Disposal strategy of proton irradiated mercury from high power spallation sources

Suresh Chiriki

Mitglied der Helmholtz-Gemeinschaft

JÜLICH
FORSCHUNGSZENTRUM

Schriften des Forschungszentrums Jülich
Reihe Energie & Umwelt / Energy & Environment Band / Volume 67

Forschungszentrum Jülich GmbH
Institute of Energy Research (IEF)
Safety Research and Reactor Technology (IEF-6)

Disposal strategy of proton irradiated mercury from high power spallation sources

Suresh Chiriki

Schriften des Forschungszentrums Jülich
Reihe Energie & Umwelt / Energy & Environment Band / Volume 67

ISSN 1866-1793 ISBN 978-3-89336-632-3

Bibliographic information published by the Deutsche Nationalbibliothek.
The Deutsche Nationalbibliothek lists this publication in the Deutsche Nationalbibliografie; detailed bibliographic data are available in the Internet at http://dnb.d-nb.de.

Publisher and Distributor:	Forschungszentrum Jülich GmbH Zentralbibliothek 52425 Jülich Phone +49 (0) 24 61 61-53 68 · Fax +49 (0) 24 61 61-61 03 e-mail: zb-publikation@fz-juelich.de Internet: http://www.fz-juelich.de/zb
Cover Design:	Grafische Medien, Forschungszentrum Jülich GmbH
Printer:	Grafische Medien, Forschungszentrum Jülich GmbH
Copyright:	Forschungszentrum Jülich 2010

Schriften des Forschungszentrums Jülich
Reihe Energie & Umwelt / Energy & Environment Band / Volume 67

D 82 (Diss., RWTH Aachen, Univ., 2010)

ISSN 1866-1793
ISBN 978-3-89336-632-3

The complete volume ist freely available on the Internet on the Jülicher Open Access Server (JUWEL) at http://www.fz-juelich.de/zb/juwel

Abstract:

Large spallation sources are intended to be constructed in Europe (EURISOL: nuclear physics research facility and ESS: European Spallation Source). These facilities would accumulate more than 20 metric tons of irradiated mercury in the target, which has to be treated as highly radioactive and chemo-toxic waste. Liquid waste cannot be tolerated in European repositories. As part of this work on safety/decommissioning of high-power spallation sources, our investigations were focused mainly to study experimentally and theoretically the solidification of liquid mercury waste (selection of an adequate solid mercury form and of an immobilization matrix, chemical engineering process studies on solidification/stabilization and on encapsulating in a matrix). Based on experimental results and supported by literature Hg-chalcogens (HgS, HgSe) will be more stable in repositories than amalgams. Our irradiation experimental studies on mercury waste revealed that mercury sulfide is a reasonable solid for disposal and shows larger stability in possible accidents with water ingress in a repository. Additionally immobilization of mercury in a cement matrix and polysiloxane matrix were tested. HgS formation from liquid target mercury by a wet process is identified as a suitable formation procedure. These investigations reveal that an almost 99.9% elementary Hg conversion can be achieved and that wet process can be reasonably handled under hot cell conditions.

Zusammenfassung:

Hochleistungs-Spallationsquellen sollen mittelfristig in Europa errichtet werden (EURISOL für die kernphysikalische Forschung und ESS für die Materialforschung). Nach aktuellem Planungsstand werden die Targets dieser Spallationsquellen etwa 20 t bestrahltes Quecksilber enthalten, welches als hochradioaktiver und chemisch toxischer Abfall verfestigt und endgelagert werden muss: Flüssiger Abfall ist in Europäischen Endlagern nicht zulässig. Als Teil eines Arbeitspakets zu Sicherheit/Genehmigung von Hochleistungs-Spallationsquellen befasst sich diese Arbeit schwerpunktmässig experimentell und theoretisch mit der Verfestigung von flüssigem radioaktivem Quecksilber-Abfall. Dazu gehören die Auswahl einer geeigneten festen Quecksilberverbindung, eines geeigneten Matrixmaterials und chemisch-technische Untersuchungen zur Verfestigung und Einbindung in die Matrix. Aufgrund eigener Untersuchungen und gestützt auf Literaturresultate wurde gefunden, dass Chalcogenide unter Endlagerbedingungen die höchste Stabilität aufweisen.

Das gilt besonders für störfall Bedingungen entsprechend einem Wassereinbruch unter Berücksichtigung von Radiolyse. Daher wird HgS für die Endlagerung bevorzugt. Von diversen möglichen Alternativen zur HgS-Darstellung aus Hg wurde die Auflösung in HNO_3 und Fällung von HgS mit Ammoniumsulfid ausgewählt. Dieser Prozess führt zu einer praktisch vollständigen Umwandlung und lässt sich relativ gut unter ein Arbeits Bedingungen in einer heissen Zelle ausführen. Als Matrixmaterialien für das Abfallgebinde wurden Zement und Polysiloxan getestet

Abbreviations

ADA. Inc	ADA Technologies, Inc.
ANDRA	The French National Radioactive Waste Management Agency is responsible for the long-term management of all radioactive waste in France
BfS	Das Bundesamt für Strahlenschutz (The Federal Office for Radiation Protection in Germany)
BFS	Blast Furnace Slag
CBPC	Chemical Bonded phosphate Ceramic
CSF	Ceramic Silicon Foam
DBE	Die Deutsche Gesellschaft zum Bau und Betrieb von Endlagern für Abfallstoffe mbH
DOE	Department of energy (USA)
EPA	Environmental Protection Agency (USA)
ESS	European Spallation Source, Lund, Sweden
EURISOL	EURopean Isotope Separation On-Line (Radioactive Ion Beam)
FRJ- II	Forschungsreaktor Jülich II
FRM-II	Forschungsreaktor München II
GBq	Gigabecquerel
GeV	Gigaelectron Volt
HAW	Higher Active waste
Hg°	Elemental mercury
HLW	High Level Waste

IAEA	International Atomic Energy Agency
ILL	Institute Laue-Langevin, Grenoble, France
INEEL	Idaho National Engineering and Environmental Laboratory
IPNS	Intense Pulsed Neutron Source (IPNS), Argonne National laboratory
ISIS	Pulsed neutron and muon source at the Rutherford Appleton Laboratory in Oxfordshire
JSNS	Japanese Spallation Neutron Source
LBE	Lead Bismuth Eutectic
LILW	Low and Intermediate Level waste
MEGAPIE	Megawatt Pilot Experimental facility at PSI, Villigen, Switzerland
MTR	Materials Testing Reactor
MW_b	Megawatt beam power
MWFA	Mixed Waste Focus Area
NAGRA	Nationale Genossenschaft für die Lagerung Radioaktiver Abfälle (Swiss National Cooperative for the Disposal of Radioactive Waste)
NDA	Nuclear Decommissioning Authority (UK)
NFS	National Fuel Service Inc.
NIREX	Nuclear Industry Radioactive Waste Executive (United Kingdom body set up in 1982 by the UK nuclear industry to examine safe, environmental and economic aspects of deep geological disposal of intermediate-level and low-level radioactive waste)
NUMO	Nuclear Waste Management Organization of Japan (Responsible for final disposal and the recycling of nuclear fuel and high level radioactive waste)
ONDRAF/NIRAS	Agency concerned with radioactive waste and its management in Belgium

OPC	Ordinary Portland cement
PAC	Powered Activated Carbon
PFA	Pulverized Fly Ash
POSIVA OY	Posiva is the Finnish expert organization in nuclear waste management
SKB	Svensk Kärnbränslehantering AB (SKB, Swedish Nuclear Fuel and Waste Management Company)
SNS	Spallation Neutron Source, Oakridge national laboratory, USA
SPSS	Sulphur polymer stabilization/solidification
StrlSchV	Strahlenschutzverordnung
TCLP	Toxic Characteristic Leaching Procedure
TRU	Transuranium (TRU) Elements
WIPP	the U.S. Department of Energy's (DOE's) Waste Isolation Pilot Plant, Carlsbad, New Mexico
ZWILAG	Zwischenlager Würenlingen AG (Intermediate storage facility for the low and medium-level radioactive waste from Swiss nuclear power plants)

Table of Contents

List of Figures

List of Tables

1. Introduction and objectives

In the present world, there exist two kinds of neutron sources: fission reactors and accelerator driven spallation sources (ADS) where neutrons are produced by the interaction of protons in the energy range of GeV with a heavy material target. Considering the history, the relative merits of using pulsed accelerator spallation sources and nuclear reactors have been debated. Recently, the research for energy generation and waste transmutation by using high energy proton accelerator driven subcritical nuclear system (ADS) has gained considerable attention. The spallation neutron targets have very important link for transmutation and other applications too [1]. A consensus from the neutron scattering experiments community has finally emerged endorsing pulsed spallation sources as the preferred option for the future [2, 3].

These high power targets are the heart of many applications of spallation to science and technology, especially as neutron sources and neutrino factories [4]. With many projects aiming to utilize proton beams in the multi megawatt power range, solid targets, in particular stationary ones become increasingly difficult to cool. Liquid metal targets are thus often the concept of choice. An advantage of liquid target lies in the fact that the heat removal is easier, because no direct cooling is required. Liquid mercury is favored by most concepts, but (liquid) lead bismuth-eutectic (LBE) and lead based liquid targets are in discussion too. LBE (PbBi) is the preferred target material in systems where neutron absorption must be minimized in order to obtain a high time average neutron flux or where, as in a power generating systems, a high operating temperature is desirable. Since both is not the case in the upcoming class of pulsed spallation neutron sources [5], these facilities prefer mercury as a target material, mainly because it does not require auxiliary heating, has a higher density than PbBi and does not produce alpha-active isotopes.

So elemental mercury (Hg^0) will be used as high power spallation target material, e.g. within of the nuclear physics research programme EURISOL a $4MW_b$ (Megawatts beam powers) project or in advanced spallation neutron sources for materials research like ESS-$5MW_b$, SNS-$2MW_b$, JSNS-$1MW_b$, where a high energetic proton beam (GeV range) generates neutrons by spallation interactions with mercury. A final decision about the European projects (EURISOL and ESS) is still in discussions. Coming to explain the basic terms associated with these projects, spallation sources consist mainly of an accelerator (1-$10MW_b$ beam power, 1-2 GeV proton energy), in SNS [6] and JSNS a storage ring for short pulse proton

beam generation, and one or more target stations where neutrons are generated by spallation. For the planned EURISOL facility (4-5MW_b), mercury as main power proton target to generate neurons will be used. It will not be exchanged during the facility operation time of (5000 hr/y), e.g. about 40 years. After closure the facility, there remains at maximum 2 m^3, i.e. about that 30 tons, mercury contaminated with radioactive nuclides (List of nuclides and activity levels are shown in Table-2) [7]. Detailed calculations on inventories of irradiated Hg-targets were performed for SNS, ESS, EURISOL and JSNS facilities [6, 8]. Also the chemical behavior of the target hull for liquid mercury is of importance with respect to the safe operation and post irradiation handling of the target systems and materials as well as for an assessment of the potential risk under various accident scenarios [7]. The spent mercury is thereby considered as high level radioactive waste and must be treated and disposed off in a safe way. Present nuclear facilities indicate that costs for these waste management issues are very high. Special attention must be paid to treatment and disposal of the irradiated mercury target due to its potential chemical (bio-toxic) as well as radiological hazards in a repository. Therefore, this radioactive waste must be disposed off in the well-designed repository in order to be safely isolated from the biosphere for a sufficient time span until radiotoxic nuclides have decayed. A repository may be constructed near the surface, typically for the emplacement of short lived, low and intermediate level waste. Concentrating and confining this radioactive waste and isolating it are the accepted strategy. Radioactive waste confinement can be provided by a number of methods and depends on waste product packaging, back fill materials and host geology. For long lived and high-level waste, a repository with engineered and multiple barriers at depths up to several hundred meters in geological stable formation is preferred. Germany, Switzerland and some other European countries have decided to dispose all kinds of radioactive waste in a deep geological repository.

Because the EURISOL facility site is not yet identified and thus the regulations of a specific host country can not be applied, it was decided to use in this study the waste management methodology recommended by the European and IAEA regulations [9]. This approach is based on the concept of clearance. Clearance is defined as the removal of the radioactive materials or radioactive objects within the authorized practices from any further regulatory control by the regulatory body. The classification system proposed by the IAEA places the radioactive waste into one of following three classes [10]:

1. **HLW: High Level Wastes**
   Highly radioactive liquid (> 10^{14} Bq/m^3)
   Heat generating waste (> 2 kW m^{-3})

2. LILW: Low and Intermediate Level Wastes (< 10^{14} Bq/m^3) divided in:

2.1 LILW-LL: Low and Intermediate Level Wastes -Long Lived

Half life > 30 years

Long lived alpha emitters: > 400 Bq g^{-1} average

2.2 LILW-SL: Low and Intermediate Level Wastes -Short Lived

Half life < 30 years

3. EW: Exempted Wastes

Disposal of mercury in a liquid form is not acceptable in Europe. Different types of treatment are possible to transform the mercury to a solid waste form. Whereas non Hg-nuclides can be separated, the separation of activated Hg-nuclides from mercury target is virtually impossible. ^{194}Hg ($t_{1/2}$ = 512 y) and its short-lived daughter nuclide ^{194}Au ($t_{1/2}$ = 38.02 hr) are an important nuclides because of their emitting high energetic γ-radiation. For that, even after separation of non - Hg nuclides the irradiated mercury has to be considered as high-level radioactive waste. As mentioned before, besides of the radiotoxic impact of mercury, its pronounced chemical or bio-toxicity has to be taken into account. In this thesis, the demonstration of a complete disposal strategy for proton-irradiated mercury is the main objective. This work was performed as part of the EURISOL project of 6th European framework program (see also www.eurisol.org) [11].

Present work is divided in order to solve this main objective as follows:

- ✓ R&D on behavior of mercury compounds in repository conditions
- ✓ Selection of a solid mercury compound and an embedding matrix formation, suitable for safe disposal of proton irradiated mercury
- ✓ A detailed chemical engineering study on the mercury solidification and matrix embedding processes
- ✓ Design, construction and application of experimental setup solidification with main the point effort to be workable in hot cell laboratories

2. Literature review

2.1. Basic terminology

There are two distinct approaches for neutron production: spallation sources, in which accelerated protons smash or "spall" neutrons out of a heavy metal target, and nuclear fission reactors. Public concern over the present operational safety of nuclear reactors, together with problems associated with long-term management of radioactive waste, has made construction of new reactors increasingly difficult. Further, the neutron generation by fission system has reached its maximum capacity with ILL (Institute Laue-Langevin) reactor for thermo hydraulic reasons. Considerable efforts have thus been made to investigate the use of accelerator-based systems as an alternative in almost all areas traditionally covered by research reactors. In particular, these are:

- ✓ Material structure research by neutron backscattering method
- ✓ Material irradiation studies
- ✓ Isotope production
- ✓ Transmutation of radioactive waste

A comparison between reactors, spallation sources, and the recently proposed but still far-sighted inertial fusion source in figure 1 provides a short overview of future neutron research based applications demand.

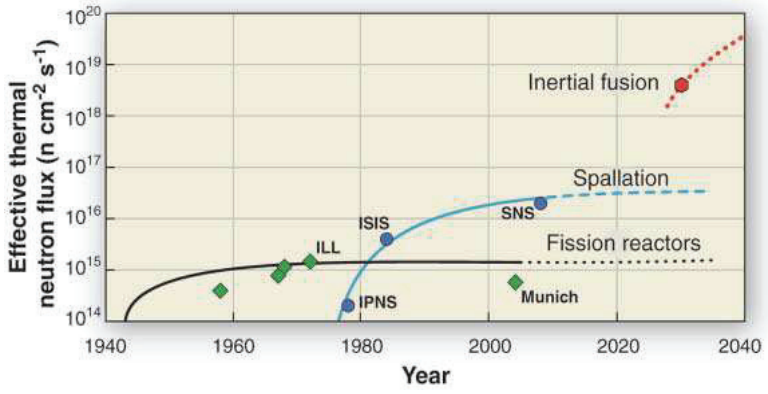

Figure 1: Neutron source flux facilities versus year of operation start [12]*

* *Shown in figure 1 "Effective flux" values are notional equivalent reactor core fluxes that provide an accepted approximate comparison between the different types of sources for many classes of experiments. The figure.1 includes the existing Intense Pulsed Neutron Source (IPNS) at Argonne, ISIS -pulsed neutron and muon source located at the UK Rutherford Appleton Laboratory in Oxford, the new high-flux reactor FRM-II in Munich, the reactor at Institute Laue-Langevin (ILL) in France and spallation neutron source (SNS) in USA, which started to operate 2006*.

Spallation sources generally employ a high intensity proton beam with high energy of typically 1-2 GeV, although beam energies up to 10 GeV are proposed too. Key element is an efficient target system to produce the high neutron fluxes. Besides being a research instrument with neutrons, spallation neutrons can also be used to transmute the highly-radiotoxic nuclei which are present in nuclear waste into stable or very short lived isotopes that can be disposed easier. The various uses impose, in detail, different requirement for targets. The main challenge for the target designer is to optimize the neutron production within the practical engineering constraints and taking into account the radiation damage on the target (if solid) structural materials and target (if liquid) hull damage by pulses. The above figure 1 illustrates how currently available neutron sources are reaching the limits of existing technologies.

2.1.1. Spallation and Fission

Neutrons have been for many years an ideal probe for understanding the microscopic structure of the matter and its behavior, in particular for technically important materials like polymers, metals and super-conductors. Fission, the first method for neutron production, is efficiently induced by thermal neutron capture in U-235 or Pu-239 and results in the prompt evaporation of 2-3 neutrons from the excited heavy nucleus. Fission based sources produce also a small fraction of delayed neutrons caused by one or more steps of β-decay. A number of important differences between irradiation facilities with a fission source or an accelerator-based spallation source should be noted. The spallation process is illustrated in the figure 2. Protons are accelerated and injected into a target by a particle accelerator and make multiple collisions with nucleons in a nucleus causing spallation (an intra-nuclear cascade). The high-energy particles such as neutrons and protons emitted during this process of collision with other nuclei, causing similar reactions (inter-nuclear cascade). We can see the incoming proton from the left striking a nucleus, which includes both spallation of the nucleus into smaller products and the evaporation of neutrons from these new atomic products. In this process, a minimum of ten fast neutrons are emitted for each proton.

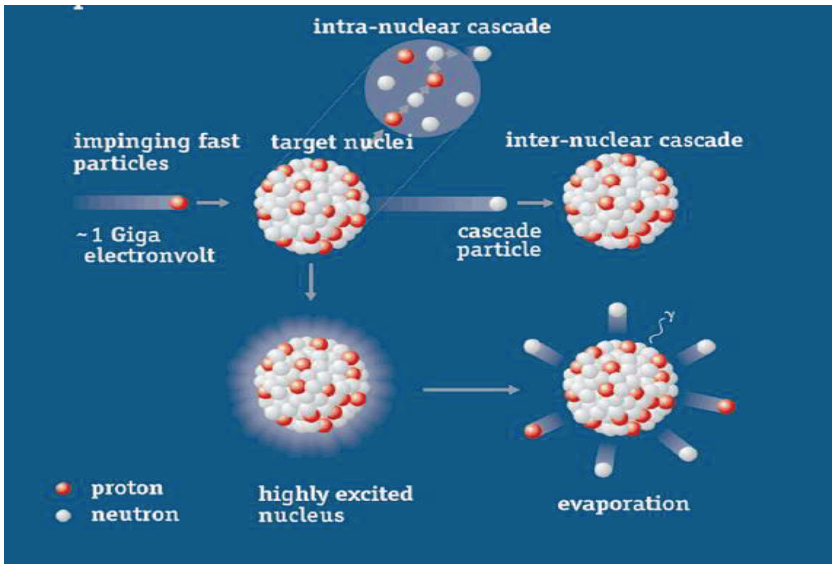

Figure 2: Schematic representation of spallation reaction

2.1.2. Multi megawatt spallation sources and target configurations

For any target, the dependence of the field of neutrons per proton as a function of beam energy (E [GeV]) and target material (atomic mass number A), is approximately given by equations 1&2 : [13]

Yield = 0.1 (A+20) (E-0.12) (A<238) ⟶ (1)

= 50 (E-0.12) (Fissionable targets) ⟶ (2)

The desirable properties of a spallation target materials are:

- ✓ High atomic number
- ✓ High density
- ✓ High boiling point (to reduce the target volatilization)
- ✓ Chemically inert, low corrosion
- ✓ Low neutron absorption cross section
- ✓ Resistance to radiation damage (for solids only)

The most important properties are the high atomic number and the high density to maximize the neutron production. The usual materials considered are tungsten, molybdenum and tantalum (and their alloys) for solid targets. Liquid metals in consideration are lead, lead/bismuth eutectic (LBE) and mercury. Liquid metal targets have several advantages: As irradiation damage does not occur much, so lifetime of a facility should last long. Thus minimizes the waste disposal problem. Additionally the mean density of the liquid metal target is not diluted by a coolant because the target itself acts as the coolant. They do not suffer from radiation damage. However in short pulse operation, shock waves are a major problem in liquid metal targets. On the other hand, the crystal lattice of solid targets serves as an activity retention barrier. But there are limited data available for irradiation effects on solid materials in a high intensity proton beam [14].

Liquid PbBi (LBE) (lead bismuth eutectic), based project called **MEGAPIE** (**MEGA**watt **PI**lot **E**xperiment) [15], is supported by a large international collaboration interested in the development of liquid metal targets for accelerated driven systems (ADS). It is expected to increase its neutron flux by another 40-50% mainly due to the higher average density compared to solid targets. The reduced amount of structural material and the absence of water in the beam are additional advantages. That is the reason why it is the preferred target material in systems where neutron absorption must be minimized in order to obtain a high average neutron flux over the time or where, as in power generating systems, a high operating temperature is desired. Since it is not intended to drain the liquid metal from container during extended shutdown periods, the PbBi must be kept in the liquid state all times because it is known to expand after solidification, which damages the target structures. A separate heating is thus required. Uncertainty in the effects of radiation damage and transient thermal stress on solid targets has resulted in mercury target being chosen for ESS and SNS. Currently EURISOL is designing their facility with a target similar to ESS.

Mercury has the advantage that no heating system is required to keep it liquid. As in all liquid targets, the retention of volatile radioactivity is small. This creates problems in the case of enclosure failure and may have problems of volatilization (because of low boiling points) and disposal as solid. Liquid target (mercury) compared to a solid target (tungsten), it seems to be more advantages of liquid target (mercury) for cooling reasons. The operation power of solid targets at 5 MW_b questions the whole system. This is respected particularly for the safety and licensing. But disposal problems are more extensive to be solved in case of liquid mercury target than solid target. On that basis, many preliminary investigations are carried out continuously at different facilities.

A mercury target can handle increasing power, but pulses are a problem. Preliminary experiment studies at SNS confirm that when the pulse of the beam hits the mercury, bubbles are created which lead to cavitations [16]. When these occur near the surface of the vessel, they can collapse, gouge into the container material [17], and erode its surface. Damages caused by cavitations erosion decrease the lifetime of the target container material and may require frequent exchanges of the container. This becomes more of a concern as operation of the SNS and JSNS compared to long pulse spallation facilities (EURISOL-5MW_b, ESS- 5MW_b,). The concept was first proposed for the 5 MW_b target of the European Spallation Source (ESS) and was then adopted and slightly modified for the USA-SNS and the Japanese JSNS projects.

All spallation concepts are based on horizontal beam injection and laterally extended ("slab") target geometry. The concept of a coalescing hollow jet is also the ruling idea in the target system considered for the next generation radioactive beam facility (EURISOL). Apart from having different flow rates due to different design power levels ((EURISOL - 5 MW_b, ESS - 5 MW_b, JSNS - 1 MW_b) the three targets differ mainly by the way in which the flow is directed across the window. ESS follows essentially the **MEGAPIE** philosophy to direct part of the flow across the window by providing a bottom inlet channel.

The SNS team decided to use a double walled container with a narrow channel to guide a partial flow all the way across the window and out of the target again (figure 3) [18], while the JSNS group developed an elaborate system of blades to establish a horizontal flow across the window and in the whole beam interaction zone. In the following figure 3 different flow patterns of liquid mercury in each high-power target test facility are shown. These assessments of the most compelling issues for pulsed liquid metal spallation targets have changed recently. As a result it was planned to research to master issues in the critical areas identified initially and furthermore of the discovery of an additional degradation phenomenon. The most prominent key areas identified originally were radiation effects in the target container structural material and compatibility of that material with liquid mercury or liquid lead–bismuth. Much progress has been made in these areas and we now have quantitative bases for target design parameters and lifetime estimations which indicate that the new spallation targets will meet their service requirements. During this time, however, the additional phenomenon of cavitations erosion or pitting of the liquid mercury contact surface of specimen containers that simulate aspects of the actual spallation targets has to be investigated.

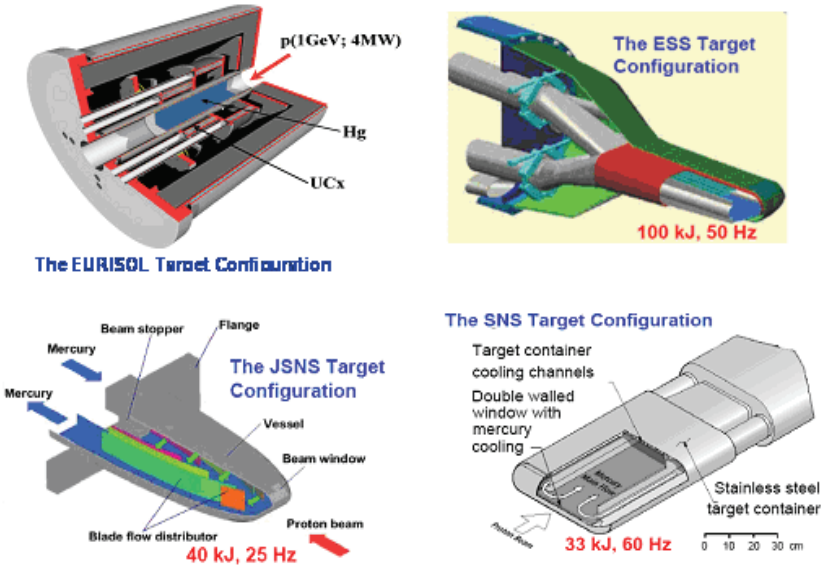

Figure 3: Schematic view of the "realistic" different target configurations [19]

2.1.3. Liquid mercury target inventory

The good knowledge of the radioactive inventory within of the ESS and EURISOL targets and of its radiotoxicity are of major relevance for safety analyses. The radioactive inventory in Hg-target was calculated for SNS, ESS and JSNS and the most relevant nuclides present in an Hg-target were identified. Based on volatility, nuclides were divided into 3 categories:

1. High volatile nuclides (tritium, iodine, noble gases)
2. Mercury isotopes (having an average volatility)
3. Low volatile nuclides (most metals other than Hg)

It should be noted that for a short time periods (1000 years after shut down) the inventory of a 4-5 MW Hg-target is even larger than an accumulated activity of a 20 MW_{th} research reactor as indicated in figure 4.

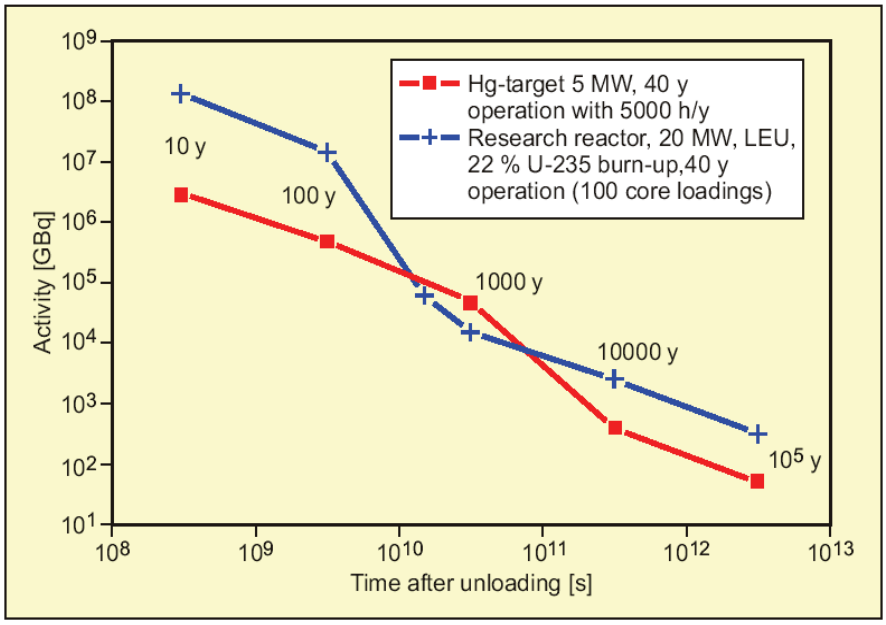

Figure 4: Comparison of activities in an Hg-target and in the core of a 20 MW_{th} research reactor (accumulated activities, relevant to waste disposal) [7]

As advantage, very long-lived actinides are not formed in an Hg-target in contrast to fission reactor and non-fissile long-lived nuclides are not present in Hg-target, too. But summarizing safety and disposal items, activity/power produced in spallation sources is of similar order as that of fission reactors.

The most relevant nuclides in the ESS and EURISOL target from a handling safety but not disposal point of view are given in table-1 together with their estimated inventories, their half-lives, their radiation type and their boiling points. The radio toxicity is presented in terms of the dose, which results from an emitted activity of one GBq (assuming dispersion, incorporation, external irradiation etc. as in [StrlSchV, 2001]) [20, 21]. Dominating nuclides for the different pathways are given in full-tone. For tritium, the inventory in the target is presented as scaled up from SNS-calculations; other values are calculated by ESS. The inventories are mainly best estimate values, multiplied by a factor of 1.6 in order to obtain conservative figures [22]. The selection of table-1 assumes that volatile nuclides are more relevant than low volatile ones due to the more limited accidental release of the latter [23].

nuclide	ESS target inventory [GBq]	Half life [d]	boiling point [K]	radia-tion type	dose/emission* ground- shine (γ) [Sv/GBq]	cloud-	inhalation	ingestion
H-3/HTO	7.9e5 total	4500	373	weak β	0	0	2.3e-9	4.6e-8
H-3/HT			14		0	0	1.5e-11	3.3e-9
I-124	3100	4.2	387	β,γ	1.9e-6	1.0e-8	3.0e-5	3.4e-3
I-125	14000	60	„	γ	1.2e-6	1.0e-10	1.8e-5	**2.3e-3**
I-126	630	13	„	β,γ	2.6e-6	4.2e-9	6.3e-5	7.6e-3
Hg-193	1.9e6	0.16	629	γ	2.4e-8	1.7e-9	6.5e-9	2.5e-10
Hg-194	1.4e5	1.4e5	„	γ	**5.4e-3**	1.3e-13	1.3e-6	3.7e-7
Hg-195	3.2e6	0.42	„	γ	5.0e-8	1.7e-9	8.1e-9	6.3e-10
Hg-197	2.2e7	2.67	„	γ	7.4e-8	5.2e-10	2.0e-8	3.0e-9
Hg-203	1.5e7	47	„	β, γ	4.9e-6	2.2e-9	1.8e-7	8.1e-9
Sr-90	14000	1.05e4	1653	β	0	0	3.5e-5	**5.2E-3**
Gd-148	3.5e4	2.72e4	3546	α	0	0	**2.2e-3**	3.6e-7
Hf-172	7.3e5	683	4875	γ	1.9e-4	7.7e-10	1.3e-5	1.9e-9
Au-195	4.2e6	186	3081	γ	2.1e-6	6.2e-10	2.2e-8	5.9e-10

*German directives for design basis accidents in nuclear facilities (dose build-up by internal and external irradiation for 70 y), infant, effective doses except for incorporation of iodine (thyroid) and strontium (red bone mark), emission height: 25 m, distance emission – imission point: 250 m

Table 1: Radiological most relevant nuclides in a 5 MW mercury target (40 y operations with 5000 h/y) Inventories as in [Bongardt 2006] [20]

The conservative dose/emission factors of table-1 should only cautiously be used in realistic accident analysis. A comparison of the radiotoxicity of mercury with its chemical toxicity was performed for the inhalation pathway. Main result is that the radiotoxicity dominates within the licensing framework, but the chemical toxicity cannot be neglected, particularly for beyond licensing events.

Table-2 contains the nuclides most relevant for target waste disposal with their halve lives and radiation energies data: these data are taken from SNS and ESS calculations, by criteria as of activity 100 years after shutdown >0.1 GBq. Fortunately, several of the nuclides listed play a relevant role in fission reactor disposal too. Accordingly, some knowledge is already available concerning their management. The total activity 100 years after shutdown is 8 X 10^5 GBq for a 5 MW mercury target, as it is shown in figure 4. As shown in table-2, the dominant activity (>10^5 GBq) is resulting from isotopes ^{193}Pt and ^{194}Hg. These nuclides don't exist in solid tungsten target. This will lead to total activity of only 10% compared to mercury one. It can be observed from the table-2 that, long-lived ^{194}Hg (512 years half-life), a hard gamma-emitter with high radio-toxicity by its daughter nuclide ^{194}Au (38h), is produced in

large quantities in mercury and LBE targets (shown in the figure 5). A new total radioactivity estimate of EURISOL 4 MW_b Hg target as a function of cooling time is depicted in figure 5.

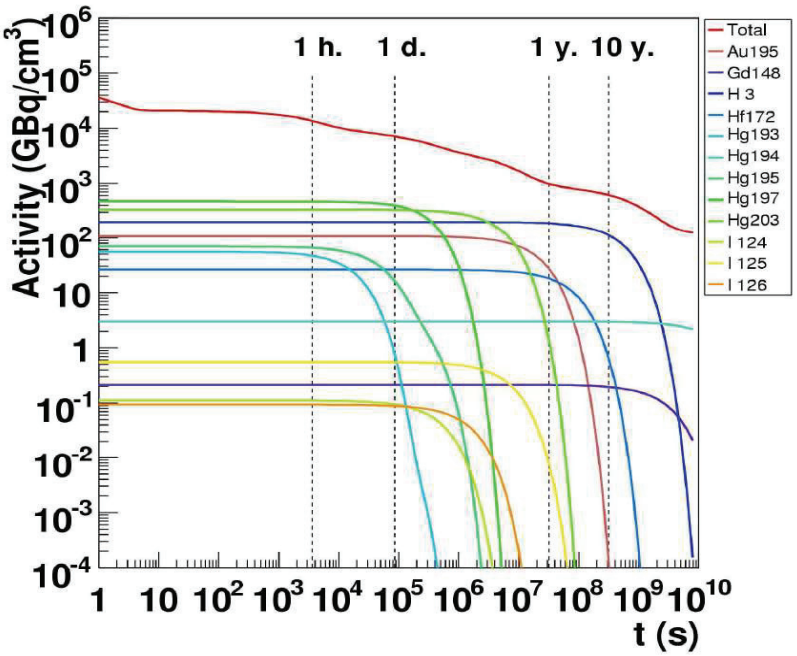

Figure 5: Total radioactivity estimate of EURISOL 4 MW_b Hg target as a function of cooling time [24]

These new calculations have been done for a continuous irradiation time of 40 years with the proton beam intensity of 2.28 mA (milliampere) (up 1 GeV protons and 4 MW target), representing an average load of the installation. Figure 5 shows the "most probable" radionuclide inventory obtained with three different models or model combinations. The contribution to the total activity of high volatility nuclides (tritium, iodine), some of the mercury isotopes with an intermediate volatility, and low volatile but long-lived nuclides (^{148}Gd, ^{172}Hf, ^{195}Au) are shown explicitly. Broad practical scenarios for decommissioning have to be studied in terms of transportation, conditioning and other nuclear waste management issue relevant for the inventories of nuclides in the mercury [25].

	Nuclide	Activity [GBq]	$t_{1/2}$ [h,d,y]	Energy of decay products [MeV]
α-Decay				*α-particles*
	Gd-148*	$2 \cdot 10^4$	75 y	3.2
	Gd-150	1.5	$2 \cdot 10^6$ y	2.7
	Dy-154	1.2	$3 \cdot 10^6$ y	2.9
β-Decay				*Average for* $\beta^{\pm}$ */ Max. for* γ
	H-3*	$2.9 \cdot 10^3$	12 y	0.006
	C-14	24	5730 y	0.05
	Si-32	$1.7 \cdot 10^3$	172 y	0.07
	P-32 **(daugther)**	$1.8 \cdot 10^3$	14 d	0.7
	Cl-36	0.7	$3 \cdot 10^5$ y	0.25
	Ar-39	$2.2 \cdot 10^3$	270 y	0.22
	Ar-42	$1.8 \cdot 10^3$	33 y	0.23
	K-42 **(daugther)**	$1.8 \cdot 10^3$	12 h	1.43 / **2.4**
	Fe-60	0.5	$1.3 \cdot 10^6$ y	0.05 / **0.06**
	Co-60	0.6	5.2 y	0.1 / **2.5**
	Ni-63	$5.5 \cdot 10^3$	100 y	0.02
	Se-79	3.1	$6.5 \cdot 10^5$ y	0.05
	Sr-90	1500	29 y	0.2
	Y-90 **(daugther)**	1500	64 h	0.94 / **2.2**
	Zr-93	0.6	$1.5 \cdot 10^6$ y	0.02 / **0.03**
	Nb-94	23	$2.3 \cdot 10^4$ y	0.14 / **0.87**
	Tc-98	0.2	$4.2 \cdot 10^6$ y	0.12 / **0.75**
	Tc-99	5	$2.1 \cdot 10^5$ y	0.09 / **0.09**
	Pd-107	0.2	$6.5 \cdot 10^6$ y	0.01
	Cd-113m	0.6	14 y	0.1 / **0.26**
	Sm-151	390	90 y	0.02 / **0.02**
	Eu-154	0.8	9 y	0.22 / **1.9**
γ-Emitter				*Max. for* γ */ Average for* $\beta^{\pm}$
	Ca-41	1.6	$1 \cdot 10^5$ y	X-rays
	Sc-44 **(daugther)**	45	4 h	3.3 / **0.6**
	Ti-44	45	49 y	0.15 / **0.06**
	Kr-81	80	$2 \cdot 10^5$ y	0.28 / **0.15**
	Nb-91	600	680 y	X-rays / **0.005**
	Nb-93m **(daugther)**	50	16 y	X-rays / **0.03**
	Mo-93	55	$4 \cdot 10^3$ y	X-rays / **0.04**
	Tc-97	0.2	$2.6 \cdot 10^6$ y	X-rays / **0.01**
	Sn-121m	60	55 y	X-rays / **0.01**
	Ba-133	90	10.5 y	0.28 / **0.22**
	La-137	100	$6 \cdot 10^4$ y	0.6 / **0.2**
	Pm-145	$4.5 \cdot 10^3$	18 y	X-rays / **0.1**
	Pm-146	0.3	5.5 y	X-rays / **0.08**
	Eu-150	$6 \cdot 10^3$	37 y	1.8 / **0.2**
	Tb-158	$6 \cdot 10^4$	180 y	1.2 / **0.05**
	Ho-163	$1.9 \cdot 10^3$	4570 y	X-rays
	Pt-193	$4 \cdot 10^5$	50 y	X-rays / **0.013**
	Au-194 **(daugther)**	$1.4 \cdot 10^5$	38 h	2.4 / **0.03**
	Hg-194	$1.4 \cdot 10^5$	520 y	X-rays

Table 2: **Disposal of relevant nuclides in a 5 MW mercury target 100 y after end of operation (40 y operation, 5000 hr/y) inventories from [7]**

2.2. Overview of aspects for safe disposal of mercury and liquid wastes

As mentioned before, special attention must be paid to treatment and disposal of the irradiated mercury target due to its potential chemical as well as radiological hazards in a repository. Some major aspects are following hereafter, based on the acceptance requirements of the German repository proposed by BfS [20]. Disposal of ADS - target is considered as high active waste (HAW), because, the overall activity of the target is $8x10^5$ GBq, even 100 years after shutdown. Often, the spent nuclear fuel arising from reactor operations is chemically reprocessed. The respective radioactive wastes include highly concentrated liquid solutions of nuclear fission products. These are later solidified generally in a glass matrix form in a process know as vitrification. Other solidification processes for HAW (high active waste) like ceramization are not available but in lab-scale developed. However, the above mentioned vitrification process is not suitable for liquid mercury target inventory because elementary mercury has a low boiling e.g. high volatilization at vitrification temperature of 1200℃.

As in fission systems nuclides relevant for long-term disposal are not fully identical to those relevant for operational time safety. ^{194}Hg is expected to be the most relevant nuclide for disposal considerations. It takes at least 5000 y (halve life 520 y) to decay to normal level for handling and further options. Also, the Hg target inventory generates such intense levels of radioactivity that heavy shielding would be required during handling and temporary storage, and in the following disposal.

The basic requirement for any geological formation is its ability to contain and isolate the radioactive mercury target until the radiotoxicity of the waste has decayed to non-hazardous levels. In order to increase the safety of geological disposal, most such disposal concepts rely on a system of independent and often redundant barriers to the movement of radionuclides [26]. These barriers generally include

(1) The leach-resistant waste form itself

(2) Corrosion-resistant containers into which the wastes are encapsulated

(3) Special radionuclides and groundwater- retarding material placed around the waste containers, commonly referred to as backfill material for gallery and shafts.

(4) The geological formation itself -- the principal barrier -- which should have to retard the transport of radionuclides against circulating deep underground water (depends on disposal land) and isolate the waste from human's environment.

There are five important reasons why deep geological disposal on land has evolved into the disposal method of choice for virtually most countries involved with such programs[27]:

- ✓ It is an entirely passive disposal system with no requirement for continuous human involvement to ensure its safety.
- ✓ Radioactive wastes present no hazard while they remain in a deep underground repository. Because of their depth of burial (several hundreds of meters), the possibility of intentional human intrusion is virtually eliminated.
- ✓ Flexibility and convenience are provided by the large variety of geological environments suitable for disposal. Geological units under consideration are rock salt, argillaceous formations (clays), and a range of crystalline rock formations [28]
- ✓ The disposal option is demonstrably practical and feasible with currently existing technology used in other mining and civil engineering practices.
- ✓ Although waste disposal implies the lack of intention to retrieve the waste, the repository can be designed so that the waste can be recovered, during repository operation or even after closure.

The following general basic requirements must be met by all kinds of waste packages:

- ❖ Waste package must be suitable for handling and transportation
- ❖ Waste must be in solid form with high chemical durability and long-term (thermodynamic) stability
- ❖ Compatibility with geological environment and resistance to bio-degradation
- ❖ Waste packages must be sufficiently radiation resistant
- ❖ Waste packages must not contain explosives or fissile materials to a certain extent

In following chapters, final waste forms of mercury also embedded in an immobilizing matrix material (e.g. cement, concrete, and polymer compounds as polysiloxanes) are discussed in more detail under irradiation conditions. Especially the selection of a solid mercury compound and clear-cut strategy on synthesis or preparation under radiation or active conditions has to be done before final disposal. A preliminary scheme for disposal of Hg-target with all process steps is following in figure 6.

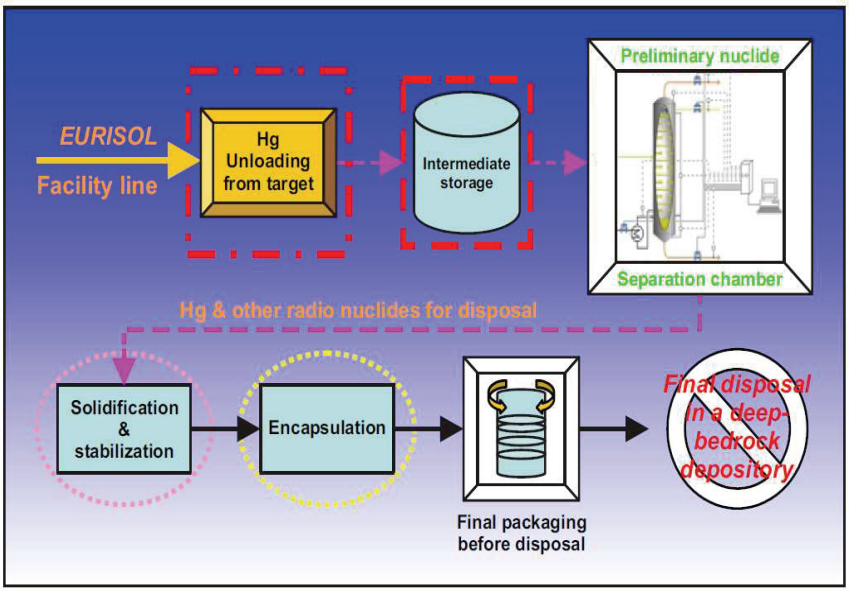

Figure 6: **One of the possible schematic layouts for Hg-target waste management strategy**

2.3. Decommissioning and final waste disposal

A considerable number of nuclear power plants have been built in the European Community since the 1950s, ranging from low power materials test reactors, through various medium power prototype/experimental reactors, up to high power commercial stations. There is a number of fuel fabrication and reprocessing plants associated with the nuclear fuel cycle and additionally military reactors in France and UK for plutonium (Pu) production. The responsibility of the waste producers is to reduce the quantities of waste generated. However it is stated as a general principle of rationalized radioactive waste management by the nuclear regulatory bodies and organizations to take care for disposal of resulting waste streams with long-term planning and decision-making associated with nuclear energy production [27]. These bodies also point out that, in order to treat the waste appropriately, it is necessary to consider safe performance, economic factors, the radioactive levels and types of radioactive materials included, so that the waste can be classified appropriately and managed and disposed of in an optimized manner. Hence, it is necessary to consider whether to adopt managed disposal at shallow or intermediate depths, or to implement deep geological disposal to ensure isolation from the human environment and to prevent the future

influence of human activities. The main sources of radioactive waste are nuclear power generation and reprocessing of waste. The radioactive waste from accelerators like spallation sources facilities played a minor role so far. In some facilities dedicated to scientific research, the amounts of nuclear waste stemming from targets (depend on liquid targets or solid targets) and shielding materials have to be considered. Large accelerators were not dismantled up to now. The increasing size of spallation facilities requires appropriate disposal methods for accelerator/target wastes which contain a wide range of nuclide concentrations [29]. Since country's availed options, it is considered that the repository site selection is an important issue and that the present disposal concept (clearance, shallow disposal, intermediate-depth disposal, geological disposal) must be implemented effectively and flexibly in order to ensure the safety of the environment [30].

Most countries with nuclear power now seem to have opted for geological disposal as the ultimate solution for the problem of processed or non-processed spent nuclear fuel or non commercial rad-waste. No state has yet made a definitive decision concerning for high level disposal siting. Although different policies for radioactive waste management have been developed in different countries, the basic problem is the same everywhere: to find a location and a method for long time isolating radioactive waste from the biosphere. A flexible stepwise by public accepted approach is required to radioactive waste management. It depends on the country for final waste disposal [30]. Countries that are planning, or that have considered, repositories for radioactive wastes equivalent to high level waste and other intermediate wastes include, Belgium (ONDRAF/NIRAS), Canada (Ontario Power Generation), Finland (POSIVA OY), France (ANDRA), Germany (BfS), Japan (NUMO), Spain (ENRESA), Sweden (SKB), Switzerland (NAGRA), the United Kingdom (Nirex), and the United States (OCRWM).

The US has an operational facility (Waste Isolation Pilot Plant (WIPP)) which is disposing transuranic wastes (broadly equivalent to LL-ILW) and is about to apply for a license to construct a geological disposal facility. In France, surface disposal for low - level and transuranic – free waste is in operation. The geological disposal facility is planned to be partitioned for separate disposal of transuranic waste (TRU) waste, HLW and spent fuel. This plan avoids interaction between each waste group. In order to minimize interaction of TRU waste, HLW and spent fuel, disposal areas would be separated by several 100 m to ensure isolation of the wastes. In relatively homogeneous sedimentary rock, it is considered that separations of several 100 m would be sufficient to rule out interaction of these wastes.
As mentioned before, the producers of radioactive waste are responsible for its safe management. The disposal remains in the hand of governments. This means permanent,

safe disposal of the waste in government owned repositories. Each power utility is responsible for waste management of the operational waste and for the decommissioning of its nuclear power plants. In Switzerland, the National Cooperative for the Disposal of Radioactive Waste (NAGRA) is responsible for the research and development work associated with the final disposal of all categories of radioactive waste. Other aspects of the waste management system, such as conditioning and interim storage of wastes, are carried out by the individual producers or by organizations set up by the producers specifically for these purposes (i.e. ZWILAG for interim storage of radioactive wastes). The central interim storage in Würenlingen (ZWILAG) has started operation in 2001 [31]. The ZWILAG facility is to be used for interim storage of all categories of radioactive waste, from spent fuel to medical and industrial waste, and comprises equipment for the conditioning and incineration of low- and medium-level waste. There is no national strategy on the way of decommissioning nuclear installations. NAGRA operates two rock research laboratories: one at the Grimsel site (granite) and one at Mont Terri (Opalinus clay). Since the quantities of high level radioactive waste (HLW) and low level radioactive waste (LLW) in Switzerland are very small, an international repository is considered as well as a national repository. However, the political environment is not yet ready for an international approach.

Swedish nuclear utilities, Svensk Kärnbränslehantering AB (SKB) is responsible for all handling, transport and storage of the nuclear wastes outside of the nuclear power stations. According to Swedish law, SKB is also responsible for an R&D-programme required to deal with radioactive wastes (SKB, 1996a) [32]. The programme comprises, among others, a general supportive geo-scientific R&D and the Äspö Hard Rock Laboratory (HRL) for more in-situ specific tasks (SKB, 1995a) [33]. A repository concept involving deep geological disposal has to be adapted to the overall geologic and tectonic conditions. The Swedish reference repository concept thus considers an excavated vault at ca. 500m depth in crystalline rocks. In this concept (KBS-3), copper canisters with high level waste will be placed in deposition holes from a system of tunnels. These disposal holes, with a diameter of 1.75m and a spacing of 6m, are drilled vertically downwards. Blocks of highly compacted swelling bentonite clay are placed in the holes leaving ample space for the canisters. At the final closure of the repository, the galleries are backfilled with a mixture of sand and bentonite or crushed rock (SKB, 1995b) [34]. This repository design aims to make the disposal system as redundant as possible. Although the KBS-3 concept is the reference concept, alternative concepts and/or repository lay-outs are also studied. The main alternative, currently under development at SKB, is disposal in boreholes of 4-5 km in depth [35]. The geoscientific research of SKB is thus related to crystalline rock and the KBS-3 repository concept. The scope of this research will, to a great extent, be guided by the

demands posed by the performance and safety assessments. Furthermore, the constructability issues are emphasized [36]. Likewise, the criteria for safety of mercury disposal are based on the protection of human health at an individual level. The estimation of an acceptable mercury load is based on WHO's threshold value for tolerable daily intake and the Swedish standard for drinking water. The Swedish EPA (Environmental Protection Agency) suggests that 0.5-10 g mercury per year is an acceptable leakage from the repository [37]. The calculation involves a number of elements, such as character of recipient, water flows, etc.

Germany has taken a decision to have disposal facilities for all waste available by 2030 or later (studies at the proposed Gorleben facility are under consideration), and is preparing to operate the Konrad facility for non-heat generating wastes in 2014: The Morsleben facility which contains LLW is in the process of backfilling it [38]. In Germany, the responsibility for the final disposal of radioactive waste is with the federal government: It has charged the Federal office for Radiation Protection (BfS) at Salzgitter with the final disposal of radioactive waste. With respect to planning, erection and operation of these installations, the BfS is using the services of the German Company for Construction and Operation of Final Repositories (DBE) at Peine as a third party [39]. For some of these disposal sites exist based on waste acceptance requirements, e.g. amount of chemo-toxic substances in the final repository or the allowed maximum concentration of radioactive/nuclide specific material. As previously stated, in Germany all radioactive wastes are to be disposed of in deep geological formations.

The mentioned Konrad iron ore mine near Salzgitter in the Federal State of Lower Saxony was selected for disposal of radioactive waste with negligible heat generation [28], i.e. waste packages which do not increase the host rock temperature by more than 3K on an average (for LLW, ILW) [40]. For the former Asse salt mine, which was used as an experimental disposal facility for nuclear waste and as an underground research laboratory, a closure concept is in preparation. Some operational information is given: In total, 124494 drums of low level radioactive waste (approximately 1.9×10^{15} Bq) and 1293 drums of intermediate level radioactive waste (approximately 1.2×10^{15} Bq) were disposed of there before 1978. The disposal of nuclear waste was started in 1967 and was stopped in 1978 because the license was expired. Since that time the Asse salt mine was used as an underground laboratory for research and development on the safe disposal of radioactive waste [41]. The Gorleben facility is intended to be the only one in the Federal Republic of Germany that will get a license for the long-term storage of vitrified high-level radioactive waste from the reprocessing of German fuel elements abroad. These conditions have to be assumed in case

of final disposal of spallation targets are opted into German or Switzerland facilities. The general nuclear waste management scheme is shown in figure 7. However the common principle practices have to be applied to the types of wastes and on national laws.

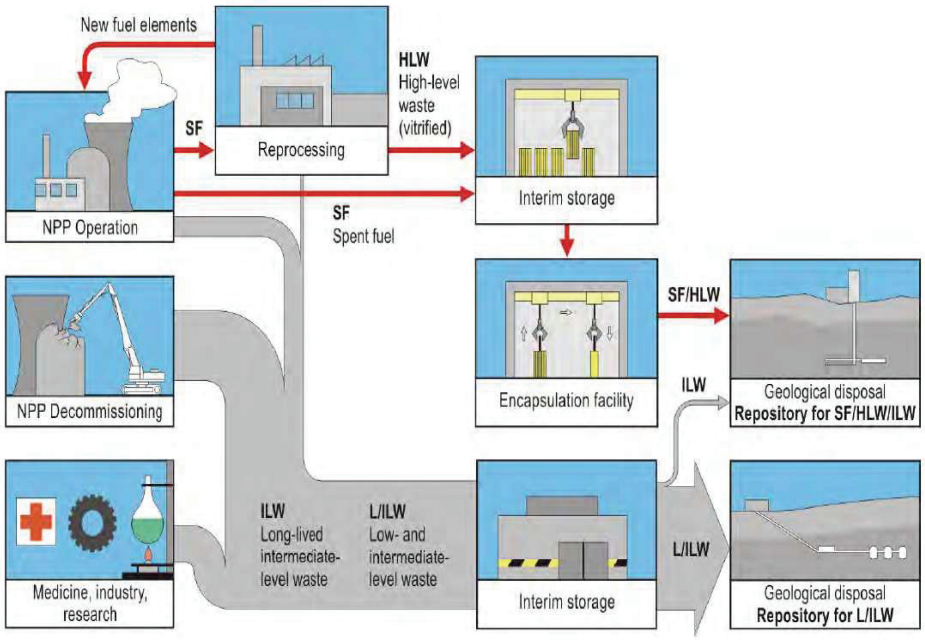

Figure 7: General scheme for nuclear waste management

2.4. Mercury and its compounds

In order to evaluate handling for the spallation target system using mercury, it is necessary to have a better overview on physical and thermo-chemical data of inorganic mercury compounds formed with other elements including spallation products. Radionuclides are important for decay studies and for disposal too. The most important isotopes of mercury with respect to radiological consequences are Hg-189, Hg-193, Hg-194, Hg-195, Hg-197 and Hg-203. Most of them are however short-lived in terms of disposal considerations. A list of natural isotopes of mercury is given in table-3. The generated radioactive mercury isotopes are homogeneously diluted in stable mercury matrix, the origin of the target [42].

Isotope	Natural isotope mass % abundance
^{202}Hg	29.7%
^{200}Hg	23.1%
^{199}Hg	17.0%
^{201}Hg	13.2%
^{198}Hg	10.1%
^{204}Hg	6.8%
^{196}Hg	0.15%
There exist 24 nuclides of Hg. Unstable nuclides have half-life ($t_{1/2}$) between 520 y (for ^{194}Hg) to 0.17 sec (for ^{177}Hg)	

Table 3: Mercury isotopes (ordered according to decreasing abundance) [42-44]

The most important physical properties [42] are listed in the table-4. Mercury is chemically inert toward water so the interaction of mercury and water is treated on purely physical considerations in the accident analyses. Important physical characteristics of mercury include its high density of 13600 kg/m^3, substantial surface tension, and its slow evaporation at the temperatures of interest in accident scenarios. The density difference between water and

mercury and the mercury surface tension restrict its contact with water under accident conditions; usually, such contact would involve only a limited amount of surface between pools of mercury and overlying water. Mercury exists in the oxidation states 0, +1, +2. It forms many compounds in environment as organic and inorganic forms. Liquid mercury is an aggressive solvent toward many other metals, forming alloys called amalgams. In sufficient amounts, these amalgams may crystallize out of solution. Most of them are lighter than mercury, so they will float on a mercury pool.

Color	Silver white
Mol. Wt	200.5 g/mol
Melting point (*mp*)	-38.9℃
Boiling point (*bp*)	357.3℃
Density (0℃)	13.6 g/cm ^{3}
Specific heat capacity c_p (0℃)	0.1397 J g^{-1} K^{-1}
Heat of fusion	11.807 J/g
Heat of evaporation (375℃)	59.453 kJ/mol
Thermal conductivity (17℃)	0.052 W cm $^{-1}$ K^{-1}
Thermal expansion coefficient β (0-100℃)	1.826E-4 K^{-1}
Electrical conductivity (0℃)	1.063E-4 mΩ^{-1} mm^{-2}
Dynamic viscosity η (20℃)	1.554 mPa· s
Surface tension	480.3E-5 N/cm
t_{crit}	1450℃
p_{crit}	105.5 MPa
Critical density	5 g/cm^{3}
Evaporation number (25℃)	0.085 mg K^{-1} cm^{-2}
Saturation vapor pressure (t- 20℃)	0.170 Pa

Table 4: Physical properties of elemental mercury (Hg⁰) [42]

The redox potentials at 298.1 K and 101.325 kPa relative to standard hydrogen electrode are shown in table-5. The standard potential shows that mercury is a relatively noble metal. There are many organic, inorganic, and metallic Hg compounds available in present chemistry world, out of them only very few compounds as stable under normal conditions. The high-temperature stability of all mercury compounds is limited. Inorganic compounds of mercury are easier to handle than organic compounds of mercury because organics are far more toxic.

						E°, Volts
Hg^{2+}	+		$2e^-$	$\Longleftrightarrow$	Hg	+0.851
$2Hg^{2+}$	+		$2e^-$	$\Longleftrightarrow$	Hg_2^{2+}	+0.920
Hg_2^{2+}	+		$2e^-$	$\Longleftrightarrow$	2Hg	+0.797
$Hg_2(CH_3COO)_2$	+		$2e^-$	$\Longleftrightarrow$	$2Hg + 2(CH_3OO)^-$	+0.511

Table 5: Redox potentials of mercury compounds with different oxidation states[43, 45]

These organic compounds are out of discussion for disposal considerations under highly radioactive conditions also because of their limited stability. The main properties of inorganic mercury compounds such as density, melting point and boiling points, standard enthalpy of formation, standard Gibbs energy of formation, constant-pressure heat capacity, vapor pressure and solubility in water are presented in following pages. In this work, mercury solid compounds are discussed from disposal point of view, i.e. stability under strong hydrolysis conditions, high thermal conditions and stability under radiation. The long term behavior of the compounds under geological disposal conditions has to be considered seriously. The conventional toxicity of mercury and its compounds have resulted in a strong effort to control the disposal of mercury. Solidification is required for elemental mercury. There is thus a stringent need for an appropriate solid form of mercury for final disposal. A few solid compounds of mercury are chosen in our present study and are shown following in the table-6. These are stable at normal conditions and available in solids form. Merits and demerits of compounds will be discussed in the following paragraphs.

2.4.1. Mercury salts

Compounds of mono-valent mercury contain ions in the form of Hg^{2+}_2. These compounds are not very stable and disproportionate easily to form elemental mercury and corresponding divalent mercury derivative [46]. Most of the mono-valent compounds are sparingly soluble in water, such as sulfate (Hg_2SO_4), chloride (Hg_2Cl_2) (calomel) and nitrate $Hg_2(NO_3)_2$, and undergo considerable hydrolytic cleavage in water. The more soluble salts, e.g., the nitrate, are partially hydrolyzed in aqueous solution: After acidification of these solutions, the poorly soluble compounds can be obtained by precipitation. The compounds of divalent mercury can be divided into those that are strongly dissociated and those that are weakly dissociated. The weakly dissociated compounds, e.g. the chlorides $HgCl_2$, are less prone to hydrolysis by water. But with excess anions, they form complexes that are more soluble than the salts themselves. Other compounds of mercury, called mercury chalconides are divalent mercury compounds that exist in nature as minerals: the oxide (HgO) as montroydite, the sulfide (HgS) as cinnabar and metacinnabar, finally the selenide (HgSe) as tiemannite. For these compounds the solubility data are given in the table-6.

Chemical formula	Compound name	Solubility (g/l)
Hg_2Cl_2 (Calomel)	Mercury (I) Chloride	2
$HgCl_2$	Mercury (II) Chloride	7000
HgO	Mercury (II) Oxide	395
Hg_2SO_4	Mercury (II) Sulfate	500
HgS(Cinnabar, Meta cinnabar)	Mercury (II) Sulfide	0.0041
HgSe	Mercury (II) Selenide	00012
$HgNH_2Cl$	Mercury(II) amidochloride	0.094
Hg	Elemental Mercury	0.06

Table 6: Solubility data of inorganic salts of Hg and elemental Hg in water (at room temperature and standard conditions)

From the table-6, it is easily predictable that the mercury sulfide (HgS) and mercury selenide (HgSe) are extremely low water soluble and in addition from literature, they are insoluble in non-oxidizing mineral acids and in caustic alkali too. They dissolve only in aqueous solutions and release sulfur and selenium, and alkali sulfide solutions, to form thio-complex-salt ions, such as $[HgS_2]^{2-}$. Mercury sulfide has also a well-defined chemistry under standard conditions. Mercury selenide is a highly toxic compound. For the disposal point of view, these are the most favorable options from inorganic compounds to convert the elemental mercury into a solid form. Even from heat of formation enthalpies and vapor pressure date with respect to temperature, Hg-chalcogenides have better stability than Hg-halogenides (shown in figure 8 and figure 9). Radiation stability data are still to be investigated.

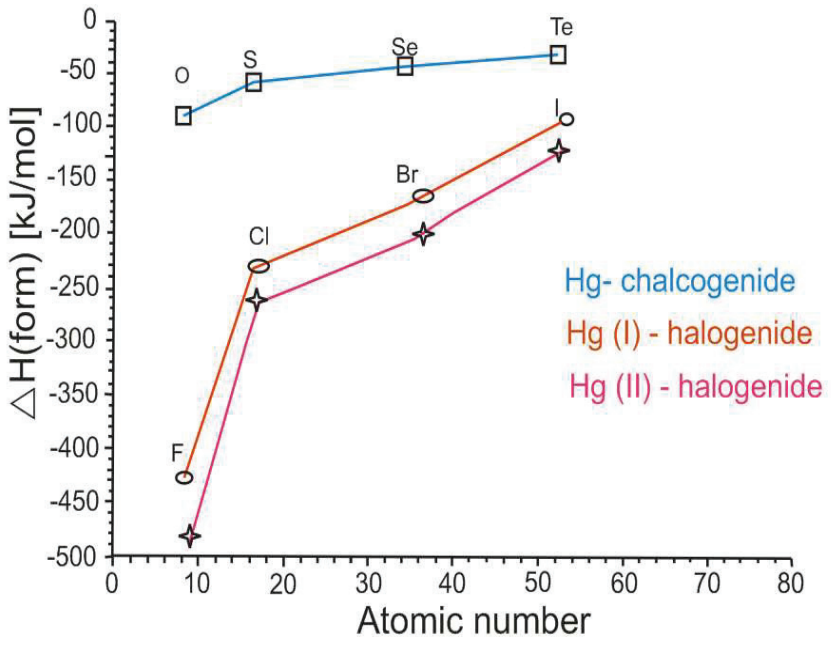

Figure 8: **Heat of formation for mercury halogenides and chalcogenides with respect to atomic number [47]**

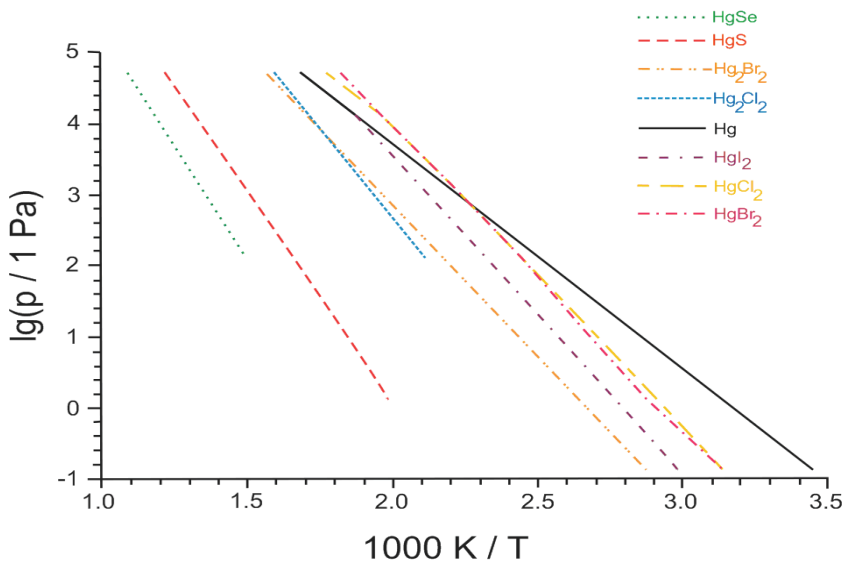

Figure 9: **Vapor pressure of mercury and mercury compounds as function of reciprocal temperature [46]**

2.4.2. Metal alloys or amalgams

The alloys of mercury (amalgams) are solid and semi-solid at room temperature. Solid amalgams contain intermediated phases, and often may contain liquid-phase inclusions [48]. The solubility of metals in mercury depends strongly on temperature (shown in figure 10). The amalgam formation may be endothermic or exothermic depending on the metal. Technically important amalgams are those of tin-copper-silver used in dental application. Still the formation of amalgams under low temperatures is not well developed. Amalgams are typically chemically very reactive [49]. Depending on the elements involved, they may react spontaneously with air, water, or even organic materials. The resulting oxides, or other products of such reactions, are typically very insoluble in liquid mercury. As these oxides are generated, they will form a skin or dross on the surface of the mercury pool, but some may collect on the surface of the mercury vessels and piping. The heat of formation enthalpies of amalgams shows that Hg_x-M_y (amalgams- M stands for metal) has better solubility [50] than Hg-inorganic compounds (as shown in figure 11). Most of heats of formation values are just below the zero. Their thermal and dissolution behaviors are more discussed in subsequent paragraphs.

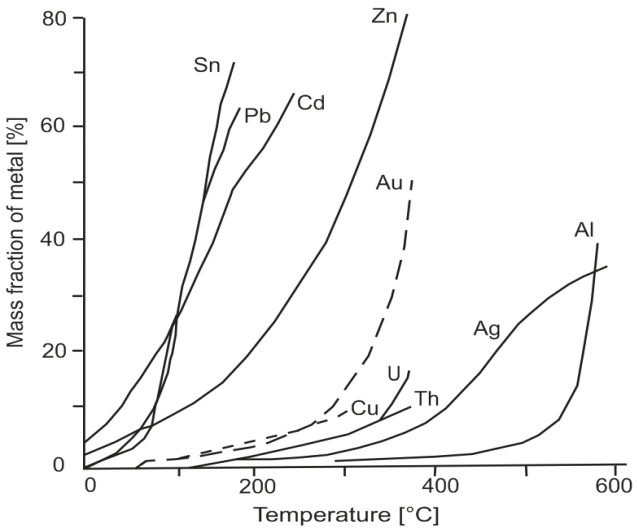

Figure 10: Solubility of some metals in mercury as function of temperature [51]

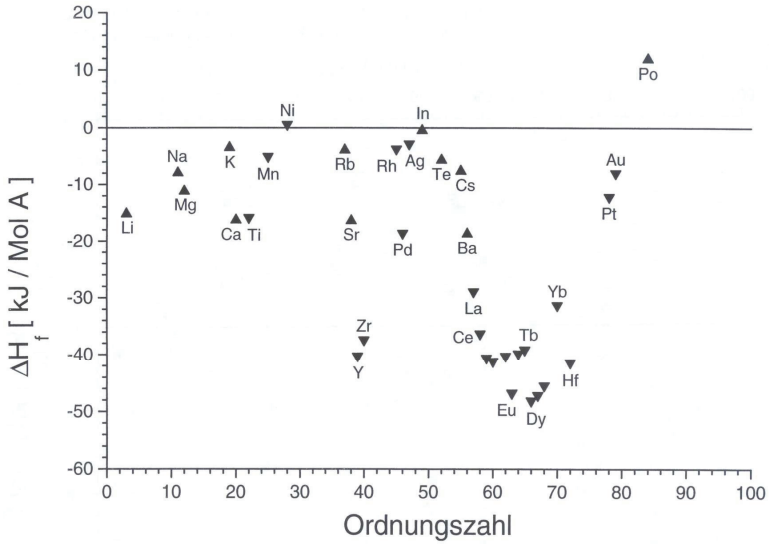

Figure 11: Heat of formation for mercury amalgams with respect to atomic number[52]

2.4.3. Stabilities of mercury compounds as chalcogenides and amalgams

In order to evaluate fully the various potential release mechanisms, supporting analyses include assessments of the behavior of mercury inorganic spallation products and metal alloys (amalgams) of the mercury and metallic spallation products have to be considered. This subsection briefly summarizes some of the results of the assessments. The full scale processing of highly level radioactive wastes requires certain parameters for final waste form. Therefore, a standard approach has to be developed for waste treat forms that should meet the final disposal requirements. However, this approach is not completely applicable to a mercury target, because of cross contamination problems associated with mercury contaminated with many nuclides (shown in table-2), including tritium oxide. Because accidents considered release of tritium either in elementary form (HT) or as water vapor (HTO) can result in contamination of plants in the form of tritium water. This leads to classification of activated mercury or mercury target inventory as hard as mixed waste. For that, separation of other nuclides from mercury is still under study to lower is classification.

Mercury sulfide

As a mercury compound in a geological repository, mercury sulfide (HgS) is one of the most favorable options. Before discussing the synthesis parameters, the geological factors of mercury sulfide are important for a disposal point view. Two modifications of HgS exist: red (cinnabar or α-HgS) and black (metacinnabar β-HgS). Both forms have been found as stable mineral in the earth crust. In hot brines metacinnabar is formed as crystallized form and transformed into more stable cinnabar [53]. In the following figure 12 examples of HgS minerals are shown. The stability relations and formation of cinnabar and metacinnabar have not been well understood. It was assumed that in that past cinnabar and metacinnabar were formed in the nature as mercury ore deposits. Cinnabar or red mercury sulfide (α-HgS) was considered as the generally stable modification of HgS. However, the results of previous studies on HgS indicate that the red HgS (cinnabar) inverts to black HgS (metacinnabar) at 386℃, at one atmosphere. The inversion is comparat ively rapid and is reversible. In presence of small amounts of iron or other impurities, an equilibrium reaction takes place between the two forms. The thermodynamic correlation [54] between metacinnabar and cinnabar and its activation energies also during the reaction are shown in the following figure 13. In general, HgS formation clearly shows that it is stable even at high temperatures above 350℃ (in absence of oxygen), and that the reaction also proceeds at low temperatures

forming metacinnabar from elemental mercury and solid sulfur power and inverts at 345℃ to form stable cinnabar[55].

Figure 12: Metacinnabar (β-HgS) (Left) and cinnabar (α-HgS) (Right)

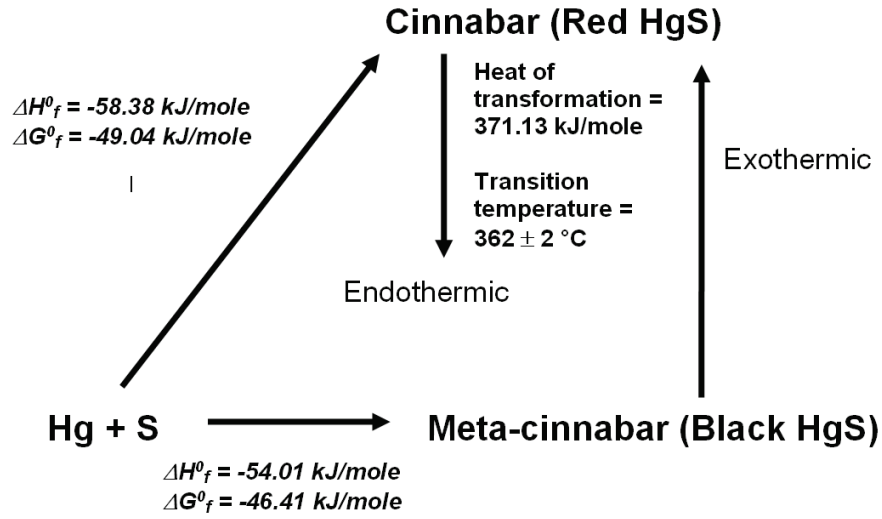

Figure 13: Thermodynamic data for the sulfide process reaction [56]

The preferred chemical state for mercury in geological repository conditions should be stable even under different salt brines (chloride environments) and aqueous acidic conditions. Earlier mercury extractability studies from cinnabar and metacinnabar were conducted by Nevenka et al. 2003 and Martinez et al. 1998, especially on soil matrices [57]. They observed that both forms of HgS were insoluble in all HNO_3 and HCl concentrations in aqua region as pure compounds. The aim of their study was to check the influence and feasibility of two common extracting agents (50% v/v HCl and 50% v/v HNO_3) on the leaching of mercury from soils containing HgS[58]. These observations were made at room temperatures and at higher temperatures between 70℃ and 100℃. This was done mainly to evaluate the soil matrix influence on the HgS solubility.

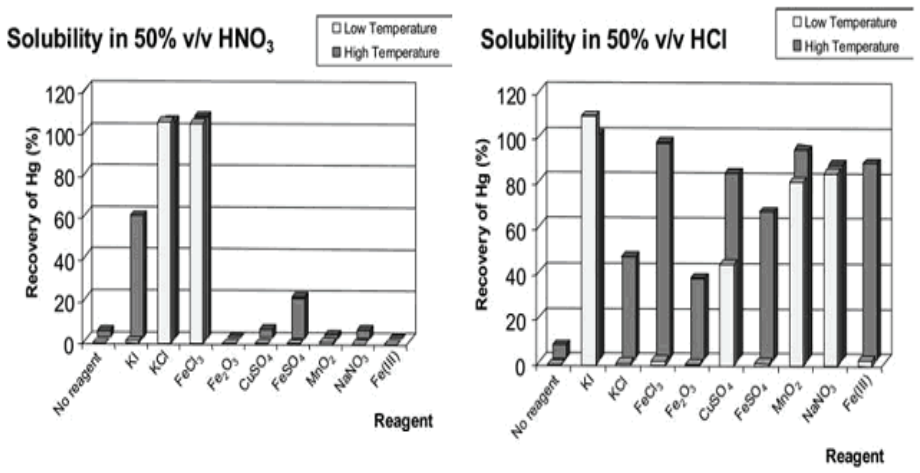

Figure 14: Solubility of HgS in soil matrix) (50% v/v HNO_3 and HCl) [57]

Several studies indicate that certain compounds can promote the solubility of HgS in acid solutions. A similar effect was observed in alkaline solutions. Sulfate and halide salts of metal at their highest valence state, such as Cu (II) or Fe (III), may partially induce dissolution of the HgS in hydrochloric acids. The behavior of HgS in the presence of Fe (II) was also investigated. Dissolved iron increases the solubility HgS and other mercury species in acids under reducing conditions as is clearly shown in the above figure 14. Of course, these are extreme conditions compared to disposal state. It is shown only the behavior of mercury sulfide in behavior highly oxidizing conditions. The effect of pH on leaching of Hg from soil

containing HgS in the presence of iron compounds, acts as container material, is plotted in figure 15. The Hg concentration gradually increased by dissolution as the pH of the suspension increases from pH 2 to 10.6. However, the presence of Fe (III) reduced the concentration of dissolved Hg significantly at all pH conditions. The change in pH conditions also changed the redox-condition of the suspension: as the pH increases the suspension becomes reducing. Bound mercury in waste form was in the stabilized forms $HgS_{(s)}$ and $HgCl_{2(s)}$ and did not leach as oxidizing condition prevailed. Alkaline and reducing conditions were found to enhance the soluble level of Hg. At high pH, the solubility of HgS in waters increases measurably by forming various bisulfide species (Clever et. al,. 1985) [59].

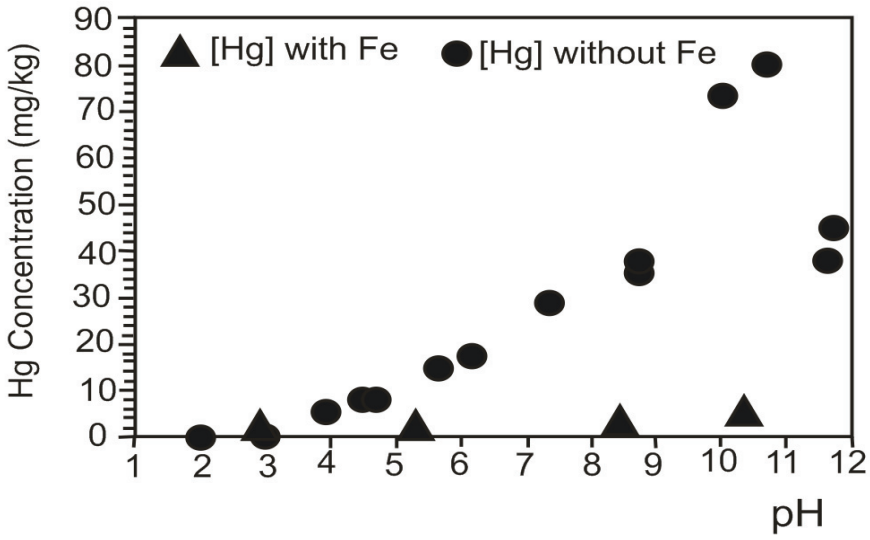

Figure 15: Concentrations of Hg in the leachate at different pH values

The high solubility of Hg as HgS complexes in solutions within the stability field of cinnabar in high concentrations of reduced S and neutral to alkaline pH is well known. A number of Hg–S solution species have been proposed to account for this solubility. Schwarzenbach and Widmer (1963)[60] proposed the (pH dependent) species $Hg(HS)_2$, $HgS(HS)^-$ and HgS_2^{2-}. In contrast, Barnes et al. (1967) proposed four possible complexes, $HgS(H_2S)_2$, $Hg(HS)_3^-$, $HgS(HS)_2^{2-}$ and HgS_2^{2-}, to model results from experiments in which Hg(II) was dissolved in 2.5 M sulfide solutions[60]. According to Barnes (1979) [61], $Hg(HS)_2$ is the dominant species

at pHs less than 6, $HgS(HS)^-$ between pH=6 and 8, and HgS_2^{2-} above pH=8; $HgS(HS)(OH)^{2-}$ requires high pHs which are outside the pH range of natural waters.

Allen, Crenshaw, and Merwin et al. studied aspects of the chemical and thermal behavior of HgS, with the aim of determining the conditions under which cinnabar and metacinnabar are formed [53]. Red HgS and black HgS were heated in evacuated vessels in the presence of substances such as ammonium sulfide and sulfuric acid, at temperatures ranging from 100℃ to 570℃, for times varying from one-half day to five days. After cooling the samples were examined under the microscope for evidences of inversion. Red HgS was reported to be unchanged, but black HgS was either partially or completely altered to red HgS. They concluded that red HgS was stable at all temperatures up to 570℃ and that metacinnabar was not stable under any of the conditions of their experiments. They found the thermal behavior of HgS to be rather confusing, however. They reported that HgS, initially red, heated to 445° C appeared black to the naked eye, but after the samples were ground fine and examined under the microscope they were seen to be made up mostly of cinnabar [62]. The black color of the underground samples was apparently caused by a thin layer of metacinnabar on the cinnabar-particles. No satisfactory explanation was presented for the appearance of black HgS, which had formed from red HgS in contradiction to their conclusion that red HgS was the stable phase at 445℃.

Amalgams behavior

As mentioned in the previous chapters, mercury forms semi solid solutions, known as amalgams, with varieties of metals. Essentially, amalgamation relies on dissolution of mercury in the solid metal or vice verse to form a solid solution, and this technique has previously found application in the extraction of precious metal, such as gold and silver from their ores. Following amalgamation, the amalgam is subject to a thermal treatment to volatilize the mercury and thereby recover the precious metal[63]. While the technique of amalgamation is a convenient, speedy and relatively inexpensive process for the handling of small amount of elemental mercury, it can be difficult to scale up. The amalgamation process requires the assistance of dilute nitric acid in order to achieve high efficiency but there is the problem of hydroxide formation. Of course, this technique is generally applicable to the disposal of elemental mercury, which is contaminated with radioactive materials. The amalgamation process mainly depends on the solubility of metals in the elemental mercury. The selection of a metal for amalgamation depends on waste disposal scheme, in terms of operating conditions and price.

Dental amalgams behavior

Silver is the major component of the dental amalgam and the alloy most consists of other metals like tin and copper. First the metal alloy mixed with mercury in an about 1:1 mass ratio. Then the amalgam reaction starts at high pressure, leading to the hardening of the mixture. A number of intermetallic mercury compounds originate in the course of this reaction [64, 65]. In overview, the most important mercury phases are shown in table-7:

Phase	Composition of metals
γ	Ag – Sn (Ag_3Sn_7)
γ1	Ag - Hg –Sn (Ag_3SnHg_2)
γ2	Sn – Hg (Sn_7Hg)

Table 7: Structural phases of dental amalgams with Hg

This process is not feasible in large quantities and especially for disposal application. In dental amalgams, many intermediate phases are formed during mixing, and these phases depend on inter-atomic reactions. γ_1-Ag_3SnHg_2 and γ_2-Sn_7Hg are stable phases and γ2-Sn_7Hg forms a protective layer during the oxidation process in mouth environments. However γ_2-Sn_7Hg phase is thermally unstable. Based on heat of formations (as shown before in figure 11), only silver-amalgam, copper and gold amalgam could be possible solutions for immobilization of large amounts of elemental mercury under highly activated conditions. For this reason, solubility data of amalgam powder in elemental mercury are necessary to predict the operating conditions and formation of stable phases. Phase diagrams of mercury with gold, silver and copper are given in the following figure.16. Although copper is readily wetted by mercury, the solubility of copper in mercury at room temperature is very low. Lindhal et al. have carried out a detailed examination on copper-mercury solid solutions and found the following phases in the solid solutions: Cu_7Hg_6, Cu_4Hg_3 and $Cu_{15}Hg_{11}$ at different temperatures. The debate about composition ended in favor of Cu_7Hg_6 and at maximum miscibility was observed from phase diagrams [66]. Lugscheider et al. determined that the stable phase is formed at a temperature of 128℃, whereas Costa et al. proposed slightly higher temperatures of 140℃. Here only one phase of copper (Cu_7Hg_6) is considered.

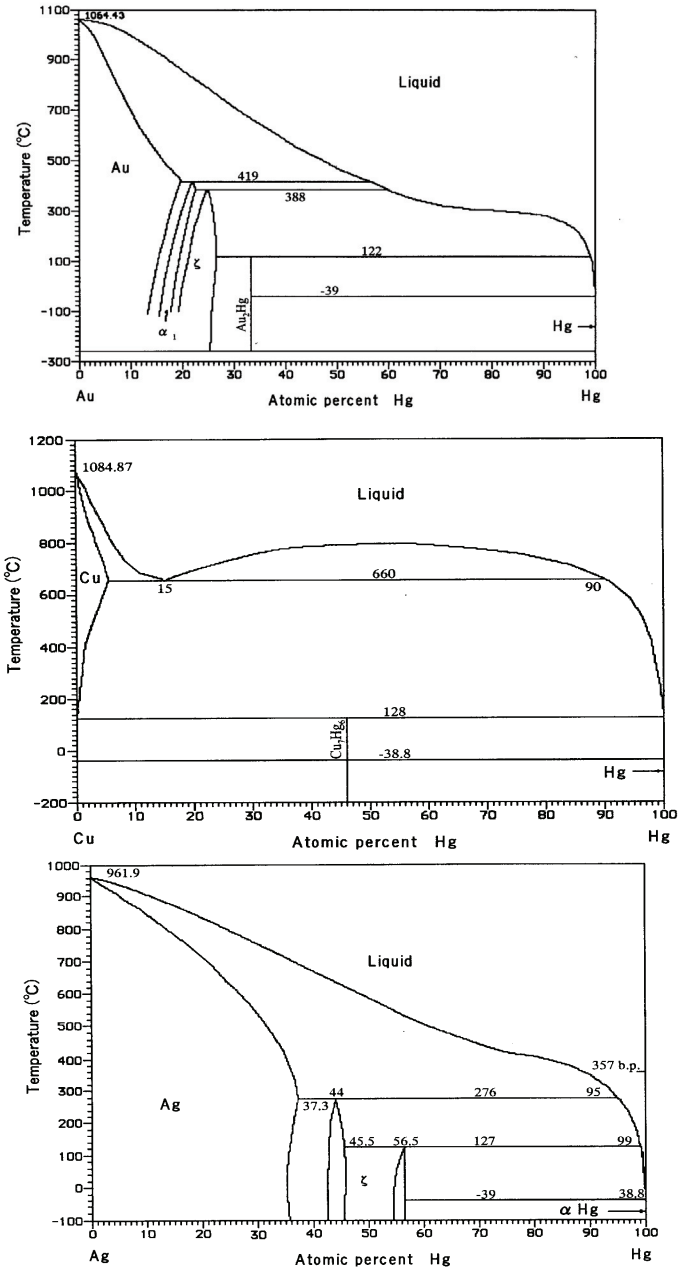

Figure 16: Phase diagrams of gold, copper and silver in elemental mercury

Similarly the mercury-silver phase is also studied [67]. The maximum miscibility with elemental mercury at room temperature solubility is good. This holds even more for the gold. Details of gold are not discussed here because it is economically not a favorable option for disposal.

In terms of dissolution and thermal stabilities of mercury in amalgam form, there are enough data available for the pure single metal amalgams, like Cu and Ag amalgams. Much information are based on dental amalgam studies: Tsutsumi et al. performed a thermal analysis for dental amalgams at a temperature range of 25-130℃, heating in air and observed local melting of amalgam structures because of a solid-state diffusion for different amalgam phases without accompanying the weight loss. Dental amalgam is not completely stable in the corrosive environment of the mouth and leads to dissolution of mercury from amalgam even in less saline conditions like saliva [68]. The level of mercury release depends mainly on the amount of Sn-Hg phase (γ_2-Sn_7Hg) and on the amount of copper in the mixture too. The composition of the alloy used for the preparation of dental amalgam affects both phase structures and corrosion resistance of resulting materials. With existing information, the use of the amalgams process for large quantities of mercury is a very questionable option. It may lead to continuous release of mercury from the matrix at any stage. Still amalgam's radiation stability is also questionable in long term nuclear application. More detailed information about amalgams is going in next chapters.

2.5. Mercury solidification/stabilization in a compound

2.5.1. Safety aspects consideration during chemical processes

After sufficient "beam on" operations, the mercury target contains radioactive mercury atoms and radioactive spallation product atoms. This includes both radioactive isotopes of many elements and unstable isotopes for each of these elements after 40 years of operation. As mentioned in the previous chapters, this irradiated mercury has to be solidified before disposal. This is because liquids are not permitted in a radioactive repository. A sufficient separation of radioactive nuclides from mercury is virtually impossible because of its significant content of long-lived Hg-194. This work mostly deals with disposal of elemental irradiated mercury. Most particularly, it is concerned with techniques for the treatment and safe disposal [69]. Currently a good number mainly inactive mercury treatment processes are available in the world. The selection of a solidification process however, involves many

factors, mainly method and material properties. It should demonstrate the effectiveness of chemical process technologies that can achieve the following:

- ✓ Minimize secondary waste generation
- ✓ Minimize worker exposure
- ✓ Maximize operational safety-flexibility and radionuclide containment

2.5.2. Overview of mercury stabilization technologies

Earlier the U.S environmental protection Agency's recommended as technology for radioactively contaminated mercury treatment is amalgamation process called DeHg™ (de-merk) process. It is an ambient-temperature, chemical process that converts the mercury component in mixed waste to a non-hazardous final waste form suitable for land disposal. The process was developed by Nuclear Fuel Services, Inc. (NFS) to address elemental, ionic, and complex forms of mercury in mixed waste. NFS has applied the chemistry specific to their process over a variety of processing configurations for different waste matrices [70] (i.e., shred/slurry treatment for debris, damp blending treatment for soils, decontamination treatment for non-shreddable debris, and batch treatment of bulk elemental mercury). The NFS process consists of a two-stage treatment that addresses the treatment of elemental or ionic mercury species alone or in combination. The general features of the DeHg process [71] are depicted in figure.17. The process uses standard equipment connected in typical fashion. The first stage of the process involves amalgamation of the elemental mercury component (if present). Before amalgamation, sample preparation (shredding, grinding or slurrying) may be necessary, depending on the capability of the mixing equipment to be used. The second stage of the process is the stabilization of soluble mercury species using a proprietary reagent. This reagent has the capability to free mercury from stable form. Sulfur polymer cement offers some potential for mercury stabilization. However, this process is sensitive to water content of the subject material and requires elevated temperature for application. Sulfur polymer cement would be as useful as other competing technologies, such as the DeHg process, given the high water content and the relatively low decomposition temperature of ion-exchange material. Nuclear Fuel Services, Inc. (NFS) focus on mixed waste mainly generated from nuclear fuel production, high-enriched Uranium recovery/conversion, decommissioning and decontamination (D&D), environmental services and process development/metals recovery mercury Mixed Waste treatability treatment

facilities. Mercury mixed waste had consisted mainly metal like lead, nickel, chromium, mercury and zinc. There was no specific radioactivity data available at the moment [72].

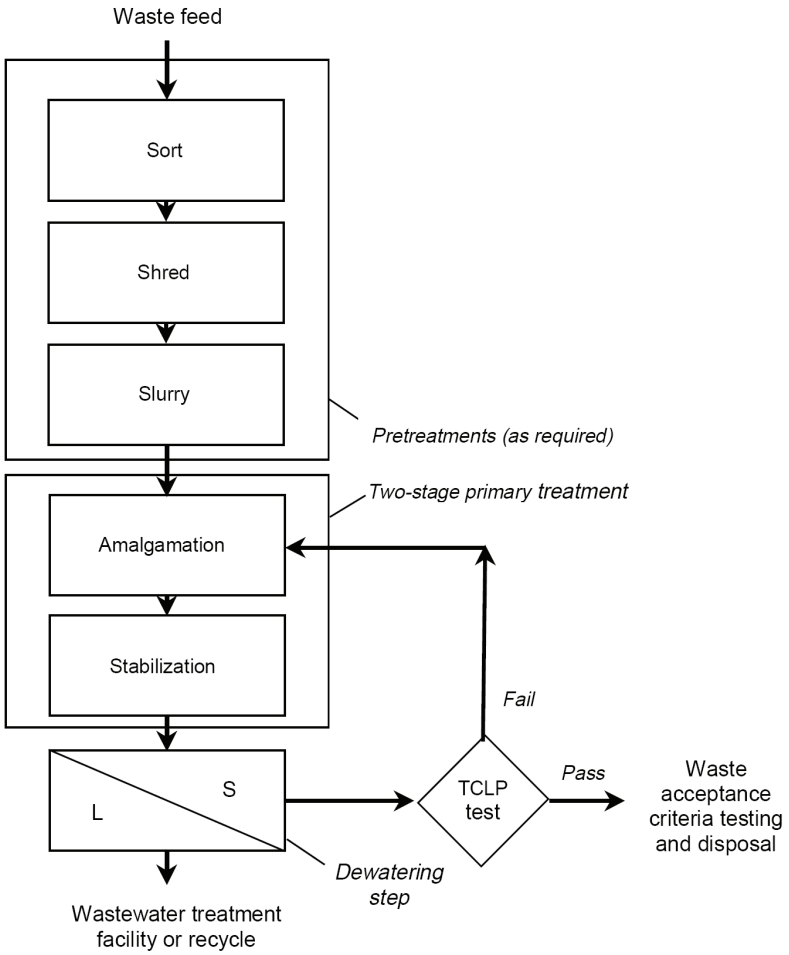

Figure 17: Block flow diagram of NFS DeHg process

ADA Technologies, Inc. (ADA) and its subcontractors demonstrated a process for stabilizing radioactively contaminated elemental mercury with sulfur [72]. The process combines and mixes waste mercury with sulfur in a commercially available pug mill to produce a stable mercury sulfide product. Initial testing was performed on surrogate waste, followed by

demonstrations on two actual mixed waste streams. ADA's treatment of liquid mercury involves adding powdered sulfur and mercury to the pug mill. As the mill continues to mix and reactions take place, additional chemicals are added. The temperature of the mixture is monitored, and samples are taken periodically and analyzed on their mercury content. Processing is performed at ambient conditions without the addition of heat. Water vapor and heat are evolved during processing. Room air is swept over the pug mill and then filtered to remove mercury vapors from the mixing area. The pug mill is manually decontaminated after processing each waste stream. ADA's sulfur treatment process was successfully demonstrated. By use of a proprietary additive mixture the process achieved a more than 90% completion of reaction and met vapor pressure requirements. The final waste product consistently achieved toxic characteristic leaching procedure (TCLP) results below 0.1 mg/L. The pug mill is well-suited to the mercury and sulfur mixing process because of its ability to adequately mix the components and control the residence time to ensure complete reaction. Moreover, the process demonstrated the use of a commercially available mixer. Radioactive contamination control requirements were readily implemented using the pug mill. This process is easily scalable to match the treatment needs at individual DOE (department of energy) sites. Consequently, the primary technical issue associated with the amalgamation of mixed waste mercury was related to scale-up of the process to a cost-effective operations level.

However, it was mentioned in previous paragraphs that an alternative of the amalgam process is the mercury sulfide process (produces more stable solid compound of mercury). In the following paragraphs, merits and demerits of mercury sulfide processes are described in more technical and chemical handling aspects for a final disposal point of view.

Formerly the formation of mercury sulfide from elements (called dry process) was done in a laboratory scale by stirring elemental sulfur powder and elemental mercury in various portions at 200℃ [Oji et al. 1998][73] and at 40℃ [Fuhrmann et al. 2002][74]. There are many chemical processes available for formation mercury sulfide like wet precipitation, adsorption, ion exchange treatment, chemical reduction and membrane separation as emerging technologies. One of the most established approaches is precipitation. The most commonly reported precipitation method is sulfide precipitation by a chemical mixing process as mentioned before. This process advantage is that it forms easily low soluble mercury sulfide (HgS). In these processes, conversion of mercury was not 100%. Unloading and failure of the reactor's stirrer question the safety of the chemical process. Recently Svensson et al. reported a room temperature process for formation of mercury sulfide from different mercury and sulfur sources [75]. They found that mercury sulfide under alkaline conditions

has maximum formation. Highest yields were observed for the samples containing elemental sulfur where both elemental mercury and mercury oxide were transformed into HgS. Sulfur may disproportionate into S (-II) and S (+VI) under anaerobic conditions, which lead to more efficient sulfide penetration whereas aerobic conditions lead to increased oxidation and content of sulphate, e.g. through following equations 3 and 4:

$$4S_{(S)} + 3Hg^{\circ} + 3/2O_2 + H_2O \longleftrightarrow 3HgS + SO_4^{2-} + 2H^+ \quad \Delta G^{\circ} = -645\ KJ/mol \longrightarrow \quad (3)$$

$$4S_{(S)} + 3HgO + H_2O \longleftrightarrow 3HgS + SO_4^{2-} + 2H^+ \quad \Delta G^{\circ} = -471\ KJ/mol \longrightarrow \quad (4)$$

The reactions are both thermodynamically favorable. The stoichometric ratio between Hg and S is important for optimal formation of HgS. There is an alternative method of producing the HgS, in which cinnabar precipitates from solutions. In this process, solutions containing Hg^+ and Hg^{2+} ($HgNO_3.2H_2O$ or $HgCl_2$) are treated with a gas phase H_2S at low temperatures, by stabile mercury sulfide formation followed by filtration step. Here one important aspect about the process is the gas phase involvement and thus controlling the reaction is difficult. That makes complications during handling of activated mercury. However, it is still under the investigation to continuation for the next steps. In addition, mercury-selenide (HgSe) is also under investigation, because it has similar properties as HgS and is the most insoluble compound of mercury. However, it is a more toxic chemical compound in handling. These methods have to be considered under irradiation aspects, long term stability of final form of mercury, chemical process engineering safety as important factors.

2.6. Immobilization by encapsulation techniques

As element, mercury cannot be destroyed but it can be converted into less soluble or leachable forms to inhibit its migration to environment after disposal. Encapsulation technologies are based primarily on solidification processes that to substantially reduce surface exposure to potential leaching media. Encapsulation technologies can also involve combination of physical entrapment through solidification and chemical stabilization through precipitation, adsorption or other interactions. Sometimes these processes are combined [76]. Conventional stabilization/solidification methods typically include the fixation of metals using Ordinary Portland cement (OPC) and fly ash or slag material. This produces an impermeable, solid waste form at high pH that limits the solubility and leachability of most metals[18]. However, it is very difficult to stabilize mercury in elemental or other mercury forms with cement based processes because it doesn't form a low soluble hydroxide.

Mercury is difficult to treat as elemental metal in solid waste. Stabilization/solidification (S/S) technologies have been proven to be effective in immobilizing of other heavy metals, such as Pb, Cd and Cr, but difficulties have been encountered to stabilize/solidify elemental mercury because of noble behavior [77]. The immobilization of mercury by solidification/stabilization involves its conversion to a stable immobile form. The role of Portland cements in nuclear waste and in other waste treatments are discussed in following chapters.

2.6.1. Solidification/stabilization in a cement matrix

Nuclear wastes can be broadly categorized as high, medium, low level, and different techniques are required for encapsulation for disposal. These wastes are frequently wet and difficult to dry. This forces the need for a water-tolerant containment matrix, and so cement is viewed as material for the choice. It is likely to be the major component in immobilization of low and medium level radioactive waste in underground repositories, as both a solidification matrix and as backfill and construction material. Favored techniques entail the encapsulation of waste by cement in containers such as steel drums [78]. The exact method used depends on the nature of waste. Firstly, cement acts as physical barrier from waste migration into biosphere because cement provides physical strength to the repository, and inhibits ground water through flow. And also the more important feature is that cement acts as chemical barrier. When cement clinker is hydrated, excess water is used to ensure that freshly mixed slurry is plastic and workable. The aqueous phase of cement is high pH, and it is this feature which makes cement so suitable for waste immobilization, as many radionuclides have reduced solubility at higher pH [79]. Furthermore, the microporosity, i.e. the high surface area of cement inhibits the transport of radionuclides out of the repository by adsorption onto surfaces. It is anticipated that the pH will decrease over time, both as result of leaching of soluble ions by groundwater and chemical attack by aggressive species such as sulfate, chloride, and magnesium. Major cement hydrate phases such $Ca(OH)_2$, C-S-H (calcium silicate hydrate), C_3Al_6 (tri calcium aluminum silicate) will be effected by aggressive ions as SO_4^{2-}, Cl^- and following degradation of cement waste form. Poon et al. (1985) found that the retention potential of the cement matrix for mercury was related to the amount of calcium in the solidified waste. Mcwhinney et al. (1990) also found evidence of close association of calcium rich deposits with mercury, and strongly supposed that physical sorption processes were closely associated with the calcium content and were mainly responsible for mercury containment in the cement matrix [48]. Poon and coworkers (1986) identified a mechanism that consisted of a combination of chemical fixation and a physical isolation process that was responsible for the containment of mercury waste form as amalgam in the cement matrix

[61]. Yang (2002) successfully solidified a mercury containing sludge using a commercially available sludge treatment agent, which was a cement-based binder with some proprietary additives. Physical and chemical durability tests were also conducted on the solidified monolith. Much more mercury was leached out after physical durability tests, which showed the significance of physical encapsulation. Therefore, it is suggested that cement-based systems alone may not fix mercury in a stable form, due to the complicated chemistry of mercury (Conner, 1990) [79]. Roy et al. (1992) [80] used a variety of microscopic and X-ray diffractive techniques to study the microstructure and microchemistry of a mercury containing sludge that had been solidified/ stabilized in ordinary Portland cement (OPC) [80]. They were unable to detect any mercury in their solidified/stabilized samples. Hamilton and Bowers (1997) attributed this to the unique potential of mercury to volatilize [81]. They investigated Hg emissions from the finished solidified/stabilized cement monolith and found that HgS showed no propensity to volatilize, while HgO or Hg^0 (liquid) led to the evolution of Hg vapor. These materials have to be studied more precisely under irradiation conditions of with impregnated mercury waste as HgS. At least it can infer from literature data that cement process could be simple and it is economical factor for final disposal cost estimation.

2.6.2. Material for immobilizing nuclear wastes

The primary objective of these encapsulation technologies is to immobilize physically the wastes to prevent contact with leaching agents or water ingress is regarded as accident scenario. Because this cannot be completely fulfilled some times by cement it self. But significant research has gone into development of other encapsulation materials that can be used as alternatives the cement-based process. Sulfur polymer stabilization or polymer stabilization/solidification (SPSS), chemical bonded phosphate ceramic (CBPC) encapsulation, and polyethylene encapsulation are few technologies that currently being tested and used to improve the long term stability of hazardous wastes [82]. Recently polysiloxanes or ceramic silicon foams (CSF) are also considered for long-term storage of low and intermediate level radioactive wastes. These materials are considered seriously in nuclear-waste processing operations. Silicon elastomers (polysiloxane materials) are based on silicon and oxygen with organic substitutes, have very good chemical, thermal and radiation stabilities to waste for long-term storage and disposal. Especially to immobilize elemental mercury, mercury-containing debris, and other mercury-contaminated wastes, there is always the problem of mercury vaporization. Therefore it is always an advantage to work at low temperature for mercury waste treatment process.

2.6.3. Polysiloxanes in nuclear waste management

Before discussing the application of polysiloxane as encapsulating material, it is good to know some basic information about polysiloxane materials and how they did arrive in nuclear waste field. Polysiloxane is a part of inorganic and part by thermosetting polymer. Once formed, the material consists of about 50% vinyl-polydimethyl-siloxane, 20% quartz (used as filler material), 25% proprietary ingredients, and <5% water. The basic polysiloxane process involves simple mixing of the base polysiloxane materials with the mixed waste in a mixer. This is followed by extruding the waste blend outside of the mixer while adding a platinum catalyst. The addition of the catalyst starts a silicon polymerization process, which results in a solid waste monolith upon curing. In terms of basic chemistry principles, polysiloxane is formed not unlike common Room Temperature Vulcanizing (RTV) of silicone foam sealants. The basic liquid chemicals SiH and SiOH (like shown in the equation 5) are thoroughly mixed with the waste and react in the presence of the catalyst to form the desired thermosetting polymer and hydrogen gas. The fundamental chemical formulation is as follows:

$$R_3SiH + R_3SiOH \longrightarrow (\text{--}R_2Si - O - Si\,R_2 \text{ -- })_N + H_2(g) \longrightarrow \qquad (5)$$

The goal is to provide sufficient mixing and cure time to allow the polymer chain to be formed around the waste at a micro level and thereby create a barrier between the waste and the environment. Examples are as follows:

Originally polysiloxane was investigated in Russia for filling material in the destroyed Chernobyl reactor. It is important to mention that Polysiloxane materials as matrices were tested first time at laboratory scale in western countries. FZ Juelich had also done some seriously investigations relevant to long term stability in connection to containers/casks for transport, interim storage, and final disposal of nuclear waste and nuclear fuel [83]. The risk dominating accident in most European repositories is water ingress. These polysiloxane encapsulation techniques are used for experimental investigation for immobilization of the mercury waste in this report.

Throughout the US Department of Energy (DOE) Complex there are large inventories of homogeneous mixed waste solids, such as soils, fly ashes, and sludges that contain relatively high concentrations (greater than 15% by weight) of salts. The inherent solubility of salts makes traditional treatment of these waste streams difficult, expensive, and challenging. Many of these materials are in a dry granular form and are the by-product of

solidifying spent acidic and metal solutions used to recover and reformulate nuclear weapons materials over the past 50 years.

At the Idaho National Engineering and Environmental Laboratory in USA (INEEL), there are approximately 8000 m^3 of salts (potassium and sodium nitrate) stored above ground only with earthen cover. One of the obvious treatment solutions for these wastes is to immobilize the hazardous components to meet US Environmental Protection Agency's stringent requirements.

One proposed solution is to use thermal treatment via melting / vitrification to immobilize the hazardous component and thereby substantially reduce the volume, as well as provide exceptional immobility. However, these electrode smelter systems involve expensive capital apparatus with complicated off gas systems. In addition, the vitrification of high salt waste may cause foaming, vaporization problems and usually requires extensive development to specify glass formulation recipes. As an alternative to thermal treatments, stabilization of these materials in cementitious grouts has also been widely employed earlier. However, salts interfere with the basic hydration reactions of cement, leading to an inadequate set or deterioration of the waste form over time. Sufficient and compliant stabilization in cement can be achieved by lowering waste loadings, but this involves a large and costly increase in the volume of material requiring handling, transporting, and disposal. As a consequence of these stabilization deficiencies associated with soluble salt containing mixed wastes, the Mixed Waste Focus Area (MWFA), a DOE program, sponsored the development of low-temperature stabilization methods as an alternative to cement grouting. One alternative is microencapsulation by polysiloxane, which in some applications provides higher waste loadings and a more durable waste form than the baseline method of cementitious grouting.
[Some introducing sentences for the next 7 points is required]

- ✓ Potential ability to adequately (i.e., comply with disposal requirements) encapsulate/stabilize salt
- ✓ Containing wastes at higher waste loadings then conventional Portland cement,
- ✓ Broad applicability to the many different types of wastes,
- ✓ Elimination of potential subsidence upon burial,
- ✓ Low cost treatment that uses no large equipment,
- ✓ Low temperatures, low emissions, and minimal secondary waste,
- ✓ Ability to control cure time.

The use of this polysiloxane material for encapsulation is patented by Orbit Technologies. The polysiloxane technology was demonstrated on salt waste surrogates, which were spiked with lead, mercury, cadmium, and chromium at 1,000 ppm levels. Up to 50 wt% waste loading was demonstrated. The final waste form had a compressive strength of 600 psi at 40 wt% loading. For high chloride salt wastes, the mercury toxic characteristic leaching procedure (TCLP) was 0.01 mg/L and for high nitrate salt wastes the mercury TCLP was 0.06 mg/L. The final waste forms for both waste types did not pass for chromium. The authors recommend pretreatment for the chemical stabilization of wastes with metals at levels greater than 500 ppm (DOE, 1999c). In addition, Miller et al. (2000) reports on the use of silicone foam to encapsulate a DOE surrogate waste containing high levels of chromium. Salt waste loadings of up to 48 wt% were achieved in their study.

These polysiloxane materials and their supportive materials play a crucial role in nuclear waste storage and as coating materials in stabilization/solidification (S/S) of mercury wastes. Recently different polysiloxane materials were also investigated under γ-irradiation as coating material for fuel elements in FZ Juelich and shown very good stability towards radiation [84].

Zhang and Bishop (2002) [85] used powdered reactivated carbon (PAC), along with Portland cement, to encapsulate mercury-contaminated wastes. Surrogate wastes were created with up to 1000 mg/kg of mercury using sand, water, and $Hg(NO_3)_2$. These wastes were mixed with PAC and then solidified with Portland cement. The wastes were successfully treated to below the U.S. EPA TCLP limit for mercury. In addition, it was determined that pretreating the PAC with CS_2 increased its adsorption capacity for mercury by a factor of 10 – 100 times depending on pH conditions. In the following chapters, real behavior of mercury waste as HgS, HgSe, with and without cement matrix and in alternative matrix form like polysiloxane under aggress leaching conditions and irradiation behaviors are discussed.

3. Experimental section

3.1. Introduction

The main objective of present work was to undertake the experimental work and develop economical and feasible waste management strategy for proton irradiated mercury generated from spallation sources like EURISOL, ESS and other similar facilities. A major part of the work was to select stable mercury compounds and study their stability under irradiation relevant to disposal conditions.

3.2. Experimental details

All these investigations were aiming to the possibility to compare stable compounds of mercury from a long term point of view with available resources and technologies of interest in the relevant geological media of practical importance for radioactive waste disposal. It is very important for comparing these results obtained from different experiments, performed under a range of conditions relevant to anticipated repository environments.

3.2.1. Reagents and materials

Elemental mercury (Hg^0), mercury sulfide (called as Cinnabar, red powder, HgS), mercury selenide (HgSe), mercurous nitrate ($Hg_2(NO_3)_2$. $2H_2O$) and mercuric nitrate ($Hg(NO_3)_2 \cdot H_2O$) were used in these present investigations and were provided by Merck, Darmstadt. They were of analytical grade of 99.6 % purity level and were used without any pretreatment for preliminary experiments. For amalgam preparation, crystalline powders, 8-20 mesh, ≥99.99% silver and copper, were used and were provided by Sigma Aldrich, Germany.

The chemicals like ammonium sulfide $(NH_4)_2S$ solution (wt.45%) and concentrated nitric acid were provided by Merck, Darmstadt and were diluted to respective standard solution molar concentrations before using for experiments. The cement type used was an ordinary Portland cement (OPC) (CEM I 52.5 R) manufactured by German Portland cement firm. In our present studies polysiloxane compound type (RT 622 Elastomer® with catalyst from Wacker Chemie GmbH, Germany) was used because it had better alcohol condensation properties compared to other type of polysiloxanes.

3.2.2. Preparation of salt brines

For long-term safety assessments of the final repository, different accident scenarios must be taken into account. One such scenario assumes groundwater penetration into the repository, accompanied by the formation of highly saturated salt brines. Compositions of naturally occurring saline solutions have variable concentrations of the main components and are controlled by temperature-dependent salt/solution equilibrium within the six-component Na-K-Ca-Mg-Cl-SO_4 system of oceanic salts. Most salt brines are saturated with halite. However, Mg-rich brines were also found during underground investigation of the Gorleben site. Commonly, three different types of highly concentrated salt brines are taken into account as relevant for the Gorleben salt dome repository. Similarly the geochemistry of the Opalinus Clay pore water represents an important scientific basis for predicting the behavior of radionuclides from deep geological repository for radioactive waste following their release into the Opalinus Clay at the Mont Terri in Northern Switzerland.

In the present work, two salt brines (Brine-2 and Brine-3), opalinus clay water and deionised waters were selected as leachates. The compositions of the leachant solutions are shown in the following table-8. Per one liter of salt brine the following salt amounts in grams were used:

Compound	Brine-2 [g/l]	Brine-3 [g/l]	Clay* water [g/l]
$MgCl_2\ 6H_2O$	937.08	-	3.457
$MgSO_4$	0.615	1.953	-
NaCl	4.13	309.4	12.38
KCl	1.42	-	0.12
$CaCl_2\ 2H_2O$	39.68	2.74	3.793
K_2SO_4	-	2.83	-
Na_2SO_4	-	2.63	2
$SrCl_2\ 6H_2O$	-	-	0.136
$NaHCO_3$	-	-	0.04
			*Opalinus clay water

Table 8: Composition of salt brines used for leaching experiments (*Opalinus clay water)

After complete dissolution of salts in deionised water at 70℃, the solution was cooled down to room temperature and its volume was adjusted to 1L in a volumetric flask.

3.3. Analytical instruments

Optical microscope (KS300)	Karl Zeiss KS300 with image processing software
SEM, EDX	JEOL JSM 840 coupled with Tractor Northern 5502
XRD	Stoe Stadi transmission diffractometer, Co-anode (CoK_α line, λ = 0.178897 nm)
Mercury analyzer ICP-MS	A Perkin-Elmer analyst 300 cold atomic absorption spectrophotometer equipped with FIMS (Flow Injection Mercury system
Raman spectrometer	PerkinElmer® Raman Station™ 400
BET	Quanta chrome Monosorb (BET) surface analyzer
Desiccator	Heraeus T-12
pH and Eh meter	Metrohm 691 pH meter
pH electrode	Orion 8103 ROSS combination pH electrode
Eh-electrode	Metrohm 6.0412.100 Pt electrode
Centrifuge	Heraeus Christ Laborfuge 15000
Analytical balance	Chyo JL-200
Digital calliper	TESA DIGIT CAL Capa calliper
Polishing machine	Struers RotoPol-22 with RotoForce-4 head
Water purification	Elga Elgastat maxima HPLC (The specific resistance of purified water is 18.2 mΩ)

3.4. Leaching experiments and sample preparation

3.4.1. Leaching experiment sample preparation using solid mercury compounds

For the leaching, commercial solid mercury compounds were selected on solubility based at standard room temperature conditions. Mercury compounds were mercury sulfide (HgS), mercury selenide (HgSe), mercury (I) nitrate, silver amalgam and copper amalgam. The aqueous solutions selected for leaching experiments are shown in table-8. The specimens (1 gram of mercury compounds) were transferred to 30 ml volume glass ampoules containing 10 ml of leaching solution, sealed and mixed thoroughly. The glass ampoules were evacuated first for anaerobic tests and then were filled with argon gas before they were

sealed by melting. The glass ampoules for aerobic tests contained air. This specific equipment was designed by Fachinger et al. and installed at FZJ hot cell laboratory. This equipment was used to evacuate and to fill argon gas in the glass ampoules. It is shown in following figure 18. Again the solutions for leaching experiments were degasified prior to experiments in vacuum and then argon saturated by bubbling. Then the glass ampoule's upper portion was removed by glass melting procedure to keep the experiment under argon gas during leaching experimental time.

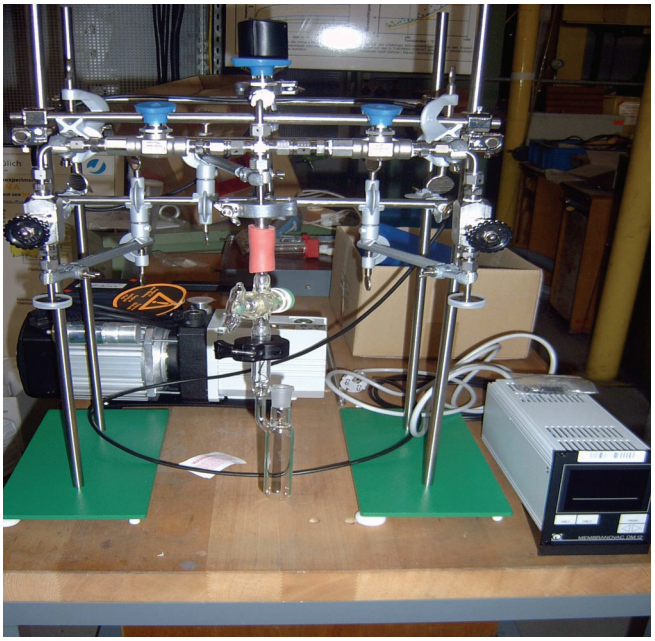

Figure 18: Evacuation and gas filling equipment for glass ampoules

3.4.2. Preparation of cement-mercury compounds as matrices

The chemical composition of Ordinary Portland Cement (OPC) used in our experiments is shown in table-9. It is used in pure form without pretreatment and mixed with sand (50-20 mesh passed) and a sand to cement ratio of 4. Cement to mercury compounds (HgS, HeSe, Hg (I) nitrate) ratio of 10, 3 and 2 were used during our experiments. A constant water-cement ratio (0.4) was used for cement pastes preparation. Cement pastes were hydrated 28

days in 98% relative humidity at 20±2℃ in cylindri cal form in plastic bottles. After 28 days curing time, the plastic caps were removed and were analyzed for chemical composition. Then these hardened cement mercury matrix samples were used in leaching experimental studies both for irradiation experiments and non-irradiation leaching experiments.

As described in chapter 3.4.1, the solutions were degasified prior to experiments in vacuum and then saturated with argon by bubbling. Then the glass ampoule's upper portion was prepared in the way such that cylindrical samples (1.5cm X 1.5cm X 4cm) fit into it directly. The upper part was removed by glass melting procedure to keep argon gas during leach experimental time. The leacheant solutions were collected to measure pH and the Hg concentrations to determine the leach rate cement –mercury matrix.

CaO	SiO_2	Al_2O_3	MgO	Fe_2O_3	SO_3	$CaSO_4$	Specific gravity	Specific surface area cm^2/g
65	22	5.1	1.4	3.2	1.6	3.1	3.17	3220

Table 9: Typical composition Ordinary Portland cement type (CEM I 52. 5 R) in wt %

3.4.3. Preparation of Polysiloxane-mercury compounds as matrix form

A general proof was performed earlier to investigate the use of polysiloxane material for coating and encapsulation/stabilization of burnt up fuel elements and nuclear waste at FZJ. The present experimental study is encapsulating three different mercury final waste forms in polysiloxane material and performing a variety of leaching, compressive strength, and durability tests on the final waste forms. In present studies polysiloxane compound type RT 622 Elastomer® with catalyst and mercury compounds (HgS, HgSe and cement matrix) were used for the preparation of polysiloxane matrices [86].

ELASTOSIL® RT 622 is a pourable, addition-curing two-component silicone rubber that vulcanizes at room temperature. It has better alcohol condensation and prevents any moisture formation during curing time. Some physical properties information is shown in the

following table-10 (uncured and cured). As it is shown, two components of polysiloxane material were mixed thoroughly in order to make a homogeneous phase at room temperature. Then HgS and HgSe (0.02 g/g of polysiloxane) were introduced in two component mixture and stirred again till uniformly mixed. The samples were placed in plastic capsules for curing. Samples were cured at room temperature for 48 hr.

Some cured samples were taken again for second coating to cover the outer surface with pure polysiloxane surface for resistance against ground water. Scanning Electron Microscope (SEM) studies were performed on polysiloxane specimens for mercury distribution in waste loading.

Property (uncured)	**Value**	
component	**A**	**B (catalyst)**
Appearance	**White**	**Reddish brown**
Viscosity at 23℃ [mPa. S]	**18000**	**800**
Density at 23℃ [g/cm ^{3}]	**1.14**	**1.01**
Cured		
Mixing ratio	**1:9**	
Appearance	**Light reddish brown**	
Density at 23℃ [g/cm ^{3}]	**1.01**	
Hardness	**27**	
Tensile strength [N/mm^2]	**6.5**	
Elongation at break [%]	**550**	

Table 10: Properties of polysiloxane type ELASTOSIL® RT 622

3.5. Leaching experiments under irradiation

In the present work, sequential leaching experiments with un-irradiated mercury waste form, Hg-cement matrix form under γ-irradiation were performed. More over the mercury waste form behavior in different conditions like oxidizing and reducing conditions were also investigated. All experiments were conducted under argon atmosphere to simulate the anaerobic conditions of the final repository. The experimental temperature was chosen to be 50-60℃, representing the conservative case of geol ogical depth temperature in repositories more than 1000m depth.

An overview of the experiments carried out is presented in table-11 and the procedure of each experiment is described in detail in the following chapters. The solutions for leaching experiments, either deionised water, salt brines or acidic solutions, were degasified prior to experiments in vacuum and then argon-saturated by bubbling as described before (chapter 3.4.1 and 3.4.2). The leaching experiments were performed in glass vessels with Teflon gas valves (except for experiments under γ- irradiation), which were pre-treated several times by 1M HNO_3 for at least 24 hours, followed by careful rinsing with deionised water. After loading the vessels were purged by argon (in the case of irradiation experiments the loading was performed in a glove bag under argon atmosphere), tightly closed and placed in a desiccator maintaining the temperature of 50-60 ℃. The pH of the solutions before and after experiments was measured at the experimental temperature under a continuous flow of argon. Before the measurements, the pH electrode was calibrated at the same temperature against two suitable buffer solutions from the set of buffers for pH 4, 7 and 10. The correction for pH values measured in highly concentrated salt brines was applied.

In order to investigate the influence of aqueous phase radiolysis on the leachability of waste forms of mercury, the leaching experiments with frequent sampling at least 60 days during first phase under γ-irradiation were performed in the MTR (Material Testing Reactor) cooling pool of the FRJ II (DIDO). The glass vessels were loaded with mercury final waste as HgS, HgSe and cement matrix form filled with 10 ml of deionised water or salt brines, and closed with screw caps. The initial surface to volume ratio of about 5 m^{-1}, similar in experiments without irradiation, was selected to simplify the comparison between these experimental series. The PVC screw caps used had a fluorine-free silicon sealing and are relatively stable with respect to irradiation. However, the caps were replaced after each sampling.

Medium	T°C	HgS	HgSe	Hg(I) Nitrate	Hg-Cement matrix
DI Water	50-60	Γ, γ	Γ, γ	γ	γ
Brine-2	50-60	Γ, γ	Γ, γ	Γ, γ	Γ, γ
Brine-3	50-60	Γ, γ	Γ, γ	γ	γ
Opalinus clay water	50-60	Γ, γ	Γ, γ	γ	γ

Γ – Static and batch leaching experiments with mercury waste form for 6 months
γ – Leaching experiments under γ-irradiation (all doubled) for 3 months

Table 11: Overview of the leaching experiments

All irradiation experiments were performed in duplicate. The vessels were placed in a closed steel sample holder (figure 19a). The sample holders were surrounded by a heating jacket (figure 19b) and placed in a waterproof irradiation container. The mounted irradiation container with heater and sample holders is presented in figure 19c. The sealed irradiation container was placed under water between four MTR fuel elements, providing the γ-field (figure 19d). Then the container was heated up to 50-60 ℃ and kept at this temperature during the experiment.

The scheme of the irradiation container is shown in figure 21. Every two months, the heating was switched off, the container cooled down and taken out of the irradiation position. The reaction vessels were opened, and samples were taken and analyzed and new sample again were placed for new or for repetition of measurements. Thereafter, the container was lowered again and kept at 50-60 ℃ till the next sa mpling. After the third sampling (about 6-8 months), the experiments were stopped, the pH and Eh of solution were measured. Then the solutions were sent for total Hg-concentration analysis.

The dose rate at the location of the irradiation container was measured several times during the experiments. The doses are presented in figure 20 show that during the first two experimental periods as the mean dose rate approximately 1.5 kGy/h. During the third period the mean dose rate was somewhat lower, amounting to approximately 1.0 kGy/h. Most of

these experiments are non-conservative type experiments because the dose rates are decreasing time scale.

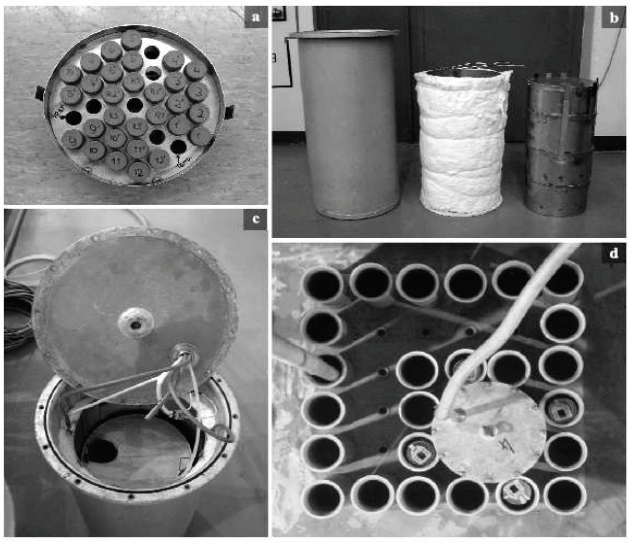

Figure 19: Experiments under γ-irradiation: reaction vessels in holder (a), container, heater and sample holders (b), mounted (c) and installed (d) container

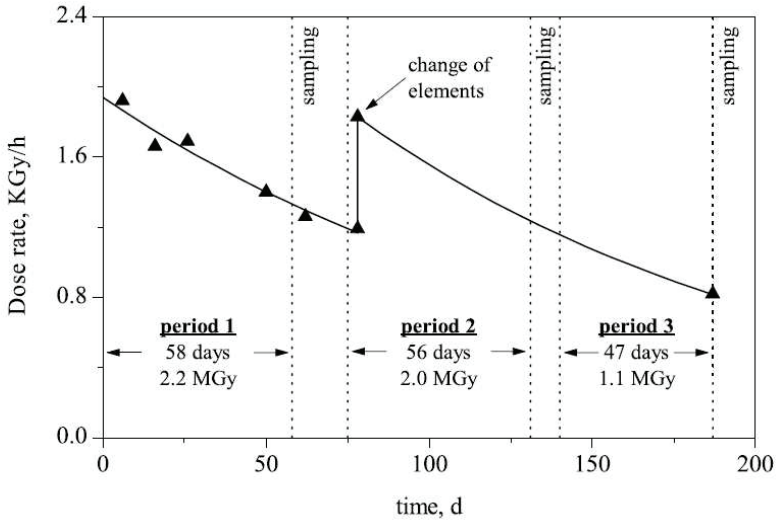

Figure 20: Evolution of average dose rate in irradiation experiments

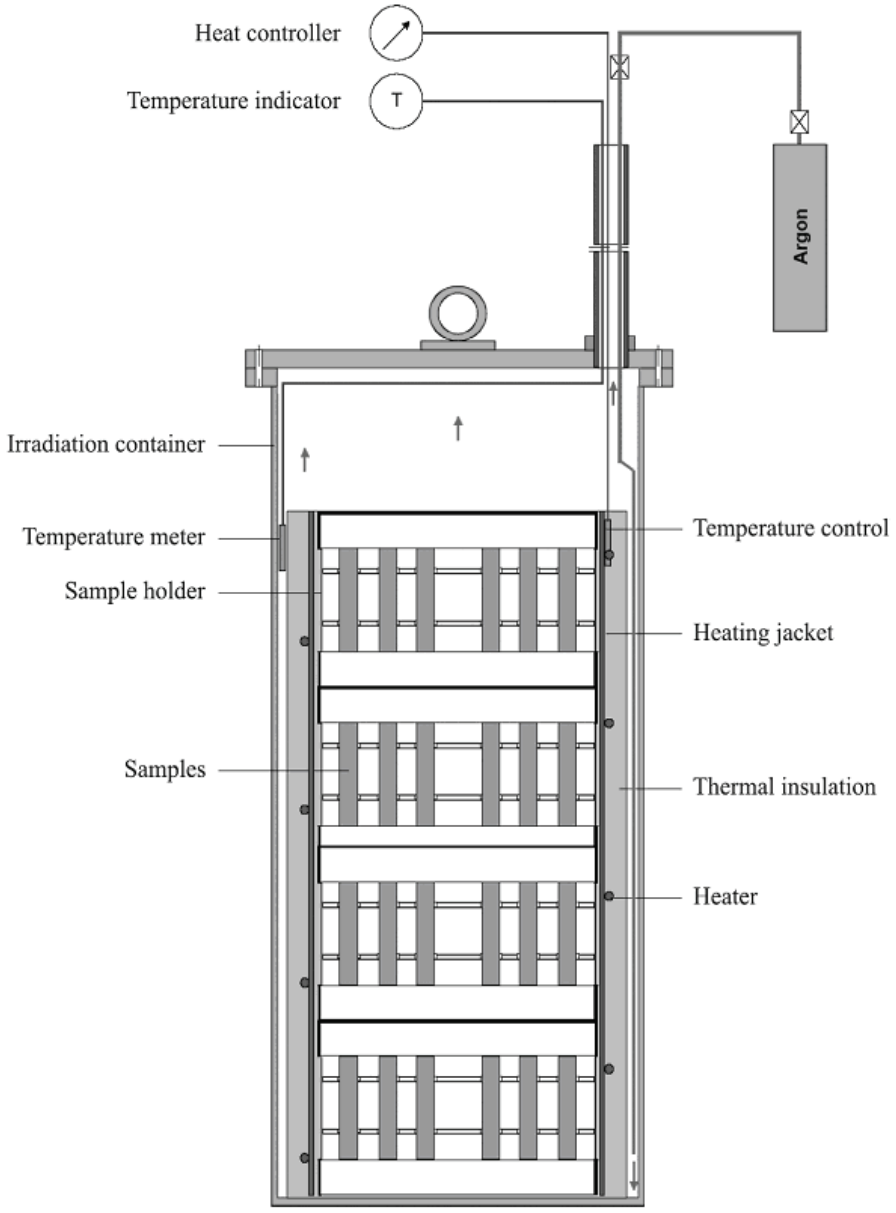

Figure 21: Irradiation container scheme

3.6. Batch leaching experiments

Polysiloxane-mercury waste matrices, mercury cement matrices and mercury solid compounds as HgS and HgSe were loaded into each vessel and they were filled with 50 ml of deionised water or salt brines. The surface to volume ratio (*S*/*V*) was constant for all experiments, amounting to 8 m^{-1}. All experimental sets were accompanied by blank tests. A set of leaching experiments at room temperature and at 50-60℃ in the oven were performed (shown in figure 22). These non irradiation experiments were carried out for a period of about one year for Hg-cement matrices, HgS and HgSe samples and 6 weeks for polysiloxane samples. After specific experimentation time, the vessels were opened and leachates and analyzed as described in previous chapters. Additionally, the samples were filtered and dried for a week in a desiccator and then analyzed to check the surface and phase changes by scanning electron microscopy (SEM) and X-ray diffractometry (XRD). Total mercury concentration was analyzed by flow injection cold vapor atomic absorption spectrophotometer. The pH of samples was measured with a glass electrode calibrated in the range pH 4 to 7, pH 7 to 10 and pH 10 to 12.

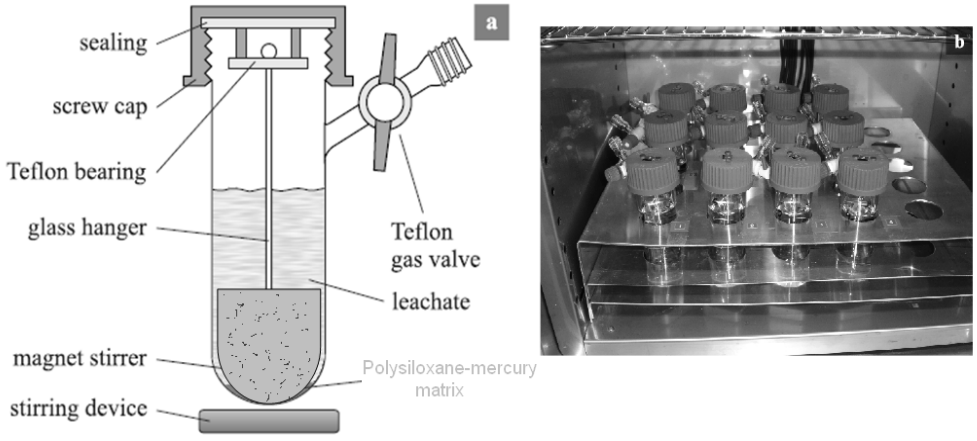

Figure 22: a) Reaction vessel with polysiloxane sample and b) set of leaching experiments in an oven

3.7. Methods and Procedures for the stabilization / solidification

The aim of current experiments was to investigate the low cost solidification/stabilization methods for the elemental mercury, i.e. transform elemental mercury to chemical insoluble mercury forms. Specifically these investigations were concentrated mainly to assess conditions for the formation of mercury sulfide (red sulfide, cinnabar, HgS) at room temperature from elemental mercury.

3.7.1. Formation of cinnabar

One of the more commonly reported precipitation methods for removal of inorganic mercury from waste water is sulfide precipitation. The same sulfide precipitation technique was used here (e.g., as hydrogen sulfide or another sulfide salt) to convert the soluble mercury compound to the relatively insoluble mercury sulfide form.

The following two solidification variables were investigated: ratio of HNO_3/mercury (Hg^0) and $(NH_4)_2S$ /mercury (Hg^0) for complete conversion of elemental mercury (Hg^0) to mercury sulfide (HgS). Initial solidification/stabilization reactions were started with elemental mercury and concentrated nitric acid (conc. HNO_3). All reactions were investigated with different ratios of Hg^0/Acid. At first concentrated HNO_3 was diluted and prepared in different standard molar solutions (1 - 5 molar solutions). Then HNO_3/mercury (Hg^0) molar ratios used were 1, 1.5, 2, 2.5, 3, 3.5, 4, 4.5 and 5. A respective amount of nitric acid was taken in a glass vessel and placed in a cooling tank filled with ice. The acid solution was cooled for more than 3 hr to maintain a temperature of 0-3℃. Then a respective amount of elemental mercury (Hg^0) was added drop by drop to reaction vessel to be oxidized to mercury (I) nitrate (mercurous nitrate). It was mixed 8 hrs at constant pH of 2.5 under cooling. Before the neutralization step, the samples were analyzed for mercurous nitrate concentration in solutions by Raman spectrometry.

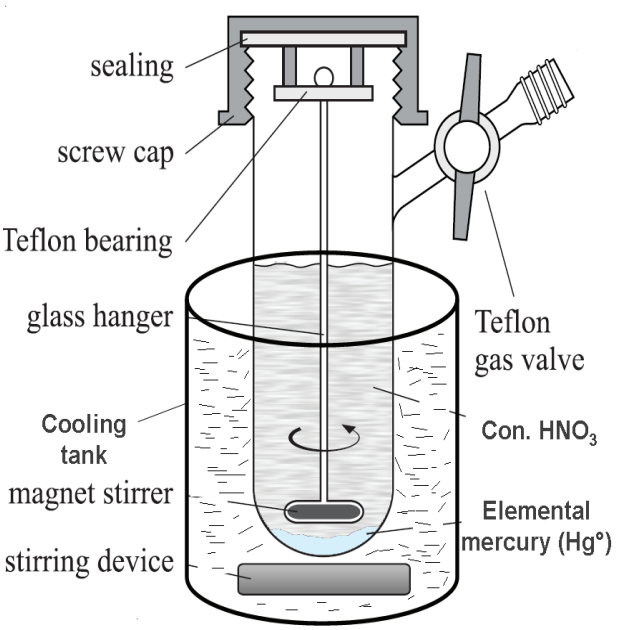

Figure 23: Preliminary batch reactor vessel set up for preparation of HgS from Nitric acid.

For secondary precipitation experiments, reagent-grade chemical ammonium sulfide $(NH_4)_2S$ solution (w/w 45 %) was used to transform the Hg(I) to Hg(II) oxidation state as in HgS or mercury sulfide. Here also the same $(NH_4)_2S$ /mercury (Hg°) molar ratios used were 1, 1.5, 2, 2.5, 3, 3.5, 4, 4.5 and 5 for precipitation experiments. The reaction times investigated were 2, 4, 8, 12 and 24 hrs with different $(NH_4)_2S$ /mercury (Hg°) ratio. Respective amount of Hg (I) nitrate was taken in glass vessel and placed on a hot plate which was preheated to a temperature of 45-50℃. Then a respective molar amo unt of ammonium sulfide $(NH_4)_2S$ solution (w/w 45 %) was added to the reaction vessel to precipitate the mercury sulfide. The reaction was taken about 2-4hrs for secondary precipitation at pH 8-9.5 and at a temperature of 45-50℃. After complete precipitation, the mixtu re was filtered through 0.45µm filters. The filtrate was analyzed for mercury concentration, and the solid part was dried in oven 25-30℃ for solidification. Then dried samples were analyzed for mercury and sulfur by XRD and XRF characterization techniques. Further experimental details and process design information are going to be in discussed in results and discussions part.

4. Results and discussions

4.1. Leaching experiments for mercury compounds

4.1.1. Performance comparison of leaching samples

The purpose of this work is to study the solubility of mercury compounds (Hg^{2+}) in four different liquid leach solutions. The investigation includes how different parameters (time, pH and (Hg^{2+})/solution ratio) effect the distribution of oxidized species and Hg° in aqueous phase. As mentioned earlier (chapter 3.1.2) the three different inorganic mercury compounds used in the leaching experiments were with equal amount of Hg^{2+} standard to ensure that the measurements would not differ too much because of different leach solution composition.

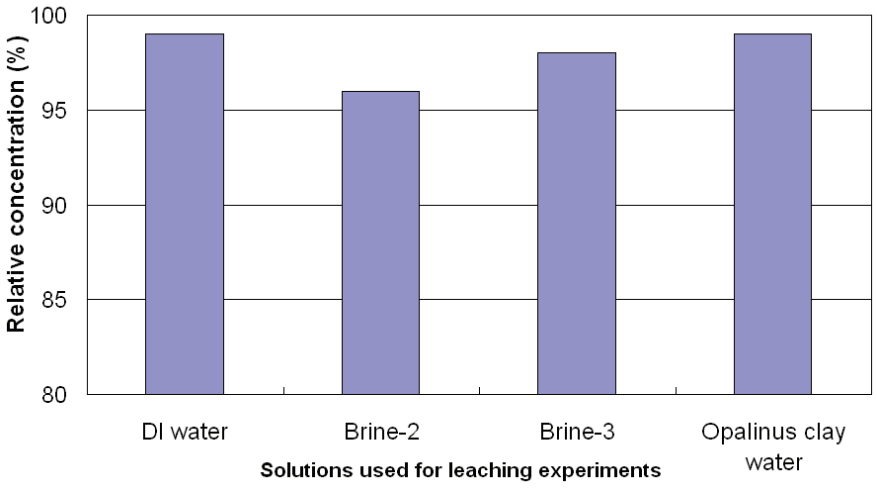

Figure 24: Relative comparison of added mercury compounds as Hg^{2+} in leaching solutions

Figure 24 visualizes the relative difference between Hg^{2+} concentrations in the four samples. A maximum of 2.3% in difference was observed between the samples. Hence, such a small difference can be neglected when comparing the solubility experiments. Because, the difference in solubility between mercury samples in solutions is in most cases of several orders of magnitude.

4.1.2. Limitations of mercury under radioactive disposal conditions

In Europe, each country has its own limitations to nuclide inventory relevant to dangerous nuclides solubility limit in ground water. An independent study at Konrad facility (a radioactive waste storage facility for non heat generating waste) had done some basic research on metallic waste migration to groundwater contamination. These studies showed that if 43.7 Kg Hg waste was contacted accidentally with deep group waters in equivalent volume of 10^6 m^3 about the time scale of 3000 years, the probable concentration of total concentration of mercury in ground water at surface level is 0.0044µg/l. In Germany, the total amount mercury allowable limit for Hg in ground water is 0.1µg/l. In repositories, a concentration up to 100µg/l is tolerable due to a requested multi barrier system.

4.1.3. Leaching experimental studies without γ-irradiation

Leaching experiments in different aqueous phases under argon atmosphere without γ-irradiation lasted for 6 weeks in sealed glass ampoules at room temperature as described in the chapter 3.4.1. After this time, the samples from the glass ampoules were taken out by breaking the seal and analyzed for mercury concentration in solutions. Our experimental results of mercury sulfide (HgS), silver amalgam (Ag-Hg), copper amalgam (Cu-Hg) and mercury selenide (HgSe) solubility in different aqueous solutions are given in the figure 25. These experiments are compared to samples under irradiation.

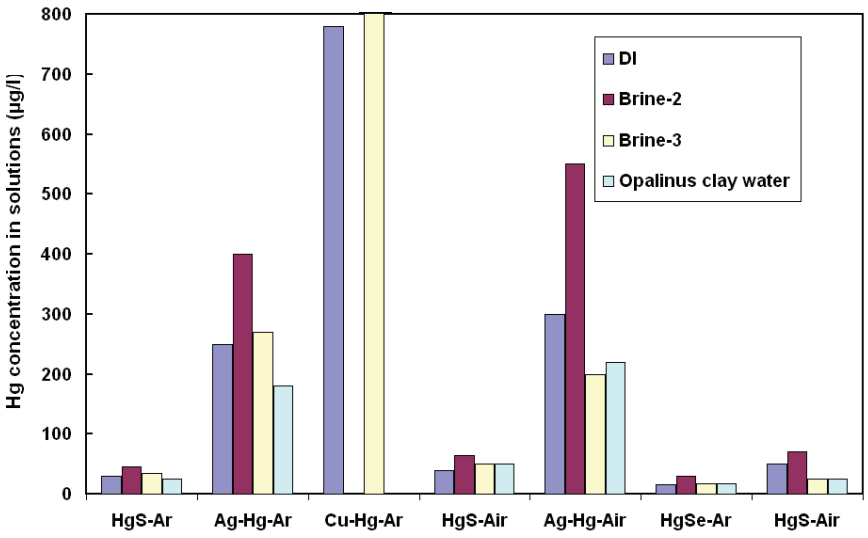

Figure 25: Dissolution behavior of HgS, HgSe, silver amalgam and copper amalgam without γ –irradiation about 3 months in different aqueous solutions at room temperature. (*Ar- Argon atmosphere)

The standard deviation of measurements of solubility, based on replicate determinations, is 12 %. This uncertainty includes all factors, such as dilutions during measurement and filtration steps. The solubility of mercury increases for aerobic conditions up to 20-30% in almost all mercury compound samples. The solution pH values are 4.5 (Brine-2), 5.6 (Brine-2), 6.8 (DI water) and 7.6 (opalinus clay water) at room temperature. Mercury solubility is high for both silver and copper amalgam compared to inorganic mercury compounds like HgS and HgSe. In the presence of these aggressive leachants, like brine-3 and brine-2, there is a clear effect on mercury solubility. Yamamoto et al. reported that presence of molecular oxygen combined with halogens, like chloride, stimulates the oxidation of dissolved elemental mercury in a linear fashion [87]. Despite the fact that the chloride concentrations in the solutions brine-2 and brine-3 are the same, the total solubility of mercury is little bit higher in brine-2 in most cases. This is likely an effect of the pH and high chloride complexes formation. Canela et al. observed in their studies of the pH dependency of mercury solubility, that at pH 7 and 8, the dominating species is $Hg°_{aq}$ (dissolved mercury in aqueous phase). They found, that in solutions with pH 7 and 8 the solubility of $Hg°_{aq}$ accounts for 74% and 58%, respectively, of the total mercury solubility[88].

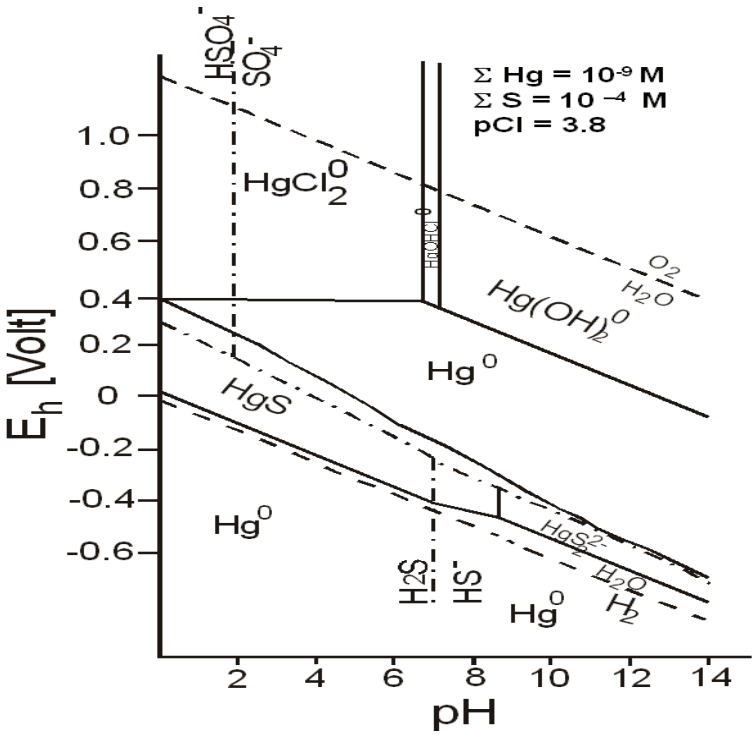

Figure 26: Pourbaix diagram of Hg-S species at room temperature

A Pourbaix diagram, also known as potential/pH diagram, maps out possible stable (equilibrium) phase of an aqueous chemical system. As such a Pourbaix diagram can be read much like a standard phase diagram. A lower pH increases the redox potential and should thus increase the oxidation rate of Hg° to H g(I) and Hg(II). From Pourbaix diagram in the above figure 26, the dominating species at pH < 4.6 and high potential are Hg complexes of chlorides and sulfates. Comparing in brine-2 (pH 4.5) with brine-3 (ph 5.8) there is a promoted oxidation which probably is due to the lowered pH (figure 25). Under aerobic conditions, there is an oxidation layer buildup on the surface and that enhances higher mercury concentrations in solutions. When the molar ratio is 1, essentially all of the Hg is in the form of insoluble mercury-sulfide. The HgS solubility is somewhat sensitive to pH.

But in the case of HgSe, it is complete different. HgSe is very little influenced by Cl^- ion and pH. In both cases the concentration of Hg in solution is below 100 µg/l. The lowest solubility happens over the pH range 6-8 and the solubility increases at both low and high pH values,

as it is supported by literature. On the other hand, HgS oxidation in the distilled water was as low as in clay water. The oxidation rate of dissolved mercury in natural water tended to be accelerated in presence of Cl^- ion irrespective of temperature. The fact that $MgCl_2$, which has 2 equivalents of chloride ions, showed nearly 2-fold higher oxidation rate than NaCl is compatible with this theory. That is the reason that brine-2 solution has a stronger effect compared to other brine solutions. Under strong oxidizing conditions in the solutions, the dissolved Hg^{2+} was suggested to form $HgCl^+$, $HgCl_2$, $HgCl^{3-}$ and $HgCl_4^{2-}$ complexes (Benes and Havlik, 1979). In Ag-amalgam, $MgCl_2$ attacks directly the reaction zone surrounding the grain boundaries of the $\gamma 1$-Ag_2Hg_3 (the matrix phase in the microstructure phase) at the surface of the amalgam. Because of that, the released mercury comes into aqueous phase via forming soluble mercury compounds. Cu-amalgam is more sensitive than Ag-amalgam in chloride environments. Dental amalgam literature reports that the mercury concentration at near neutral pH reached about 200 µg/l even in shorter time of exposure. The Ag-Hg-Sn phase of the dental amalgam released substantially less mercury than Ag-Hg phase. This difference is attributed mainly to a tin oxide surface film which forms a diffusion barrier for mercury. Our investigations are limited to Ag-Hg only because metal introduction in the amalgam needs higher temperature and high pressure. Due to safety reasons, those studies are not performed in the active laboratories for this work.

4.1.4. Leaching experimental studies under γ-irradiation

The behavior of the mercury waste form in contact with aqueous phases is quite different under γ-irradiation. The material structure undergoes several changes during irradiation: As it was observed from table-2, irradiated mercury contains many metal nuclides in soluble metallic phase. Even after transformation to solid form, their stability might be changed under irradiation. In order to investigate the irradiation stability and the effect of the aqueous phase radiolysis, the following experiments were done. Figure 27 compares the measured dose rate in these experiments and dose rates calculated for an activity of 1.4×10^5 GBq of Hg-194, which is expected in a 5 MW target. Two different geometries for an Hg-194 waste package are assumed. It becomes obvious that the experimental dose rates are sufficiently high. After irradiation the solutions are analyzed by cold vapor atomic absorption spectrometry for determination of the mercury concentrations in the aqueous phase. The aqueous phases lead to formation of additional reactive species under solution radiolysis. Concentrated chloride solutions as our salt brines, lead under radiolysis to the formation of several strong oxidative species, such as hypochlorite, chlorite and chlorate.

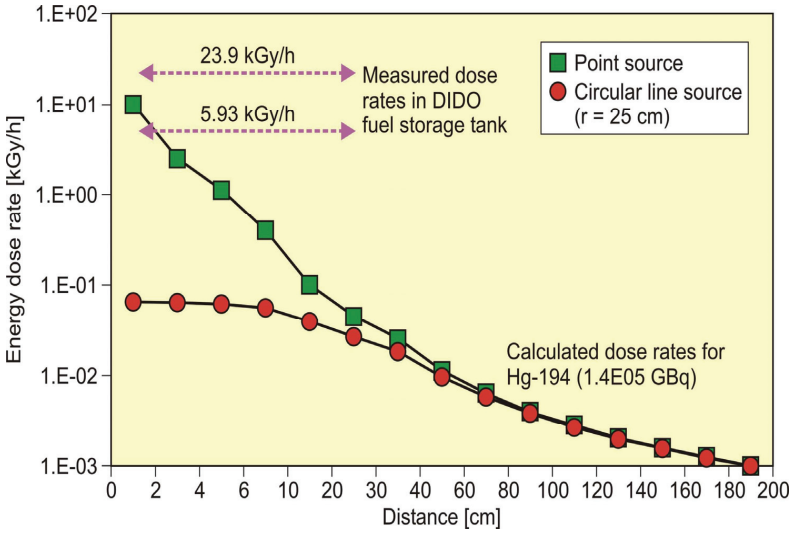

Figure 27: **Comparison of energy dose rate calculated for Hg-194 (1.4E+5 GBq) and dose rates in the fuel storage tank of the FRJ-2 reactor (Conditions: inert atmosphere, time =100 days and T = 50-60℃)**

4.1.5. Comparison studies on mercury sulfide and silver amalgam under irradiation

The first series are the long-term experiments of mercury leaching in deionised water and different salt brines at 50-60℃ under argon atmosp here and under γ-irradiation. The duration of these experiments were approximately 3 months. Before and after leaching, the pH measurements were done and did not show any significant changes during the leaching time. The values measured in the solutions after different leaching times are within the experimental error, estimated as 0.2. For initial studies, HgS and laboratory prepared Silver amalgam were taken for our investigation. Figure 29 shows the results of leaching investigations. One important result is that HgS has better stability than silver amalgam under γ-irradiation. One main objective of this set of experiments is to study the effect of irradiation and chlorides on the mercury release from waste forms. As discussed before the dissolution of mercury from amalgams depends mainly on solution conditions and on pH value. All transition metals, able to exits in more valences, generate a large number of free radicals, including most powerful ones, the hydroxyl radical, so does Hg. In amalgam, mercury concentration is the much higher solution due to free radicals reaction with chloride ions. From figure 28, it can be guessed that much of the chloride salts were deposited on the

amalgam surfaces and that enhanced the slow release of mercury in solution phase. Preparation of amalgam is another factor for mercury dissolution from silver amalgam. A thin film of oxide layer is formed on surface of Ag-Hg matrix phase, which is the main source of mercury and acts as an effective layer to dissolution (Marek, 1990). Oxide and hydroxide films of mercury are less stable at low pH. As earlier it is discussed that similar sort of behavior was identified in the case dental amalgams dissolution studies.

The mercury concentrations in opalinus clay waters are much higher compared to other brines. This gives different information on amalgams. By comparing un-irradiated leaching samples (figure 25), the behavior of amalgam is worse under irradiation and gives higher concentration in orders of magnitude. Literature report suggests that the higher mercury concentrations at higher pH has to be expected, since opalinus clay water contains high concentration of hydroxides, which form relative strong complexes with dissolved mercury and thus increases the solubility. These experiments are of non-conservative type because during repetition the experiments, the samples received a slightly less gamma dose rates. Similar investigations were carried on copper amalgams too. But it is a know fact that copper is an unstable element in corrosive and chloride environment. The values are far beyond the acceptable limit (above 1 mg/l). A comparison of concentrations of Hg in solutions from HgS and Ag-amalgam, the values below 200 µg/l in aqueous phase are taken for further investigation. Gold is ruled out because of its high price. Not only the solubility behavior of Hg/Cu system is not satisfactory at room temperature, but copper amalgam is more difficult to process than silver amalgam

The radiolysis of water produces both molecular and radical oxidants and reductants, which may influence the redox conditions in the repository and the stability of the waste, waste container and buffer materials. Several pairs of radicals or ions (primarily e^-_{aq}, OH* and H_3O^+ in pure water) are formed in small isolated volume elements (spurs) in the initial radiation process. Species within the spurs interact as they diffuse into homogeneous distribution and these interactions result in the reformation of water and in the formation of molecular products. In pure water under γ- irradiation the decomposition products which appear in homogeneous distribution are e^-_{aq}, OH, H_2 and H_2O_2.

Radiolysis of salt brines produce large amount of chloride radical in solutions. The radiation chemical reactions occurring in the presence of Cl^- ions have a great effect on solute dissolutions. This effect enhances the formation of soluble forming Hg_2Cl_2 and $HgCl_4^{2-}$ and other Hg-chloride complexes in solutions. In our investigation under irradiation, mercury dissolution increases in brine solution 10-20% values for case of HgS and even for

amalgams case. Comparing HgS un-irradiated sample in deionized water, concentration is almost the same.

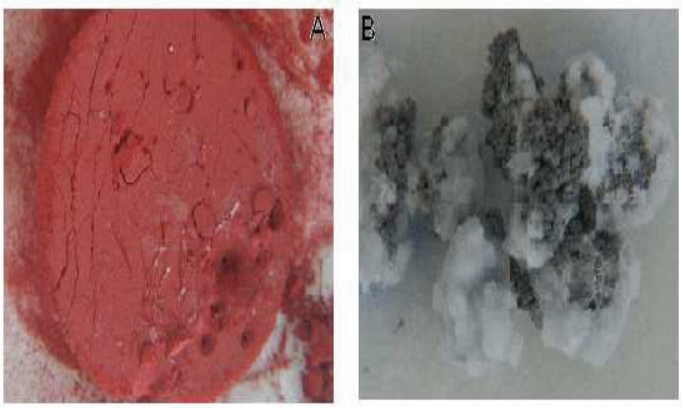

Figure 28: Samples after irradiation experiments A) HgS and B) Ag- amalgam

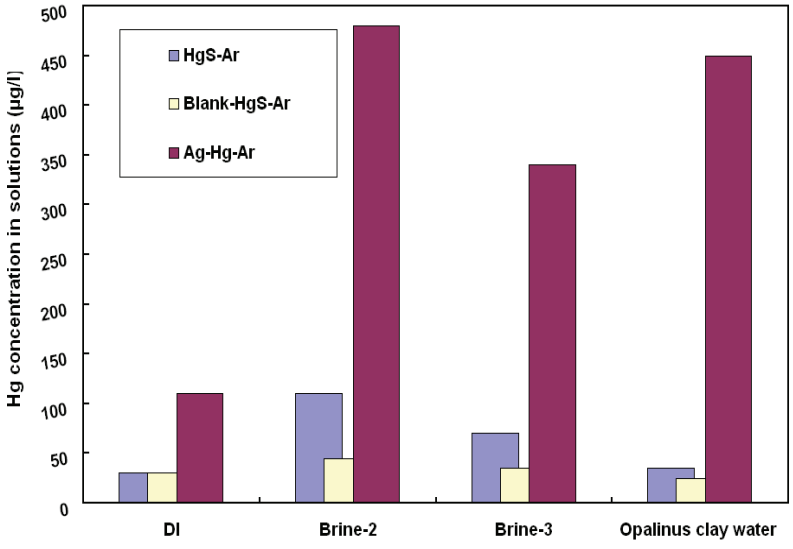

Figure 29: Mercury concentration in solution containing HgS and Ag-amalgam under γ - irradiation in diverse aqueous environments after 100days

Figure 30 gives information about stability region of HgS in soluble sulfide solutions. HgS-water systems under oxidizing condition, HgS tends to change $Hg(OH)_2$ at 4-8 pH range. Under reducing conditions, either polysulfide molecules will be generated. This is the probably the reason that the smaller concentrations of mercury in solutions are observed in the case of deionized water and opalinus clay waters.

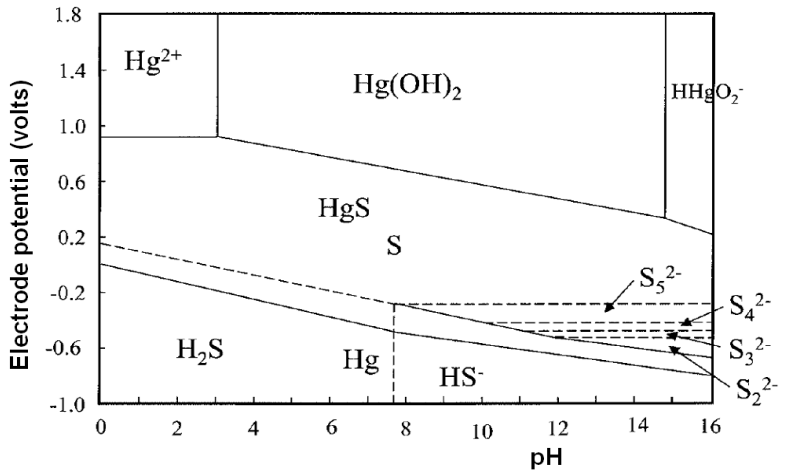

Figure 30: Metastable potential–pH diagram for the Hg---S---H_2O system at 298 K with activities of dissolved mercury and sulfur of 10^{-6} and 1, respectively, in equilibrium with HgS (c, red) and HgO (c, red, orthorh.)[89]

The metastable potential–pH diagram shown in figure 31 best predicts the kinetic behavior of HgS, at least in neutral chloride media. The upper limit of stability of HgS is the vertically hatched region. Hence, the most probable oxidation reaction appears to the following equation under irradiation condition:

$$HgS + 4Cl^- + 4H_2O \rightarrow HgCl_4^{2-} + SO_4^{2-} + 8H^+ + 8e^- \qquad \longrightarrow \qquad (6)$$

According to the potential–pH diagram illustrated in figure 30 & 31, a reducing agent with a reversible potential less −0.096 V should be capable of reducing HgS to metallic mercury at extremely low pH values. But in these investigations, no reducing agent was used at low pH value.

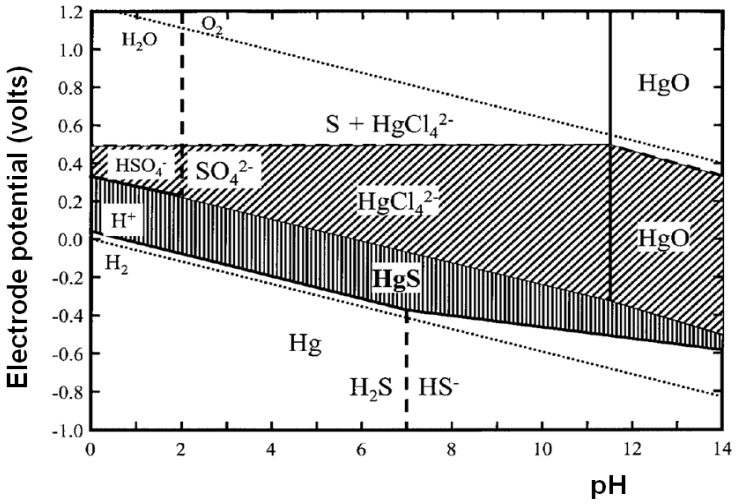

Figure 31: Metastable potential–pH diagram for the Hg---S---Cl---H_2O system at 298 K with activities of dissolved mercury, chloride and sulfur of 10^{-6}, 1 and 1, respectively, in equilibrium with HgS (c, red) and HgO (c, red, orthorh.) [89]

4.1.6. Leaching behavior of mercury sulfide and mercury selenide under irradiation

The strong influence of γ-irradiation on dissolution rates of HgS becomes obvious by comparison of the blind (un-irradiated) specimen in brine 2 with irradiated ones: HgS-specimen without irradiation reveal dissolution rates by more than an order of magnitude smaller than irradiated ones (from figure 32). The dissolution of HgS comes probably from oxidation reactions forming soluble mercury sulfate (Hg_2SO_4) or reduction reactions forming polysulfide compounds (HgS_2^{2-}) [88], but chlorine may play critical role too. The altogether small amount of mercury dissolved from HgS in salt brines and clay water shows the strong stability of HgS and its suitability as solid compound for disposal. Literature data indicate that the mobility of mercury in aquatic environments without irradiation varies with pH and redox conditions: Oxidizing environments result in medium Hg mobility, reducing environments however in very low mobility up to immobility. Acidic environments generate high mobility, but in neutral to alkaline environments, a very low mobility up to immobility was observed.

Therefore experiments were carried out under oxidizing (aerobic) [90], anaerobic/neutral and anaerobic/acidic conditions for the most promising compounds HgS (figure 32) and HgSe (figure 33). Oxidizing conditions were examined by introducing an oxidizing agent (ferric chloride) in addition to air (aerobic conditions): These experiments revealed that the mercury

mobility increased in oxidizing environments. Fe(III) chloride is reduced by Hg to Fe(II) chloride and an equivalent amount of mercury chloride is formed. Also, at low pH values the solubility increased. Comparing the dissolution behavior of HgS and of HgSe in these experiments, HgSe is found to be even some more stable than HgS, although altogether similar dissolution behavior was detected. Although not found in absence of irradiation, HgSe underlined the increased dissolution rate in presence of Cl^-. The main conclusion drawn from these results is that the stability of chalcogenides during accidents in a repository is larger than amalgams. Despite of its still better dissolution behavior mercury selenide (HgSe) was not considered for detailed studies: High costs and bio-toxicity of selenium (Se) are major disadvantages. The HgS was chosen as solid compound for final disposal. Because of that further investigations are concentrated only on HgS.

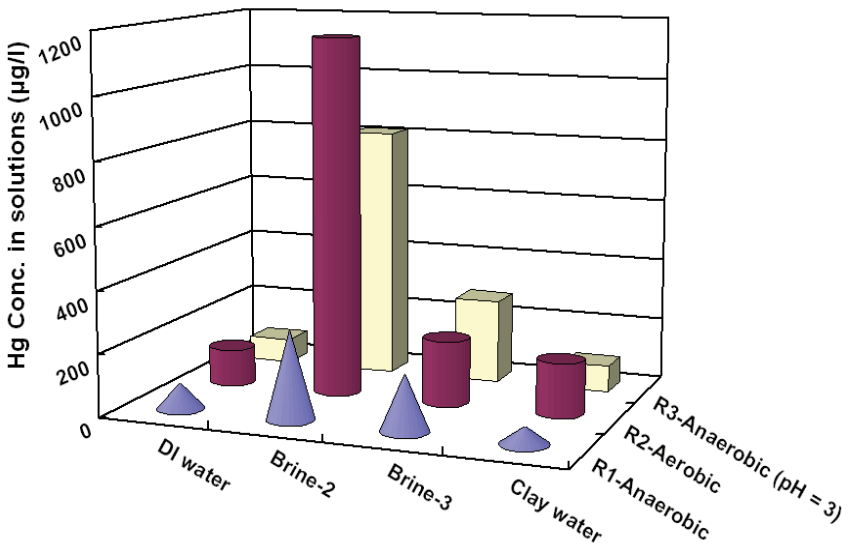

Figure 32: Dissolution behavior of HgS under γ-irradiation in different aqueous solutions and different reducing conditions

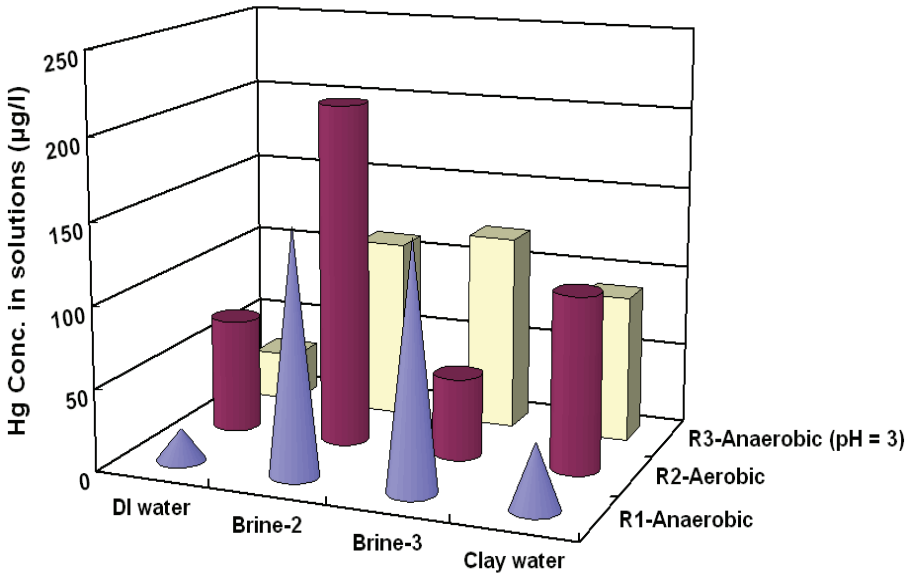

Figure 33: Dissolution behavior of HgSe under γ-irradiation in different aqueous solutions and different redox conditions

4.2. Encapsulation of mercury compounds in cement

4.2.1. Leaching behavior of mercury sulfide and Hg (I) nitrate embedded in cement matrix under irradiation

In figure 34, the dissolution behavior of mercury compounds (HgS, Hg(I)nitrate) from cement matrices is shown. As additional parameter the influence of the Hg/cement ratio on dissolution behavior is studied for HgS. A photo of diverse Hg/cement matrix specimens is presented in figure 35. Due to large density differences of mercury compounds and of cement, a homogeneous Hg distribution in cement was difficult to achieve: Here further improvements are required. As expected, the retention of soluble $HgNO_3$ is relatively small compared to HgS. Poon et al. studied the effect of heavy metal oxides (Cr, Cu, Zn, Cd, and Hg and Pb) in cement physical properties [61]. Their studies had shown that metal interaction with hydration and microstructure of the hydrated cement in the early stages of hardening and seriously affect strength devolvement.

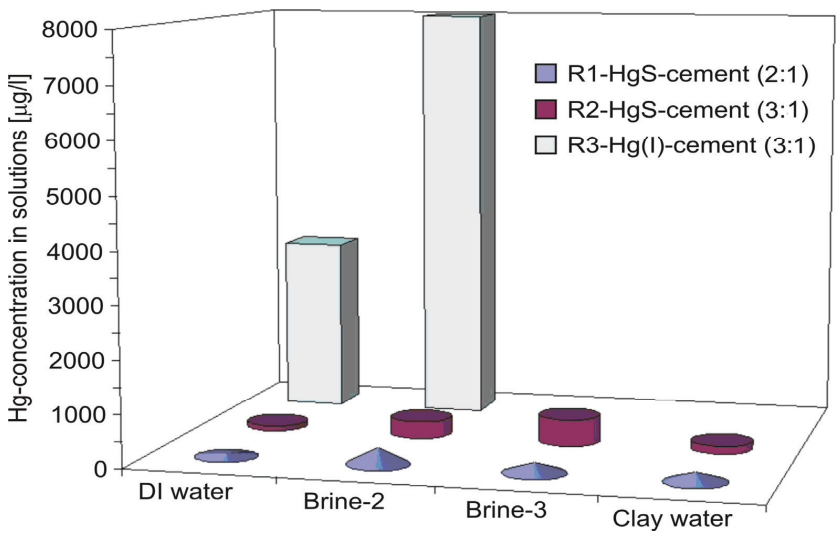

Figure 34: Dissolution behavior of mercury compounds embedded in a concrete matrix under γ-irradiation

Figure 35: Concrete specimen containing mercury compounds

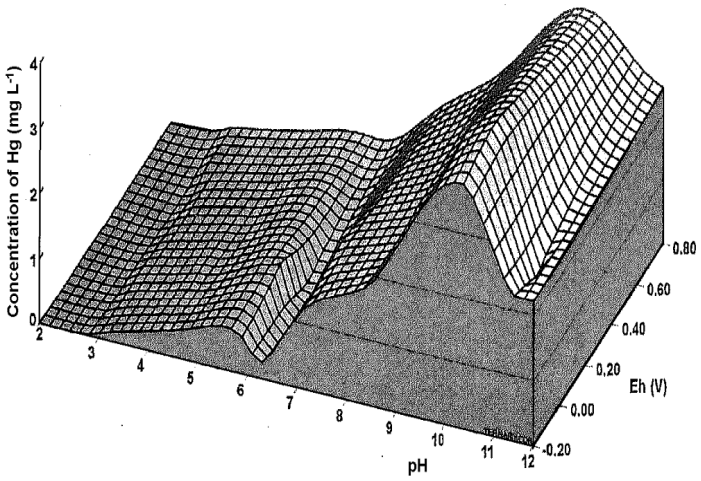

Figure 36: Composite–leaching profile of pH from waste material at different Eh and pH conditions (Randall et al., 2003)[18]

In fact the leaching kinetics is strongly affected by the experimental conditions and the frequency at which the solutions reach the pores of Hg-cement matrices. This leads to more interfacial pore reactions. More or less the Hg release is believed to be controlled by diffusion through cement matrices [91]. Stepanova et al. [92] also found that metal chlorides interact with silicate and aluminate components of cement to form complexes whose stability makes a substantially contribution to final compressive strength. Our investigations on Hg (I) nitrate and HgS with cement have given high concentrations (above 1 mg/l) due nitrates/sulfates reaction with hydration products of the cement. These reactions might have influenced the hydration and mechanical strength. And due to that porosity increased in Hg-cement matrix [93].

The irradiation conditions produce an accelerated leaching environment in the presence of Cl^- too [91]. Under these conditions the result showed that leachants had very high initial alkalinity, probably due to the dissolution of hydrated cement. Figure 36 shows the leaching profile of Hg-waste material at different pH conditions. Mentioned studies of Stepanova et al. exactly match our investigations about release of Hg in solutions [88].

Another important point for high dissolution of mercury from cement matrices is that dominant species like $Hg(OH)_2$ (90-99%) is formed during surface reaction. Due to density differences of the mercury compounds, HgS migrates to the bottom of the cylindrical shaped

specimen. This also influences the release of Hg from the sample in the olution. In addition, a number of physiochemical processes can affect the fate of solidified/stabilized Hg (shown in figure 37).

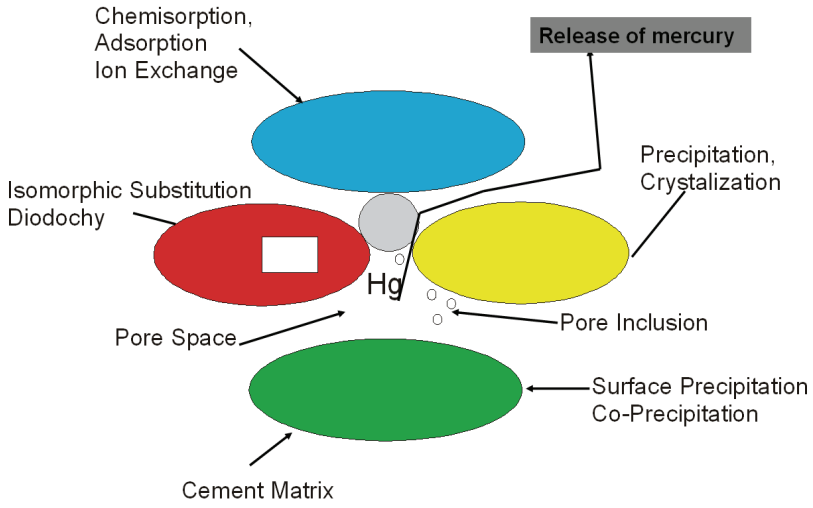

Figure 37: Possible physiochemical processes involved in the solidification/stabilization of Hg-waste in cement matrices

Under irradiation, the interstitial liquid in concretes is affected by radiolysis. Water radiolysis changes the composition of leachates and forms soluble products which influence the degradation of the cement matrix.

Gamma radiation from radioactive wastes is especially important because of its ability to deeply penetrate and degrade materials. Early studies indicated that damage to concrete will only occur for gamma doses on the order of 10^2 MGy. However, there has been little attempt to determine whether the dose rate is an important factor in concrete degradation in the long time deposition. In these investigations, samples received dose rate is below this values (it is almost below 100 KGy). So concrete irradiation induced mercury dissolution is considerable less on our samples.

4.2.2. Mercury waste (Hg) in ordinary Portland cement (OPC)

The effect of HgS/OPC ratio on embedding is shown in figure 34 already. It can be seen that the waste/OPC ratio has a small effect on the mercury concentration (Hg_{tot}) in solution. When the HgS/OPC ratio increases 2 to 3, the mercury concentration in solution is almost the same in deionized water and opalinus clay water. There is a small increase in brine solutions; this might be the influence of chloride ions in solutions. Zhang et al. reported similar results with Hg (I) nitrate samples and Hg(I)/OPC ratios above 4: There is a large increase in Hg concentration in filtrates. In the case of Hg (I) nitrate solutions, there is a large amount of mercury in solution because: It forms easily soluble hydroxides with dissolved oxygen molecules.

4.2.3. Chloride effect on mercury embedded in cement matrix

As mentioned in previous chapters, chloride ions can significantly increase the mobility of mercury. Schuster et al. (1991) [94] pointed out that, at a chloride ion concentration of 10^{-4} M (naturally occurring) increased the solubility of $Hg(OH)_2$ and HgS by a factor of 55 and 400, respectively (as shown in figure 38). The increase of Hg release with increasing Cl^- concentrations is attributed to the dissolution of the adsorbed Hg through its complexation with Cl^- (Wang et al., 1991)[95].

At low pH (as in the case of Brine-2), alkalinity originating cement from cement was increasingly consumed during the leaching. The cement matrix was weakened, leaving relatively large pores in the cementitious matrix. Additionally an intense decalcification of C-S-H (calcium silicate hydrate) in the presence of chloride occured due to greater ionic strength that they generate [96]. Figure 39 shows the pore size distribution of an initial sample and a degraded sample. The gauss mode distribution is not present in the degraded cementitious matrix: It is flattened and pores were wide opened. Perlot et al. [97] mentioned that the degradation behavior of cement paste is influenced by chloride ion diffusion through the matrix. Their investigations exhibited a chloride ion diffusion coefficient De_{Cl^-} of about 25.6 x 10^{-13} m^2 s^{-1}. Svensson et al. [98] calculated the apparent diffusion coefficient to 10^{-14} m^2 s^{-1} in OPC. The diffusion coefficient is increased by 2.5 times due to influence of chloride ion.

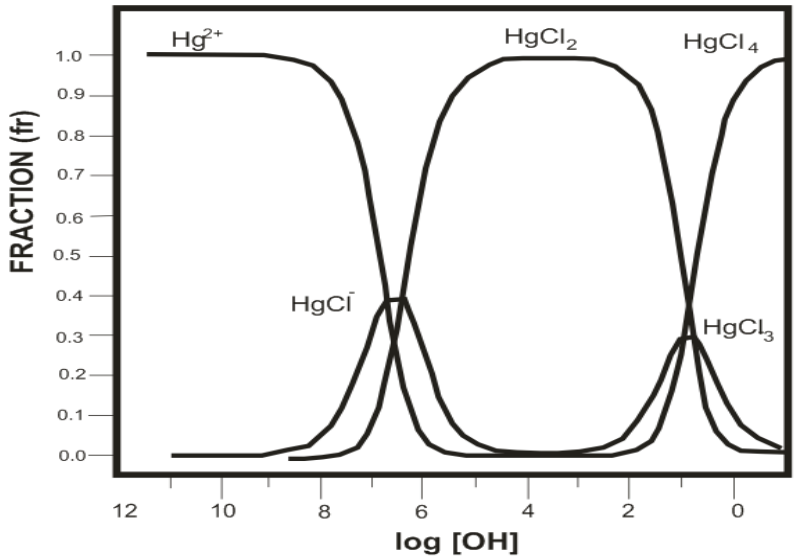

Figure 38: Predicted speciation of Hg as influenced by pH and chloride ions (Hanhe et al. 1973a)[94]

As a thumb rule, the greater the diffusion coefficient is the greater the penetration of aggressive ions from solutions to material. Recently Svensson (2008) et al. have done long-term experiments for diffusion through concrete barriers with mercury waste as Hg(II) and announced that the apparent diffusion coefficient is about 0.4 - 0.2 x 10^{-14} m^2 s^{-1}. Assuming apparent diffusion coefficient (D_a) = 10^{-14} m^2 s^{-1} in Ordinary Portland cement, it would take years to release 1% of initial mercury concentration and 35000 years for 50% through 10 cm barrier (Drevel et.al, and Freeze et al.) [99]

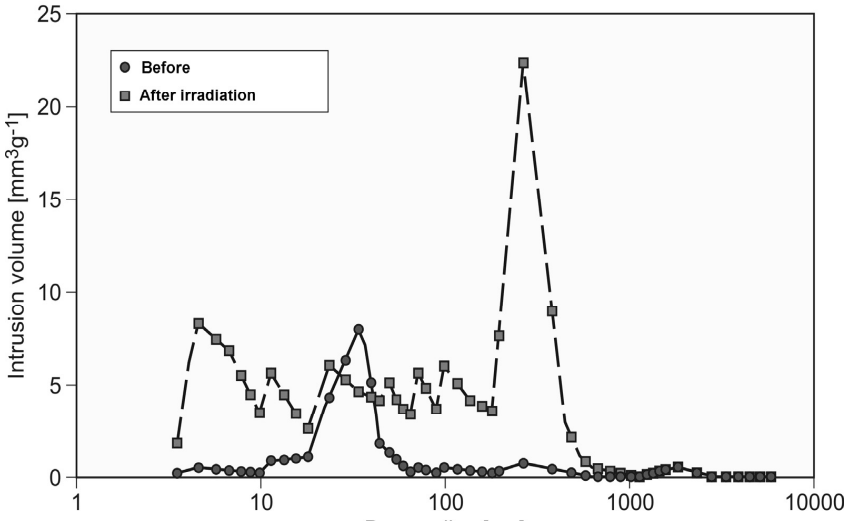

Figure 39: Pore size distribution of comparison between Hg-cement matrix before and after irradiation

4.2.4. SEM investigations on mercury sulfide embedded in cement

The evolution of the HgS-cement matrix surface during leaching experiments was investigated. During preliminary studies on matrix specimen, there are visible changes in surface of matrix after leaching studies in Brine-2. The EDX analysis on the surface of HgS-cement matrix leached in Brine -2 (figure 40) shows that Ca, Cl and Mg are the main elements of the phase formed. The presence of Mg and Cl is connected to the formation of salt precipitations on top of the surface during the leach process. The dissolution of HgS-cement matrix comes probably from surface and pore reactions with $MgCl_2$ by forming soluble cement complexes and soluble mercury sulfate (Hg_2SO_4) or reduction reactions forming polysulfide compounds (HgS_2^{2-}). The above mentioned chemical processes, make an enhanced degradation of the cement matrix. In figure 41(b), it is shown that mercury sulfide is located at one specific point and the surrounding mercury compound is leached completed by these aqueous phases. Simultaneously pore region also is affected by aqueous solutions too [96]. Because of that reason the samples become more porous after leaching time. Precipitated chloride and magnesium elements were deposited on pore walls and outer surface of the matrix (figure 41(c) and figure 41(d)). EDX analysis also revealed that the content of magnesium is relatively low compared to chloride (figure 40).

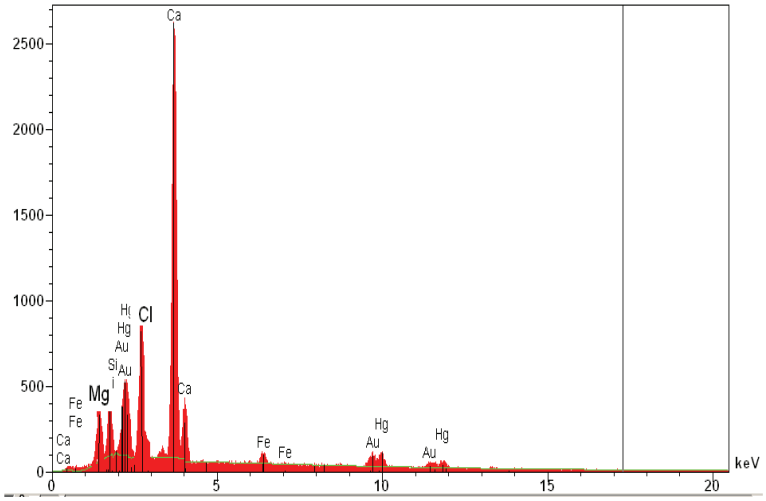

Figure 40: EDX spectrum of coverage of Hg-cement matrix after 3 months leaching in Brine-2 under γ-irradiation

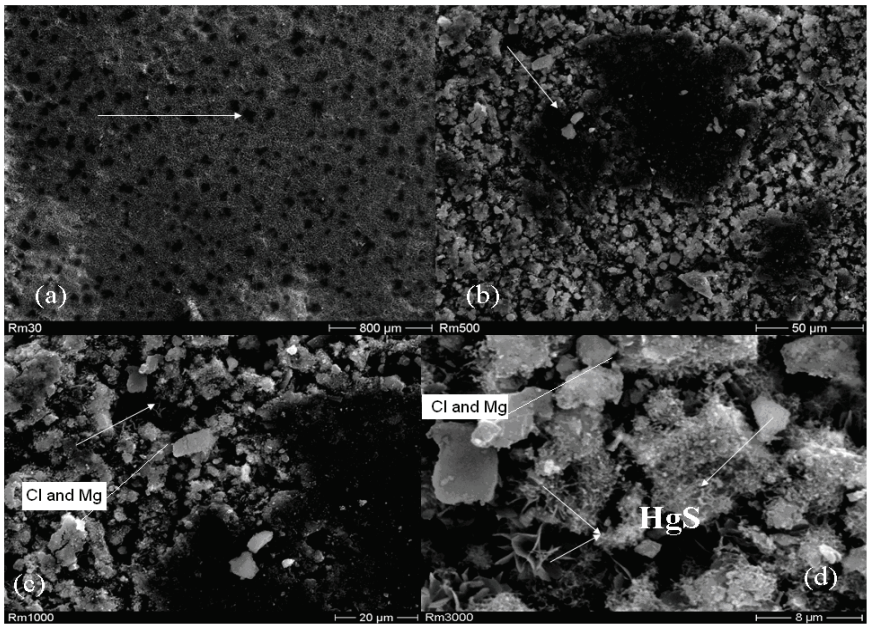

Figure 41: SEM photosgraphs of degraded HgS-cement matrix after 3-months leaching in Brine-2 under γ-irradiation a) Outer surface with distributed HgS in cement b)HgS is located specific point c) Precipitated Mg and Cl on porous surface d) HgS located on single point

The EDX line scanning was done to identify mercury distribution in the cement matrix. It revealed complex issues of the mercury and other elemental distribution. In figure 42(a), the mercury compound is located in specific points in 50 μm scale region. From figure 42(b), it can be inferred that the surface distribution of mercury is very limited. Mercury is leached by the aqueous phase and this can be either done by the direct reaction or by desorption from high surface area hydration products. However, alkaline hydrolysis of mercury compounds could lead to the formation of other soluble hydroxides and of free mobile sulfur complexes. These free sulfur complexes may form soluble mercury sulfates compound, which will be released from pore sites and eventually degrade the cement matrix. It can be concluded that pore fluid chemistry has clear a influence on Hg-cement matrix. In the long term, this is the potentially worst scenario as it leaves species free in ground water in accidental situations. In addition to that the irradiation helps the solubilization of Hg radionuclide's and migration in fast pace. The outcome from above studies is that there is a serious requirement for alternative to cement type material for mercury embedding matrix.

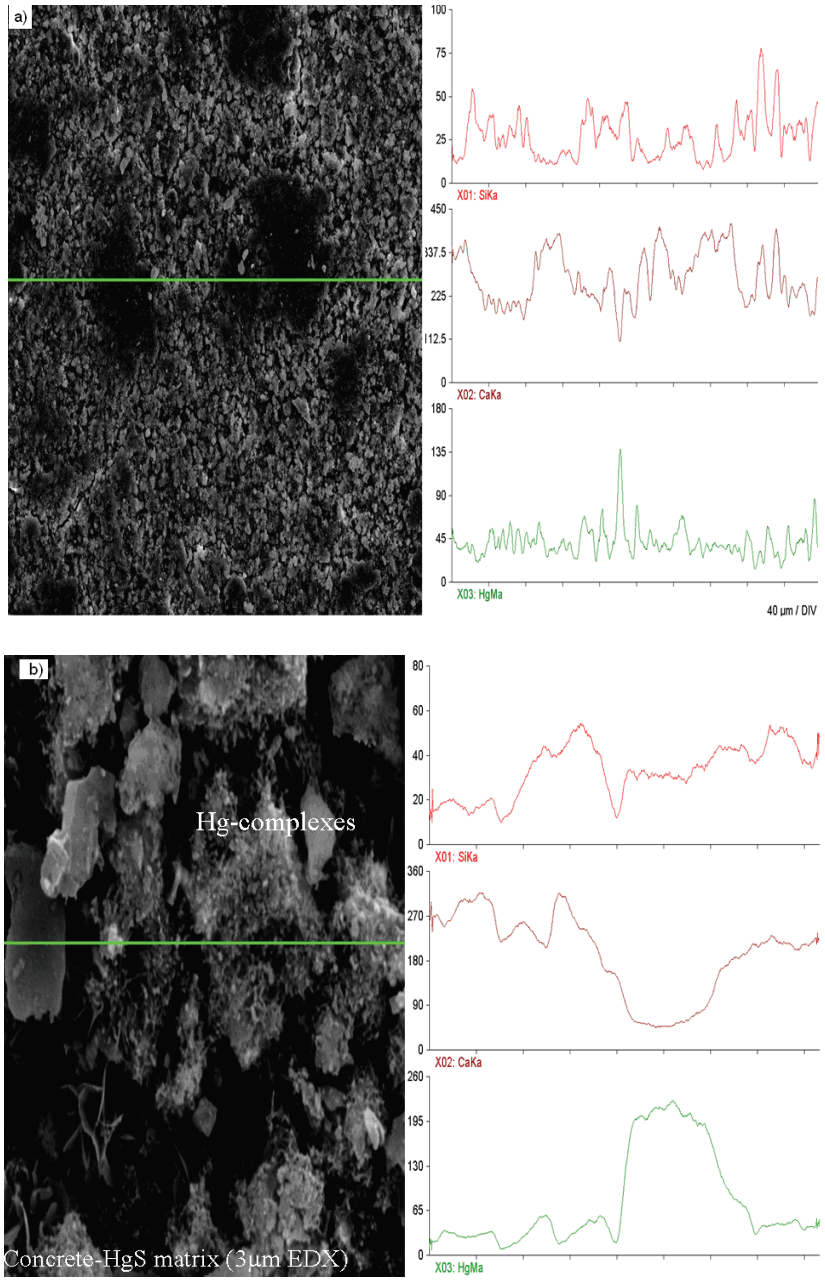

Figure 42: SEM photograph of degraded HgS-cement matrix with EDX line scan through porous surface at specific points: a) 50µm and b) at 3µm

4.3. Encapsulation studies for mercury compounds using polysiloxane material

4.3.1. Leaching behavior of mercury compounds embedded in polysiloxane matrix

Embedding nuclear waste in polysiloxanes is under examination for certain wastes from nuclear fission reactors, too. Unfortunately it was not possible to perform leaching experiments on polysiloxane with embedded HgS under γ-irradiation, because the Juelich Research Reactor was shut down and the dose rate in the fuel decay tank became too small. The transfer of the irradiation equipment to another irradiation site was examined but was found to be to time consuming. Nevertheless leaching experiments but without γ-irradiation were performed.

Besides the standard waste package, a layered polysiloxane waste package was manufactured: In a first step a polysiloxane/HgS mixture was manufactured and hardened out. After that some HgS/polysiloxane specimens were embedded in an additional but HgS free polysiloxane layer. This was done in order to compensate a possible inhomogeneous HgS distribution in the polysiloxane due to the density difference between HgS and polysiloxane.

In these experiments, polysiloxane type RT 622® Elastomer with catalyst from Wacker Chemie GmbH, Germany was used. Figure 43 contains pictures of unlayered and layered HgS/polysiloxane specimens. Leaching experiments with brines shown in table-8 were performed at 50-55℃ for 6 weeks under aerobic conditions. Besides HgS specimens also those containing HgSe were examined. Figure 44 shows specimens in leaching solutions. Figure.45 shows the results of these leaching experiments. For comparison one result of a cementitious embedded HgS specimen without radiation is presented, too. It becomes obvious that layered specimen reveal a substantial better leaching behavior than unaltered specimen. A standard cementation specimen reveals a better leaching behavior than unaltered polysiloxane specimen but a worse one than polysiloxane layered specimens. Unaltered HgSe/polysiloxane specimens reveal a better leaching resistance than unaltered HgS/polysiloxane specimens but there is no difference for layered specimens. Altogether this indicates that polysiloxane is very promising candidate as matrix material for HgS waste packages. However a layered polysiloxane waste package has to be used. Future work has to reveal details about the leaching behavior under γ-irradiation, too. It has to be noted that layered cementitious specimen are not easily to manufacture because of shrinkage effects

during hardening, potentially leading to cracks. Figure 46 shows some results on the leaching rate of unlayered polysiloxane/HgS specimen depending on time and on leaching temperature. There is obviously only a small temperature dependence of the leaching rate in the examined temperature regime 20 to 55℃.

Figure 43: HgS/polysiloxane specimen - unlayered (top) and layered (bottom)

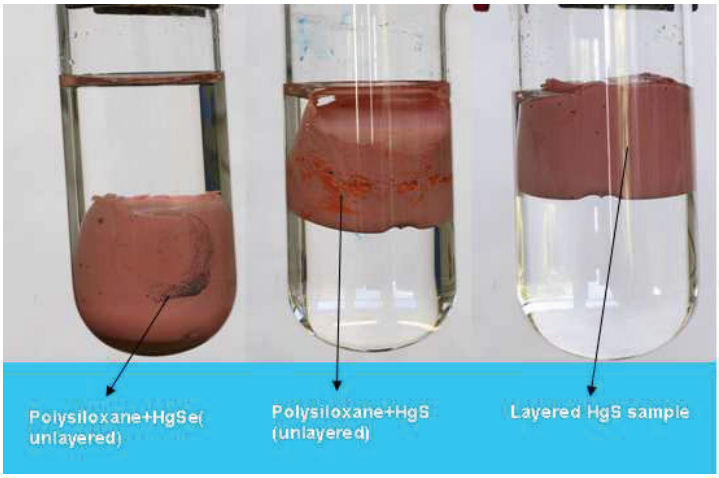

Figure 44: HgSe/ and HgS/polysiloxane specimen in leaching solutions

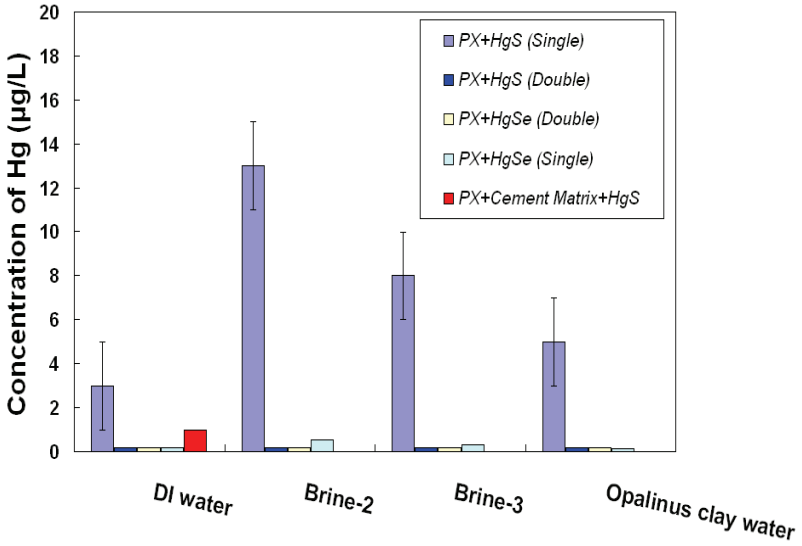

Figure 45: Leaching behavior of HgSe/ and HgS/polysiloxane specimen in 4 different leaching solutions at 50-55℃. For comparison a value of a c ementitious specimen is presented, too (single= unlayered, double=layered)

From figure 46 comparing leaching studies of unlayered HgS/polysiloxane samples at both temperatures, there is an equilibrium value reached for leaching at temperature 25℃ after 3 weeks. The HgS/polysiloxane sample at 55℃ is also behaving similar as at 25℃ up 4 weeks, after that there is slight increase in concentrations in solution about 2 µg/l. Randall et al. [82] investigated high nitrate salt waste surrogate (contains Pb, Cr, Hg salts) mixed with polysiloxane at 50% waste loading. They reported that mercury TCLP (Toxic Characteristic Leaching Procedure) result exceeded the 25µg/l level from 1 g/l of mixed metallic waste containing mercury oxide from similar time scale at room temperature [72]. From our investigations, mercury concentration in solution reached by less 20 µg/l from 18 g/l mercury sulfide (HgS). Figures 47(a) and 47(b) show the Hg distribution in HgS/polysiloxane of the outer layer and the middle of sample (double layer specimen). The outer layer of HgS/polysiloxane shows no mercury on the top and there are no shrinkage effects during hardening and no migration of Hg to the surface as in the case of cement matrices. In the middle of the layer, mercury is located at specific sites and exists as HgS only (figure 47(b)). From these investigations, it can be concluded that polysiloxane encapsulation is applicable for mercury wastes containing large amount of hazardous metals, but may require pretreatment steps for higher concentrations to ensure that distribution is homogeneous and therefore leachability limits are met. Based on the preliminary studies, the polysiloxane

encapsulation is a competitive method to the usage of cement for mixed Hg-waste stabilization.

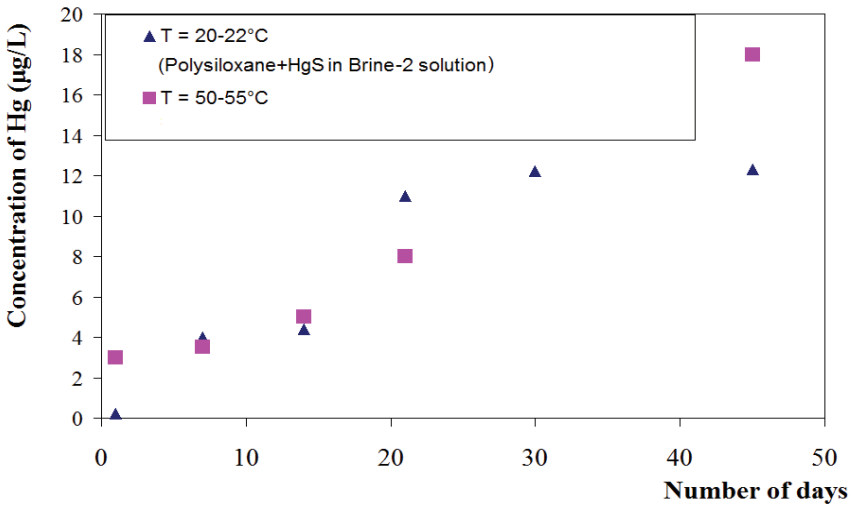

Figure 46: Temperature and time dependence of leaching behavior of unlayered HgS/polysiloxane specimens

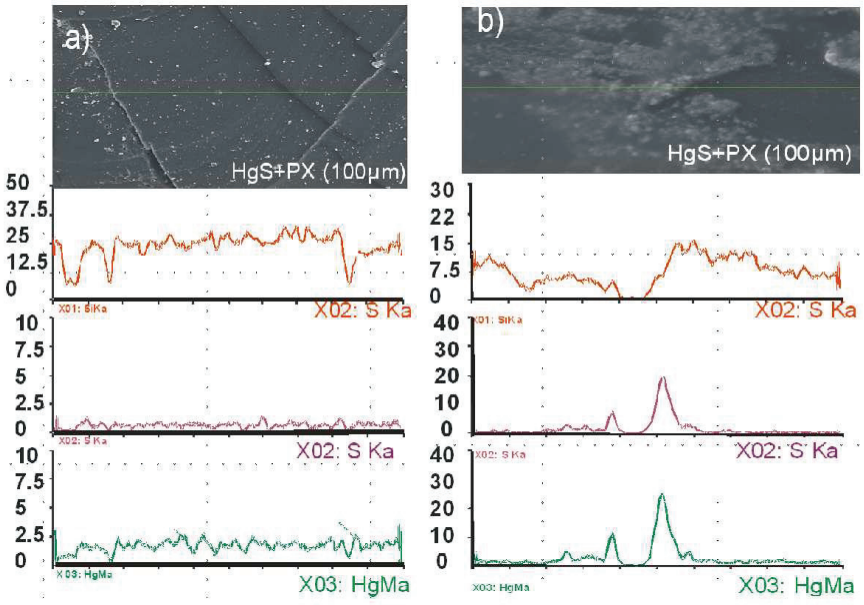

Figure 47: Hg-distribution in HgS/polysiloxane matrix by SEM/EDX a) outer layer (left) b) middle of sample (right)

4.4. Chemical engineering study of HgS generation

4.4.1. Selection of a process for formation of HgS from liquid mercury

In principle there are many different ways of formation of HgS from liquid mercury:

1. Formation by adding a solid sulfur compound (S, FeS) to liquid mercury and reaction to HgS at elevated temperatures. It is a long term process and requires continuous stirring and requires large excess of the sulfur compound for a complete reaction of Hg to HgS. Accordingly, a separation of excess sulfur from the product is required. This HgS formation process is technically relevant and called 'Dry process'. A highly water insoluble (0.0125 mg/l) mercury sulfide or meta-cinnabar is thus formed, which is converted to red sulfide or cinnabar by heating (at temperature of 386℃). Similar dry process investigations were carried in our laboratories at room temperature under aerobic and anaerobic conditions in glass ampoules. The sulfur powder is added to mercury in an S: Hg ration of 1:1, 2:1, and 3:1. These experiments were opened after 12 months. The samples were analyzed by SEM for mercury sulfide formed from elemental mercury and sulfur powder. From figure 48, still there is unreacted mercury in sample even after one year chemical stabilization. Svensson et al.[100] had done similar investigations with Hg°, HgO and different elemental sulfur sources (FeS and FeS_2) about 3-4 years in anaerobic conditions. They reported that their reaction kinetics reached only 90-95% of elemental mercury conversion under alkaline conditions. Svensson et al. results match with our investigations of elemental Hg° and elemental sulfur.

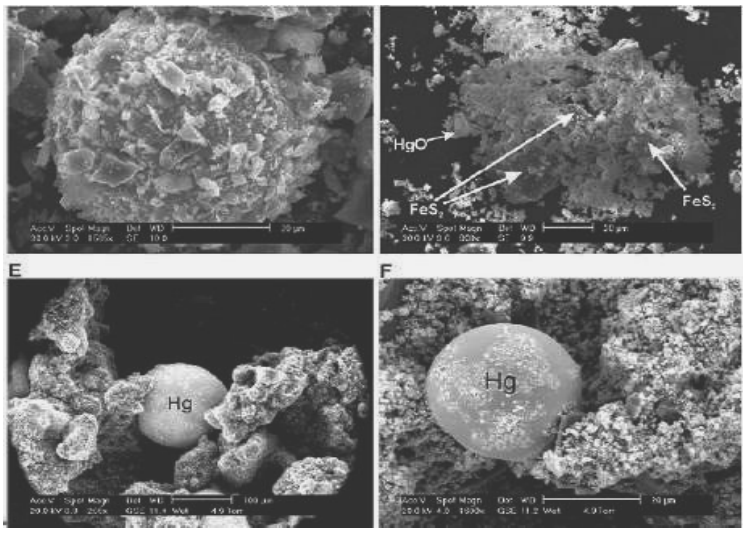

Figure 48: SEM photo of HgS form dry process

2 Formation from the gaseous elements: This process, in principle is possible, however has no technical relevance. The problem: is that the gas phase reactions with solid products are difficult to control (e.g. deposition of educts together with the product). Therefre this process requires major chemical engineering R&D for becoming mature for application under hot cell conditions.

3 Formation by dissolution of mercury in HNO_3 and subsequent precipitation of HgS by a soluble sulfide. This is process is technicall relevant. The advantages are:

- Potential for continuous or semi-batch process (i.e. only a small amount of mercury is present in the reaction step, which is safer to process operation).
- Reactions in water solutions are easy to control but It has to be mentioned that the use of water and other chemicals significantly increases the amount of waste.

After a detailed literature survey and after preliminary experiments, the gas phase reaction and the reaction from elemental mercury with sulfur compounds in the condensated phase were ruled out: For the first, major R&D on the process is required and the second because of difficulties to realize a complete reaction of mercury, because of the need of a batch process and because of the long term character of the reaction. Thus we concentrated our

examinations on the process with dissolution and precipitation, called 'Wet process' (reaction scheme shown in figure 49).

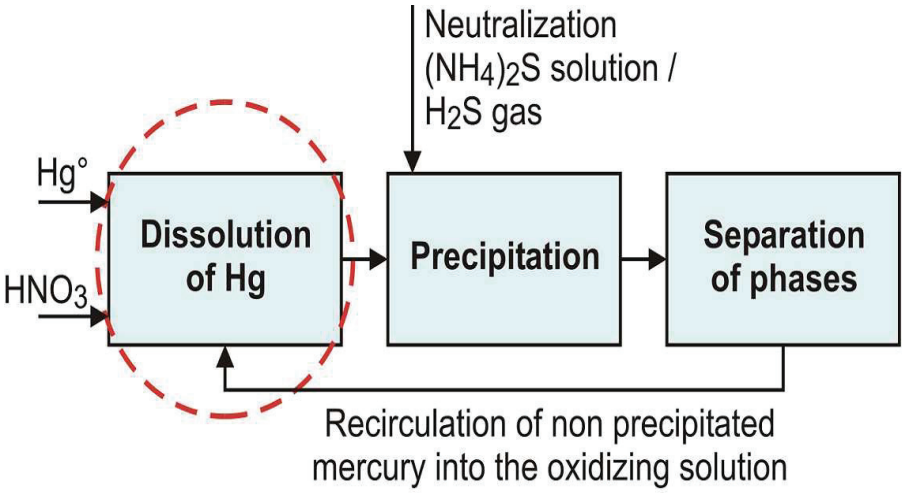

Figure 49: General reaction scheme of the wet HgS formation process

A lab scale apparatus for process studies on the formation of HgS by the wet process was constructed and operated in the chemical hot cells of FZJ. Because of its high conventional toxicity the treatment of major amounts of mercury was not permitted outside of these chemical hot cells. Figure 50 contains a scheme and figure 51 a photo of the apparatus used. Exhaust gas purification is required because of the toxicity of the nitrous oxides formed and of the hydrogen sulfide, which may occur during the precipitation step. As the figures indicate, a careful pH and temperature control in the process is required.

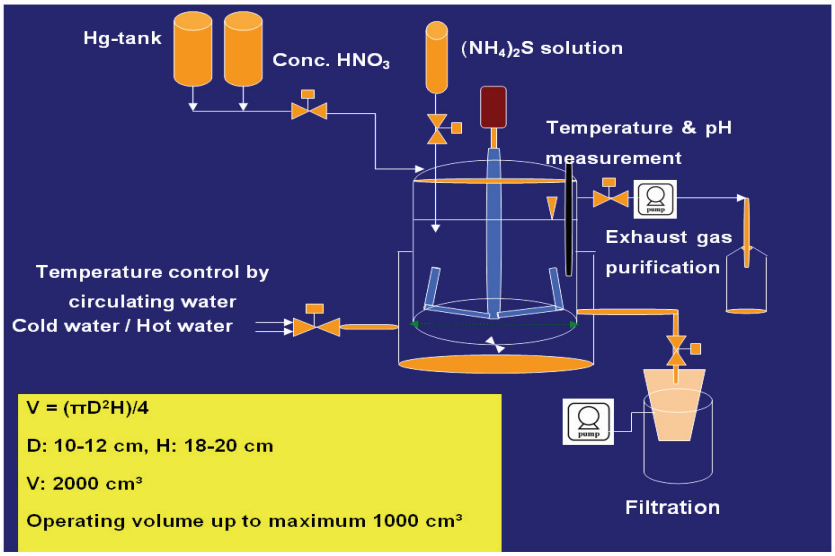

Figure 50: **Schematics of the apparatus used for HgS formation**

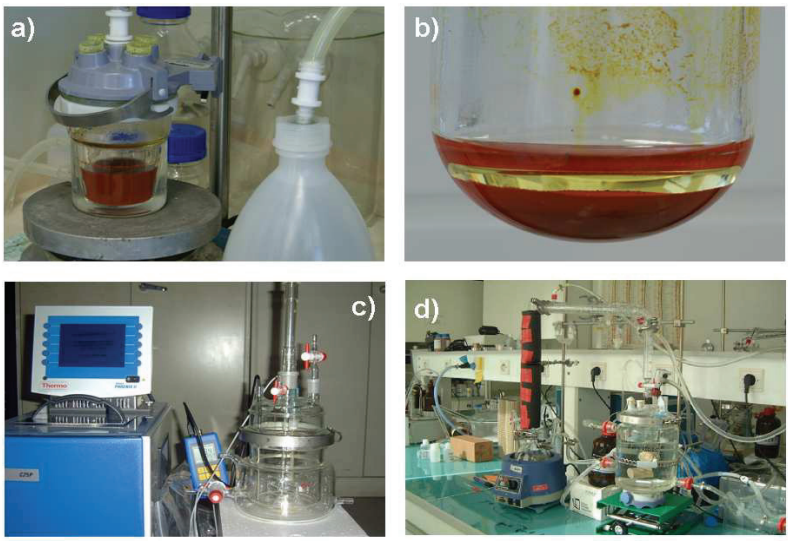

Figure 51: **Photo of the lab-scale experimental set-up constructed for formation of HgS from mercury**

4.4.2. Formation of mercury sulfide by wet chemical process

4.4.2.1. Dissolution of Hg in nitric acid:

From the general reaction scheme of the wet HgS formation process (figure 49), the dissolution of mercury metal in nitric acid is the first important step. The dissolution is a prohibitively slow reaction, but small amounts of mercury form mercurous nitrate which causes a vigorous and exothermic reaction. It is obtained by the reaction of mercury with cold nitric acid. Literature suggest that formation of $Hg_2(NO_3)_2$ which arises from mercury ion, probably mercury(I) occurs at low temperature of about 0-5℃ and at low pH of 2-3. Higher temperatures lead to formation of $Hg(NO_3)_2$, mercury (II) nitrate in nitric acid. In the course of our investigation on the mechanism for this reaction, we found that the ionic mercury, in the mercurous ion form, is unique in that it exits only in the dimeric form, Hg_2^{+2}, and never as a simple monomer. In solution this will exists only below a pH of about 2.5 to about 3 because of its reactivity with water or hydroxyl ions at higher pH values via disproportionate reaction (7). The precipitation reactions involving ionic mercury ions are complicated by disproportionate reaction yielding elemental mercury and mercuric compound as follows including the equilibrium constant for disproportionation reaction (8):

$$Hg_2^{2+} + 2OH^- \longrightarrow Hg + H_2O + HgO \longrightarrow \quad (7)$$

$$Hg + Hg^{2+} \longrightarrow Hg_2^{2+},\ K = 166 \longrightarrow \quad (8)$$

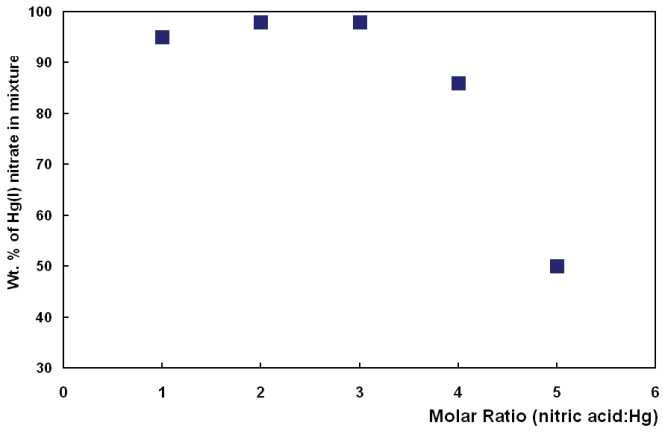

Figure 52: mercury (I) nitrate formation with respect to molar ratio (HNO_3: Hg)

Figure 52 shows the effect of excess of a amount acid in nitric acid for dissolution of mercury. An excess amount of nitric acid leads to additional formation of mercuric complexes in aqueous solutions. In addition to that reduction to elemental mercury readily achieved, but oxidation to the mercuric ion is more difficult. The oxidation potential of the elemental mercury to the mercuric ion [Hg (0) – Hg(II)] and the mercurous to the mercuric ion [Hg(I) – Hg(II)] are close. In order to determine the mercury oxidation state in solutions, the samples were periodically analyzed by Raman spectrometry [101]. Figure 53 shows the formation of mercury (I) nitrate at different molar ratios of acid to Hg. The Raman spectrum of the nitrate ion is a sensitive indicator of the nitrate ion coordination environment.

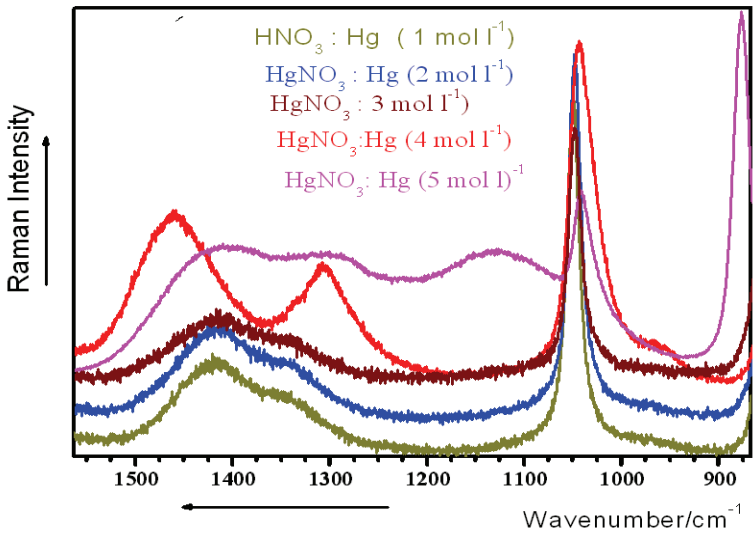

Figure 53: Mercury (I) nitrate ions identification in aqueous phase by Raman spectroscopy (wave numbers range 900-1600)

When the nitrate ion contacts a cation, it is polarized, resulting in the Raman active symmetric stretch with frequency lower than 1050 cm^{-1}; the out-of-plane infrared active mode occurs at frequencies lower than 830 cm^{-1} and becomes Raman active; the asymmetric stretch which is a doublet for the equated peak generates two more-widely separated bands, one of which is polarized in the Raman spectrum; polarization of the lower frequency member of the pair is indicative of unidentate cation-nitrate ion binding whereas polarization of the higher frequency member of the pair is indicative of bidentate orientation; the deformation mode occurs at a frequency higher than 718 cm^{-1}. The Raman peak at 1050 cm^{-1} was assigned to the (NO_3^-) (nitrate peaks) [102]. If the peak shifts to lower wave numbers,

this vibration can be assigned to the ($NO_3^-Hg^+$). The Raman signal at about 718 cm^{-1} was assigned to the $Hg^+NO_3^-$ deformation mode (shown in figure 51). In the case that this vibrational mode shifts to higher wave numbers, then it will be assigned to the $NO_3^-Hg^+$ deformation mode. A very strong band at wave numbers higher than 170 cm^{-1} can be assigned to the large non-bonded Hg-Hg stretching mode in the crystals. The absence of the band at about 1385 cm^{-1} suggests that no Hg(II) was formed (figure 54).

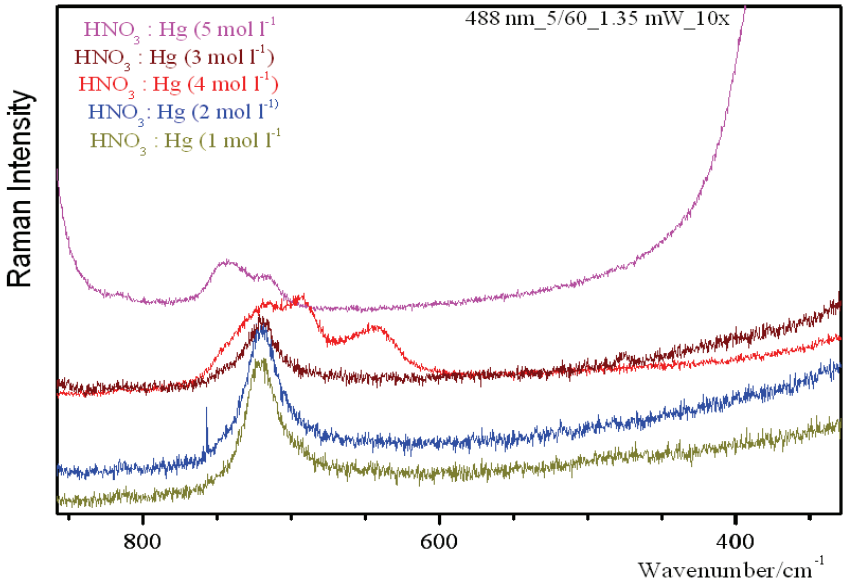

Figure 54: Mercury (I) nitrate ions identification in aqueous phase by Raman spectroscopy (wave numbers range 300-900)

At higher molar ratio, the concentration of Hg (I) is reduced in solution and leads to the formation of mercury hydroxides and oxides. Controlling the dissolution reaction of mercury in nitric acid is an important step for a secondary reaction called precipitation to HgS. Our investigations indicated that a ratio of HNO_3 to Hg of about 2 - 3 plays a critical role. Dissolution is limited by heat generation because of the exothermic reaction. This limitation is overcome by continuous cooling of the whole system for a long time (approximately 24 - 48 hrs).

Due to the complex spallation process (EURISOL/ESS targets), various nuclear reaction products will occur in different states. Many elements produced by nuclear reactions will undergo chemical reactions also with structural materials and impurities and form solid

compounds, e.g. oxides or intermetallic phases, which have a low solubility in Hg. These compounds, according to density, will tend either to float on top of the liquid metal (most probable), to sediment or to form particles dispersed in metallic mercury. Hardly soluble elements in mercury may also be precipitated at a cold surface as solid particles. The oxidative dissolution step in the wet process generates ionic soluble form of almost all metals and also of mercury in an aqueous phase that will facilitates the next step.

4.4.2.2. Precipitation of HgS from ammonium nitrates solution

A broad spectrum of technologies of mercury treatment has been described in the technical literature, ranging from established full scale applications to innovative approached investigations which are to date only at bench scale or pilot scale. The literature, however, provides only limited information on actual full scale treatment technologies performance and almost no full scale economic date of a mercury solidification process.

One of the more commonly reported in literature for precipitation methods for removal of inorganic mercury from waste water is sulfide precipitation. In this process, sulfide (e.g., as H_2S, sodium sulfide or another sulfide salt) is added to the waste stream to convert the soluble mercury to the insoluble mercury sulfide form [103]: Here also the same technique is applied to convert all the soluble mercury in aqueous phase to insoluble form as HgS with precipitating agent $(NH_4)_2S$. The sulfide precipitant as $(NH_4)_2S$ is added to the mercury nitrate solution in a stirred reaction vessel, where the soluble mercury is precipitated as mercury sulfide. The precipitated solid as HgS (Cinnabar) is then removed by gravity settling in reaction vessel as shown in figure 51 and followed by filteration step. Table-12 presents the sulfide treatment results with respect to the molar ratio of Hg and the precipitating agent $(NH_4)_2S$. Literature report suggests that for initial mercury levels in excess of one mg/L, sulfide precipitation can achieve 99% removals of mercury. In our experimental studies it was found that the dissolution of mercury occurs with a reasonable rate at temperatures of 50 – 80℃. Neutralization was performed at temperatures lower than ambient, as the precipitation of the HgS, too. The whole process went straightforward, as it is required in hot cell facility.

$$HgS + S^{2-} \longrightarrow [HgS_2]^{2-} \longrightarrow \quad (9)$$

$$[HgS2]^{2-} + H_20 \longrightarrow HgS + OH^{-1} + HS^{-} \longrightarrow \quad (10)$$

$$[HgS2]^{2-} + NH_4^{+} \longrightarrow HgS + NH_3 + HS \longrightarrow \quad (11)$$

There is some solubility of HgS in polysulphides so that an excess of sulphur in the product should be avoided. In the literature it is suggested that a maximum excess of 10 – 30 % is tolerable. For that the composition of the product was analyzed depending on the Hg/S ratio in the reacting solutions. The reaction mechanism for the formation of HgS precipitation is given in equations by 8, 9. 10. Mercuric sulfide is insoluble in hydroxide solution. But it is sufficiently acidic and that influences the HgS to dissolve at higher concentration of sulfide present in solutions via reaction 8. Such solutions precipitate the sulfide upon dilution because hydrolysis of equilibrium sulfide ion as in reaction 9. Maintenance of species in the solutions thus requires large quantities of metals, alone or with added alkali metal hydroxide.

Molar ratio Hg : $(NH_4)_2S$	Hg (mol %) in precipitate	S (mol %) in precipitate	Amount of Hg in filtrate (µg/l)
1:1	47.3	52.7	0.072
1:2	49.1	50.9	0.068
1:3	44.2	55.8	0.104
1:4	37.1	62.9	0.092
1:5	30.5	69.5	0.304

Table 12: Product and residue composition depending on the Hg/S ratio in solution

As table-12 indicates for a sulphur excess by a factor of 2 in the solution an almost stoichometric product is gained with only a slight excess of sulphur. The composition of this product is almost ideal. For a sulphur excess by a factor of 4 or 5 in solution an excess in the solid product by a factor of 1.7 was measured, which is too high. Accordingly the excess of sulphur in the solution should be restricted to about 2. The table also contains the residual mercury concentration in solution: Values of < 0.1 µg/l were found, which is sufficiently low. Altogether this means that this procedure allows a complete conversion of liquid Hg to solid HgS. As in this precipitation treatment, the process is usually combined with pH adjustment, at the beginning, the pH of solution was not fully recorded, but it remained always acidic. After the neutralization step, $(NH_4)_2S$+water was added slowly as a buffering agent to stabilization of pH and to precipitate any mercury form to mercury sulfide. The total concentration of mercury in solution was monitored for kinetic studies with pH monitoring too. Figure 55 indicates that concentration of ionic mercury during precipitation reaction. The

most effective precipitation, with regard to minimizing sulfide addition, is reported to occur in the near neutral pH range. Precipitation efficiency declines significantly at pH above 9 (Patterson, 1985). The molar ratio has clear effect on the precipitation. The prolongation of the reaction time has a negligible effect and less than 8 hrs is enough for total precipitation reaction to be finished.

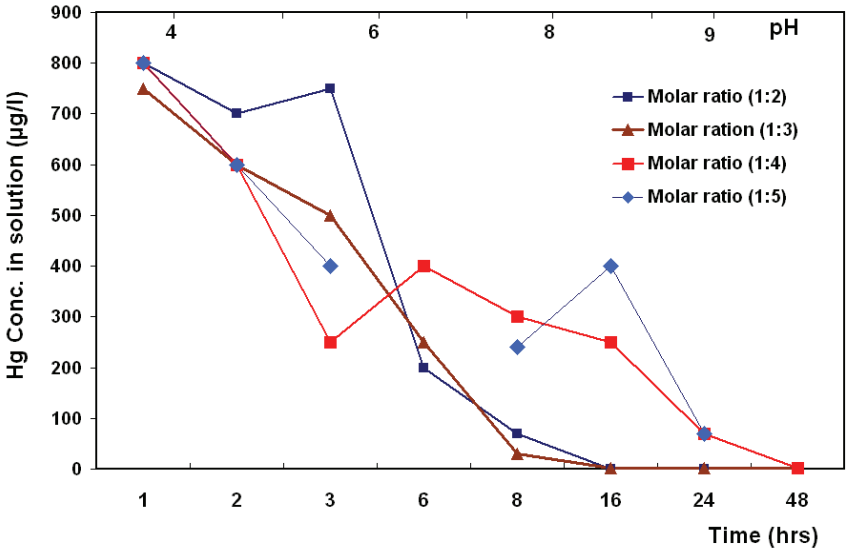

Figure 55: Concentration profile of Hg in solution during the HgS precipitation process

After that the precipitated mercury sulfide sample (shown in figure.48) was filtered and dried over 2 days in dessicator. After that the sample was analyzed for the mercury phases and purity of formed mercury sulfide. In figure 53 XRD data of formed mercuy sulfide are depicted. It suggests almost pure mercury sulfide and there is no visible unstable meta-cinnabar in the final compound.

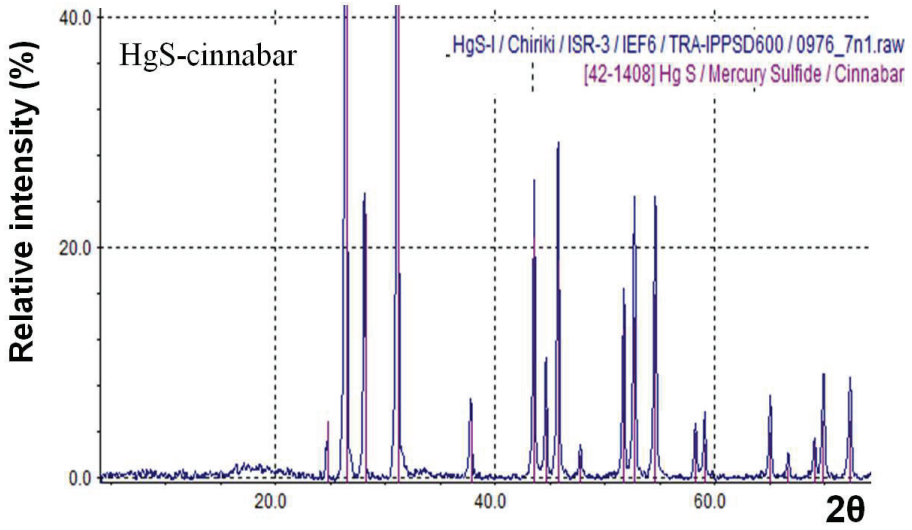

Figure 56 : XRD information of stable cinnabar phase can be synthesized by wet process

It can be conclude that the above examined process mainly depends on the dissolution acid (HNO_3) and soluble precipitating agent $(NH_4)_2S$ which is added to the elemental mercury at a ratio of 1:3 and 1:2 for complete conversion to final insoluble form of HgS. In this process, the precipitated mercury compound is removed by a physical separation process. Additionally solutions from filtration step can be recycled to remove all dissolved mercury. The main advantage is that elemental mercury conversion to solid form is almost 99.8%.

There are an extraordinary number of patents and papers that deal with the treatment of mercury. Many of the described processes are adapted and optimized to special applications of the used mercury and the removal of a certain kind of impurities. But sulfide precipitation appears to be the common practice for mercury treatment in many chlor-alkali plants already. The removal efficiencies of 95 to 99.9 percent are reported for well designed and managed processes. The same well designed chemical process engineering techniques can be applied to up scale this wet sulfide treatment process to handle large amounts of elemental radioactive mercury in batch experiments in hot cells.

4.5. Development and scale up studies

During the research and development of a new chemical process, one of the problems that merits close to attention and often proves to be problematic is the scaling up. The focus here is especially on the chemical treatment process of irradiated elemental mercury relevant to the radioactivewaste management industry. In fact, however, the problems are similar for all material conversion processes, and the methodology presented can therefore be applied equally well to the chemical and allied industries. Radiation protection guide lines have also come into considerations to up scale such chemical processes.

The starting point generally consists of laboratory results that concern chemical transformation whose translation to economic gain appears viable. Process development should serve to treat quantities of raw materials to large scale, amounting to tons, where as only grams or kilograms of the raw materials are used in laboratory. This is the precise function of change of scale or scale up. The problem is to reproduce the laboratory results on a large scale: in other words, to achieve the same conversions, yields and selectivity and in some cases, possibly improve the results.

To go directly from laboratory to large scale is rarely feasible. As a rule, one or more additional parameters are necessary. Specifically, the problem is to define these additional steps in order to gather all the information required at maximum safety and economically feasibility. It is here that the methodology of process devolvement, and hence of scale up, becomes decisive for success of the operation. Different phases are some distinguished in the devolvement of a process, by referring to scale at which the experiment is conducted.

In our laboratory-type experiments, certain aspects of the chemical process are investigated by handling relatively small amounts of mercury in order to meet safety requirement. Our investigations on mercury solidification and disposal outlined here is a first step in development of a complete disposal strategy for a mercury target. It may however be taken as an indication that the disposal of proton irradiated mercury is possible even within the strict limitations of European regulations. However because of the required solidification, which as a chemical process resembles to a small scale nuclear reprocessing step, the effort is very large compared to target materials which do not need a solidification process. Before upscaling, this type of chemical process requires a lot engineering studies and chemical safety analysis relevant to hot cell conditions.

4.6. Cost estimation studies

In principle, for a cost estimation of the whole process in a radioactive waste treatment plant, detailed knowledge of each separation step and its technical implementation is important. The detailed implementation of a suitable waste treatment plant based on distillation or aqueous treatment techniques into the EURISOL design will largely depend on the peculiarities and details of the transfer of conventional methods to a highly radioactive environment and its adaptation to the overall layout of the EURISOL facility. Furthermore, there is a complete lack of experience with the handling of large amounts of radioactive mercury. In particular, the combination of high radioactivity, chemical toxicity and volatility is special to this material and poses problems that have not been encountered before. Because of the little information available, in this report we have to confine ourselves to derive estimations for the costs of such a plant, based on the information we collected from companies that run conventional industrial purification plants. This will be combined with recommendations concerning the transfer to a radioactive environment obtained from experts in the field of radioprotection, technical radiochemistry and radioactive waste management at Julich and PSI. These estimations should give a reasonable order of magnitude for the costs that will arise from the setup and operation of a chemical treatment of the complete amount of mercury within the EURISOL multi-MW target based on conventional treatment techniques. It should be pointed out that very crude assumptions were taken for this estimation of the additional costs of radioprotection such as shielding, monitoring, filtering and venting systems and the costs caused by the disposal of the additional waste produced. Therefore, a relatively large error margin is possible here. A more detailed discussion of this estimation is presented below.

Finally, these assumptions led to the conclusion that a radioactive plant for mercury treatment should, in a conservative assessment, be at least 20 times as costly as a conventional one.

We will confine our estimations to those conventional treatment techniques that seem feasible for. Alternative chemical methods that could be especially suitable for a spallation system are discussed in the following section. Since these methods have not been applied in an industrial scale, there is no knowledge with respect to efficiency and economical practicability. For some of these methods, even fundamental research has to be completed before a technical up scaling can be envisaged. Therefore, we will not give any cost estimations for these methods.

For both conventional treatment techniques considered, i.e. amalgmation and sulphide precipitation techniques, where chemical laboratory installations allowing high levels of radioactivity are required. These have to be integrated into the hot cell of the spallation source unit. Depending on the treatment method chosen, this laboratory has to be furnished with special safety equipment and installations, i.e. double enclosures, gas monitoring and mercury gas filtering systems for a distillation plant or corrosion or acid resistant systems and installations for the handling of large amounts of acid aqueous solutions in case of a wet process. Therefore, the price for devices treating high level radioactive mercury is obviously several times higher than for conventional plants. After discussion with experts, we estimate that a reasonable cost multiplier for the transfer of a conventional mercury distillation to a plant for highly radioactive mercury would lie in the range 10 to 20. For conservative cost estimation, we will use a multiplier of 20 in the following. We stress again at this point that the following estimations are not precise and give only the order of magnitude of the costs that have to be expected.

Nuclear Fuel Services, Inc developed amalgamation process called NFS DeHg^{SM} early 1990. They projected costs for treating more than 1,500 kg were 200€/kg, assuming waste is elemental mercury (there is not data available about specific activity) and does not include disposal costs of the treated waste. At the Pacific Northwest National Laboratory, DOE conducted laboratory scale testing of the Sol-Gel process to stabilize high salt content waste. Two salt-containing, non-radioactive surrogates - one with high levels of nitrate salts and one with high levels of chloride and sulfate salts - were used for the tests to simulate wastes at DOE facilities. While a detailed cost analysis had not been performed on the process, an order of magnitude estimate indicates that the process would cost in the range of 500,000€ to 1€ million.

Idaho National Engineering and Environmental Laboratory's (INEEL) results showed that the polysiloxane process produced a durable waste form for all three high-salt content surrogates. The waste forms met the target TCLP levels for heavy metals, and the more stringent UTS standards for several of the metals tested. The process is currently limited to nonaqueous solid materials. Treatability testing is recommended for specific wastes prior to use of this technology. In addition, long-term durability testing of the polysiloxane waste forms is needed. Costs for full-scale polysiloxzane treatment are about $8/lb or $573 per cubic foot of salt waste. The cost for polysiloxane encapsulation is competitive with the baseline technology of Portland cement stabilization.

Considering non-cost criteria only, the storage options rank most favorably. If both cost and other criteria are considered, then landfill options are preferred, because they are the least expensive ones. Long term storage options ranked unfavorably on cost because: (a) even relatively small per annum costs will add up over time; and (b) storage is a temporary solution and, sooner or later, a treatment and disposal technology will be adopted, which adds to the cost. However, current analysis supports continued storage for a short period (up to a few decades) followed by permanent disposal when treatment technologies have matured.

Considering the above points, these estimations do not include the decommissioning costs of the plant after the shut-down of the facility and the disposal of the additional waste produced by each chemical and technical operations. These are not negligible. Since the costs for the decommissioning of 1 m^3 of radioactive waste are currently about 70 k€ to 100 k€

A wet process would probably be a little less expensive regarding the costs of installation and operation, but produces a large amount of liquid waste that is difficult and expensive to dispose. Depending on the frequency that is chosen for the disposal procedure, this can lead to exorbitant costs. [SNS and ESS cost estimates, see EURISOL deliverable last chapeter]

5. Summary

Radioactive mercury and radioactive waste management can be seen as extreme cases where the modern notions of risk management and product control reach almost their limits. The hazards associated with these categories of waste entail a requirement for safe handling over long term. At the same time, it is not possible to fully predict the consequences of any chosen way of waste disposal. Despite these uncertainties, those who supply the proposed solutions to mercury radioactive waste disposal cling to the notion of safety- i.e. any future leakage will be minimized to a level that is harmless to human health and the environment. In the course of achieving effective final disposal of radioactive mercury waste, there are many uncertainties. Since the issue of risk versus safety almost always becomes a major point. These investigations would argue that the adherence to the notion of predictable long-term safety and provides a path final disposal of mercury waste.

About 15000 kg (1.1 m^3) of mercury will be irradiated in the EURISOL target for about 30 years. After shut down (about 10 years) the mercury still contains an activity of about $6 \cdot 10^6$ GBq. Mercury must be solidified prior to disposal. It is advisable to start treatment of irradiated mercury for production of waste packages not earlier than after 5 – 10 years of cooling time, because in this period a decay of activity by a factor of 10 has to be expected (decay storage). The facilities therefore need an action plan for the conditioning of mercury waste.

The main objectives of the present work were to perform R&D on the behavior of mercury compounds under repository conditions and which mercury solid compounds will be embedded in a suitable matrix for safe disposal. Another major task is a chemical engineering study on the mercury solidification and the design of an experimental setup for Hg-solidification which is suitable for hot cell laboratories.

5.1. Selection of solid mercury compounds

The initial selection of mercury compounds is based on solubility data. Solid compounds of mercury considered for our investigations are inorganic compounds (HgS, HgSe and Hg(I) nitrate and alloys (Ag-amalgam and Cu-amalgam)). Organic compounds are not considered because of their smaller stability under radiation and their even more pronounced conventional toxicity and mobility.

In general the risk dominating accident in most European repositories is water ingress. In salt mines (German concept) the ingressing water will be converted into salt brine. For accidents in clay repositories (Swiss concept) solutions with low salt concentrations have to be expected. In any case γ-radiation, which from the radwaste packages induces radiolytic reactions. Experiments were performed to study stability of hardly soluble solid mercury compounds [(HgS, HgSe and Hg(I) nitrate) and alloys (Ag-amalgam and Cu-amalgam)] in water, clay water and salt brines under γ-irradiation (5 - 25 kGy/h) at temperatures of 50 – 60℃ to reciprocate the repository conditions. Thes e experiments were done for 2 - 3 months in the spent fuel storage of the FRJ-II DIDO reactor.

The main conclusion drawn from our experimental investigations is that the stability of amalgams during water ingress in a repository is less than that of chalcogenides (HgS and HgSe). Further, formation of amalgams from elements without un-reacted mercury creates chemical engineering problems under hot cell conditions. The Ag-amalgam process is a complex chemical process and it is not easy to perform it at room temperature. Loading of Hg in amalgams is therefore questionable. The presence of radiation reduces the stability HgS and HgSe in salt brines and in Opalinus clay water. Despite of its better dissolution behavior mercury selenide (HgSe) was not considered for more detailed studies: High costs and the biotoxicity of selenium (Se) are major disadvantages. Hence HgS is selected as final disposal compound for further investigations related to immobilization by encapsulation techniques

5.2. Matrix embedding studies in HgS with cement and polysiloxane materials

For the stabilization/solidification of hazardous metallic wastes cement and its supportive materials (like pulverized fly ash and blast finance slag materials) are the most commonly used encapsulation materials. In these investigations, cement was used as one of the encapsulating materials with chalcogenides (HgS and HgSe) and Hg (I) nitrate. As expected the retention of soluble $HgNO_3$ is relatively small compared to HgS in cement matrix. These investigations also reveal that the combination of HgS-cement matrix is not fully stable at all final disposal conditions. Alkaline conditions and cement chemistry destabilized Hg-cement matrix and enhances the Hg release into solutions under γ-radiation. Another important point to be considered seriously here is that the volume of waste generated is increased too. These considerations resulting in work on an alternative encapsulating material. Polysiloxanes are considered for investigations. Previously Julich research center had done

lot of investigations on thermal and radiation stabilities of polysiloxane materials extensively. These results were implicated to these investigations. Unfortunately we were not able to perform leaching experiments on polysiloxane embedded HgS under γ-irradiation due to the shut down of the facility. Our leaching experiments without γ-irradiation however have shown that encapsulating HgS in polysiloxane may potentially be the best option in relation to cement encapsulation. The high salt concentration itself seems to have virtually no influence on the dissolution of the materials investigated, and the “aggressiveness” of $MgCl_2$ - rich brine is attributed mainly to the relatively low solution pH. Our investigations proved that HgSe with polysiloxane is best encapsulating technique, but this rules out for the same reasons as discussed before. Multilayer encapsulating HgS in polysiloxane fulfills the primary purpose of the barriers in the repositories to isolate the waste, to protect human health and to protect the environment. In case of any leakage, the barriers shall impede or delay the transport of the hazardous substance to the biosphere.

5.3. Conversion of elemental mercury to mercury sulfide

The fundamental reaction for generation of mercury sulfide or cinnabar (HgS) is by mixing elemental mercury Hg° and sulfur source. As known by the negative ΔG_f°, formation of cinnabar is theoretically feasible by mixing elemental mercury and sulfur (elemental sulfur power, Fe_2S, and FeS). These investigations have shown that this reaction is not feasible at room temperature and it is time consuming and the most important Hg-conversion of 100% is not achievable. There is also the danger of stirrer break down during the operation which creats major safety and operational problems under the required hot cell conditions. All these factors lead us to develop a new process based on wet process chemistry starting from elemental mercury to HgS. Based on the requirements, a small laboratory experimental set up was built up with 2 liter capacity.

Several experiments were done on the wet process dissolving Hg by HNO_3 and precipitating HgS by adding $(NH_4)_2S$. Our investigations reveal that an almost 99.9% Hg conversion can be achieved. The analyses of HgS formed reveal that it is almost pure. Whereas for a mole ratio S/Hg of 2 in the solution the product is almost stoichometric HgS with a slight Sulfur excess, higher ratio leads to a more pronounced excess of sulfur in the precipitate. The concentration of Hg in the filtrate was negligible. This invention related was generally to the process of removing of mercury from waste streams in industrials environment. More specifically, the present invention is directed to continuous process and safe handling of mercury in hot cell condition. The whole wet chemical process is controlled easily by properly engineering techniques.

6. Outlook

This thesis work evaluated the effectiveness of diverse methods for conversion of radioactive mercury into a sufficiently stable solid, which includes encapsulation in matrices.These investigations are intended to allow decision makers sufficient insights into this problem However, this thesis should be taken as a first step and respective work has to be continued. Future work should include: Reduction of pH of concrete for a better stability of mercury compounds has to be examined. Mercury compound encapsulation with polysiloxane remains to be investigated under gamma irradiation.

Separation of other nuclides than Hg from a spent target should be studied more detailed, too. Solidification/stabilization of elemental mercury is done up to now by chemical wet process. The route for formation of mercury sulfide was done in a laboratory scale only. Up scaling to pilot plant and pilot plant to large scale studies have to be investigated seriously and safety analysis has to perform relevant to hot cell condition.

7. Acknowledgments

My special and sincere thanks are addressed to Prof. Dr. Reinhard Odoj for offering me this PhD position in his group and for motivating and supporting me during all these years.

It is a great pleasure to offer my sincere thanks to my Ph.D. supervisor, Dr. Rainer Moormann, who continuously oriented me in the correct research direction, with his constructive support and his great efforts to explain things clearly and simply, has helped me to gain a better understanding.

I am grateful to Prof. Dr. Dirk Bosbach for being reviewer of work and also for important his technical remarks and advices.

Sincere thanks to Dr. J. Fachinger for intellectual support, also supervising my work and scientific discussions especially at beginning.

Special thanks are addressed to H. K. Hinssen for his day to day technical support during my experimental set up design and problems. Sincer thanks are addressed to Chemical analytical department (ZCH juelich) people (Dr. Peica for Raman spectrometry analysis, Dr. Besmehn and Dr. E. Joussen) and for their technical support for analyzing my experimental samples.

The experiments under γ-irradiation would not have been possible without the assistance of F. Kreutz, M. Thomé, and the DIDO team. I appreciate the support from Dr. A. Bukaemskiy, who helped me in the scanning electron microscopy studies. Thanks are due to W. Jahn for solving all computer related problems.

And of course, I would like to express my gratitude to all my colleagues at the Institute for Safety Research and Reactor Technology (ISR-3) and their collaboration and help in daily routine work. For a successful thesis, not only the scientific part was important but also the ambient in the group (sincere thanks to Prof. Hans Ullmaier, Bärbel Schlögl and Dr. Karl Verfondern) at work place. I am greatly indebted to Dr. Dorothea Schumann and Dr. Jörg Neuhausen for their support and encouragement to complete of this work and I proudly can say that I learned a lot about this project during stay at the PSI.

Last, but not least, I thank my family: my parents, for giving me life, for educating me, for unconditional support and encouragement to pursue my interests, even when the interests went beyond boundaries of language and geography.

I greatly acknowledge the financial support of the European Community under the FP6 "Research Infrastructure Action - Structuring the European Research Area" EURISOL DS Project Contract no. 515768 RIDS.

8. Literature

1. Bowman, C.D., et al., *Nuclear-Energy Generation and Waste Transmutation Using an Accelerator-Driven Intense Thermal-Neutron Source.* Nuclear Instruments & Methods in Physics Research Section a-Accelerators Spectrometers Detectors and Associated Equipment, 1992. **320**(1-2): p. 336-367.

2. Jameson, R.A., G.P. Lawrence, and C.D. Bowman, *Accelerator-Driven Transmutation Technology for Incinerating Radioactive-Waste and for Advanced Application to Power Production.* Nuclear Instruments & Methods in Physics Research Section B-Beam Interactions with Materials and Atoms, 1992. **68**(1-4): p. 474-480.

3. Bauer, G.S., et al., *A target development program for beamhole spallation neutron sources in the megawatt range.* International Conference on Accelerator-Driven Transmutation Technologies and Applications, 1995. **346**: p. 105-116.

4. Bauer, G.S., *Technology issues in the design of medium-to-high power spallation targets for accelerator driven systems.* Journal De Physique Iv, 1999. **9**(P7): p. 91-113.

5. Ni, L., G.S. Bauer, and H. Spitzer, *Effects of pulsed power input into a liquid metal target.* Nuclear Instruments & Methods in Physics Research Section a-Accelerators Spectrometers Detectors and Associated Equipment, 1999. **425**(1-2): p. 57-64.

6. SNS, *SNS Preliminary Safety Analysis Report (PSAR), update 2002, DOE,.* 2002.

7. Moormann, R., *ESS-Target inventories and their radiotoxic and toxic potential, Document ESS-R-1205-R.Moormann-1-02.* 2003.

8. ESS, *http://www.neutron-eu.net: Neutrons - Documentation – Reports- ESS reports & more – Fact sheets.* 2003.

9. IAEA, *Decommissioning Techniques for Research Reactors, Technical Report Series No. 373:* . 1994: Vienna.

10. Ene, D., et al., *Radiation protection aspects of the EURISOL Multi-MW target shielding (EURISOL DS/Task5).* 2009. (http://www.eurisol.org)

11. EURISOL. (http://www.eurisol.org).

12. Taylor, A., et al., *A Route to the Brightest Possible Neutron Source?* Science, 2007. **315**(5815): p. 1092-1095.

13. Broome, T.A., *High power targets for spallation sources, RAL 96-053 and Proc EPAC 96*. 1996.

14. Henry, J., T. Auger, and Y. Dai, *Operation of High Power Liquid Metal Spallation Targets: a Challenge for the Structural Materials*. 2008: Springer Netherlands. 575-584.

15. http://megapie.web.psi.ch/documents/megapie.pdf.

16. Haines, J.R., *Cavitation-erosion in mercury spallation neutron target source.* Journal of Nuclear Materials, 2005. **343**(1-3): p. 366-366.

17. Tanaka, N., M. Suzuki, and M. Futakawa, *Numerical analysis of mercury cavitation in MW-scale spallation neutron source system.* Nuclear Instruments and Methods in Physics Research Section A: Accelerators, Spectrometers, Detectors and Associated Equipment, 2006. **562**(2): p. 680-683.

18. Randall, P. and S. Chattopadhyay, *Influence of pH and oxidation-reduction potential (Eh) on the dissolution of mercury-containing mine wastes from the Sulphur Bank Mercury Mine.* Minerals & Metallurgical Processing, 2004. **21**(2): p. 93-98.

19. http://www.gedeon.prd.fr/ATELIERS/27_28_novembre_2006/exposes/Targets_Reactor_Coolants_groeschel.pdf.

20. BfS, *The Konrad Repository Project. Published by Federal Office for Radiation Protection, Salzgitter, Germany*. 1994.

21. StrlSchV, *Verordnung über den Schutz vor Schäden durch ionisierende Strahlung (Strahlenschutzverordnung), Bundesgesetzblatt, Teil I, G5702, 26.Juli 2001, Nr. 38*. 2001.

22. Freeman, D., P.D. Ferguson, and E. Iverson. *Method for maintaining SNS target activity below regulatory limits during initial operations*. in *Proc. ICANS-XVI, 2003 Neuss*.

23. D Filges, B Lensing, K Nünighoff, Ch Pohl, H Schaal, G Sterzenbach. *Determination of Radioactivity, Energy Deposition and Radiation Damage in the TMR Components of ESS*. in *Proc. ICANS-XVI,* . 2003. Neuss.

24. Boudard, A., et al., *Applications of the spallation knowledge, two examples: EURISOL and MEGAPIE*. 2006.

25. Lowrie, R.R., *Chemistry and Physics Challenges in Spallation Neutron Source Safety Analyses*. 2001 (Internal report from SNS)

26. Brennecke, P., *Aspects of repository storage related to ground water.* Atw-Internationale Zeitschrift fur Kernenergie, 1998. **43**(12): p. 779-783.

27. Berg, H.P. and P. Brennecke, *Basic Considerations on Radioactive-Waste Classification Regarding the Different Waste Management Steps.* Kerntechnik, 1993. **58**(5): p. 264-268.

28. Berg, H.P., et al., *Safety Assessment of the Thermal Influence Upon the Host Rock of the Planned Konrad Repository.* Kerntechnik, 1995. **60**(1): p. 56-61.

29. EC, *valuation of radiological and economical consequences of decommissioning particle accelerators, European Commission, Report 19151 EN, Luxembourg*. 1999.

30. NDA:, *National policies on the long-term management of higher activity wastes*. 2008.

31. NAGRA, E*ntsorgungsprogramm und standortgebiete für geologische tiefenlager*. 2008.

32. SKB, *SKB Annual Report 1996. SKB Technical Report TR 96-25*. 1996a, SKB: Stockholm, Sweden.

33. SKB, *Treatment and final disposal of nuclear waste. Programme for encapsulation deep geological disposal and research development and demonstration* 1995a, SKB: Stockholm, Sweden.

34. SKB, *Template for safety reports with descriptive example.* . 1995b, SKB: Stockholm, Sweden

35. SKB, *Kärnkraftavfallets behandling och slutförvaring (The handling and final disposal of radioactive waste), FUD-Program 98*. 1998a, SKB: Stockholm, Sweden.

36. Ericsson, L.O., *Geoscientific R&D for high level radioactive waste disposal in Sweden -- current status and future plans.* Engineering Geology, 1999. **52**(3-4): p. 305-317.

37. Swedish-EPA, *Slutförvar av Kvicksilver. Huvudrapport (Final Disposal of Mercury. Main Report), Report No. 4752*. 1997, Swedish Environmental Protection Agency: Stockholm, Sweden.

38. Bandt, G., Spicher, G., Steyer, S., Brennecke, P. *Disposal of LLW and ILW in Germany: Characterization and Documentation of Waste Packages with Respect to the Change of Requirements*. in *Proceedings of WM08, Waste Management 2008 Symposium*. 2008. Phoenix, Arizona, .

39. Baltes, B., Brennecke, P., *Safety Requirements on Heat-generating Radioactive Waste. – In: Proceedings of the International Conference Radioactive Waste Disposal in Geological Fomations, Report GRS-S-49,Köln, Oktober*. 2008.

40. Brennecke, P. and B. Thomauske, *Final Storage in Germany.* Atomwirtschaft-Atomtechnik, 1993. **38**(4): p. 280-284.

41. Brennecke, P., K. Kugel, and W. Noack, *Morsleben waste acceptance requirements.* Atw-Internationale Zeitschrift Fur Kernenergie, 1997. **42**(4): p. 237-241.

42. Kobayashi, K., et al., *Physical and thermochemical properties for inorganic mercury compounds*. 2000.

43. Knacke, O., Kubaschewski, O. and Hesselmann, K., *Thermochemical properties of inorganic substances*. 1991: Springer-Verlag., Heidelberg. 877-890.

44. Roesmer, J., *Radiochemistry of Mercury*. 1970: U. S. Atomic Energy Commission.

45. Latimer, W.M., *The Oxidation states of the elements and their potentials in aqueous solutions*. 1952: Prentice-Hall, Inc.

46. Branden, C.I., *Structural Chemistry of Some Mercury (2) Complexes.* Svensk Kemisk Tidskrift, 1964. **76**(12): p. 715-&.

47. Eichler, B., R. Dressler, *Löslichkeit von Kernreaktionsprodukten im Quecksilber-Spallationstarget – Bedeutung für das Betriebsverhalten und Möglichkeiten der Kalkulation*, in *PSI-Report 99-02*. 1999.

48. McWhinney, H.G., et al., *An investigation of mercury solidification and stabilization in portland cement using X-ray photoelectron spectroscopy and energy dispersive spectroscopy.* Cement and Concrete Research, 1990. **20**(1): p. 79-91.

49. Hultgren, R., et al. *Selected values of the thermodynamic properties of binary alloys*. in *American Society for Metals*. 1973. Metals Park, Ohio.

50. Guminski, C., *Metals in Mercury*. IUPAC Solubility Data Series, ed. A.S.K.e. al. Vol. 25. 1985, Oxford: Pergamon Press.

51. Dewet, J.F. and R.A.W. Haul, *Zur Löslichkeit Einiger Übergangsmetalle in Quecksilber.* Zeitschrift für Anorganische und Allgemeine Chemie, 1954. **277**(1-2): p. 96-112.

52. Guminski, C., *On Some Thermodynamic Aspects of the Formation of Intermetallic Compounds in Mercury*. Zeitschrift Fur Metallkunde, 1986. **77**(2): p. 87-96.

53. Allen, E.T., J.L. Crenshaw, and H.E. Merwin, *Sulfides of zinc, Cadmium and Mercury: their Crystallinn Forms and Genetic Conditions.* American Journal of Science, 1913. **34**: p. 341-97.

54. Kullerud, G., *The mercury-sulfur system*. Vol. 64. 1965: Year Book - Carnegie Institution of Washington. 19-5.

55. Dickson, F.W. and G. Tunell, *The Stability Relations of Cinnabar and Metacinnabar.* American Mineralogist, 1959. **44**(5-6): p. 471-&.

56. Tauson, V.L., M.G. Abramovich, and L.F. Paradina, *Stoichiometry and relative stability of the alpha and beta modifications of merrcury sulfide.* Trans. from Geokhimiya, 1983(12): p. 1706-1719.

57. Mikac, N., et al., *Influence of chloride and sediment matrix on the extractability of HgS (cinnabar and metacinnabar) by nitric acid.* Analytical and Bioanalytical Chemistry, 2003. **377**(7): p. 1196-1206.

58. Mikac, N., et al., *Extractability of HgS (cinnabar and metacinnabar) by hydrochloric acid.* Analytical and Bioanalytical Chemistry, 2002. **374**(6): p. 1028-1033.

59. Clever, H.L., S.A. Johnson, and M.E. Derrick, *The Solubility of Mercury and Some Sparingly Soluble Mercury Salts in Water and Aqueous-Electrolyte Solutions.* Journal of Physical and Chemical Reference Data, 1985. **14**(3): p. 631-681.

60. Schwarzenbach, G. and W. Michael, *Die Löslichkeit von Metallsulfiden I. Schwarzes Quecksilbersulfid.* Helvetica Chimica Acta, 1963. **46**(7): p. 2613-2628.

61. Poon, C.S., et al., *Permeability study on the cement based solidification process for the disposal of hazardous wastes.* Cement and Concrete Research, 1986. **16**(2): p. 161-172.

62. Tossell, J.A., *Calculation of the Structures, Stabilities, and Properties of Mercury Sulfide Species in Aqueous Solution.* The Journal of Physical Chemistry A, 2001. **105**(5): p. 935-941.

63. Marshall, S.J. and G.W. Marshall, *Dental Amalgam - the Materials.* Advances in Dental Research, Vol 6, 1992: p. 94-99.

64. Bracho-Troconis, C., et al., *Influence of thermal treatments on Ag Sn Cu powders in order to reduce mercury contents in dental amalgam.* Journal of Materials Science: Materials in Medicine, 2000. **11**: p. 1-9.

65. Zebreva, A.I. and Kozlovsk.Mt, *Effect of Formation of Intermetallic Compounds on Amalgam Methods for Determining Metals.* Industrial Laboratory, 1965. **30**(10): p. 1477-&.

66. Carnasciali, M.M. and G.A. Costa, *CuxHgy: a puzzling compound.* Journal of Alloys and Compounds, 2001. **317**: p. 491-496.

67. Sunier, A.A. and C.B. Hess, *The solubility of silver in mercury.* Journal of the American Chemical Society, 1928. **50**: p. 662-668.

68. Okabe, T., et al., *Dissolution of Mercury from Amalgam into Saline Solution.* Journal of Dental Research, 1987. **66**(1): p. 33-37.

69. W. Hawickhorst, et al. *Liquid Waste Treatment from Source to Final Disposal*. in *Waste Management 1999*. 1999. Tucson (AZ).

70. NFS, *Demonstration of the DeHg Stabilization Process for Treatment of Radioactively Contaminated Wastes Containing < 260 ppm Mercury and Other RCRA Metals (MER02)*. 1998.

71. MWFA, *Innovative Technology Summary Report—Amalgamation Demonstration of the DeHg Process*, in *Mixed Waste Focus Area*. 1998.

72. DOE, *Stabilize High Salt Content Waste Using Polysiloxane Stabilization*, in *Mixed Waste Focus Area(DOE/EM-0474)*. 1999.

73. Oji, L.N., *Mercury disposal via sulfur reactions.* Journal of Environmental Engineering-Asce, 1998. **124**(10): p. 945-952.

74. Fuhrmann, M., et al., *Sulfur polymer solidification/stabilization of elemental mercury waste.* Waste Management, 2002. **22**(3): p. 327-333.

75. Svensson, M., A. Duker, and B. Allard, *Formation of cinnabar - estimation of favourable conditions in a proposed Swedish repository.* Journal of Hazardous Materials, 2006. **136**(3): p. 830-836.

76. Trussell, S. and R.D. Spence, *A Review of Solidification Stabilization Interferences.* Waste Management, 1994. **14**(6): p. 507-519.

77. Atkins, M. and F.P. Glasser, *Application of portland cement-based materials to radioactive waste immobilization.* Waste Management, 1992. **12**(2-3): p. 105-131.

78. M. Atkins., F.G., *Application of portland cement-based materials to radioactive waste immobilization.* Waste Management (Amsterdam, Netherlands), 1992. **12**(2-3): p. 105-31.

79. Conner, J., *Chemistry of cementitious solidfied/stabilized waste forms*. Chemistry and Mircrostructure of solidified waste forms. 1993: Lewis publishers. 41-79.

80. Roy, A., et al., *Solidification Stabilization of a Heavy-Metal Sludge by a Portland-Cement Fly-Ash Binding Mixture.* Hazardous Waste & Hazardous Materials, 1991. **8**(1): p. 33-41.

81. Hamilton, W.P. and A.R. Bowers, *Determination of acute Hg emissions from solidified/stabilized cement waste forms.* Waste Management, 1997. **17**(1): p. 25-32.

82. Randall, P. and S. Chattopadhyay, *Advances in encapsulation technologies for the management of mercury-contaminated hazardous wastes.* Journal of Hazardous Materials, 2004. **114**(1-3): p. 211-223.

83. Schneider, L. and C. Herzog, *Untersuchung von Polyorganosiloxanen als Konditionie-rungsmaterialien für radioaktive Abfallstoffe*. 155/2021 3655/HDB, Stoller Ingeni-eurtechnik GmbH Dresden, 2003. 2003.

84. Kucharczyk, P., *Qualifizierung von Polysiloxanen für die langzeitstabilie Konditionierung radioaktiver Abfälle*, PhD thesis in *Sicherheitforschung und Reaktortechnik*. 2005, RWTH Aachen: Juelich.

85. Randall, P.M., et al. *Characterization and leachability studies of mercuric sulfide sludges under simulated landfill conditions*. in *Proceedings of the Air & Waste Management Association's Annual Conference & Exhibition*. 2000. Salt Lake City, UT, United States.

86. *http://www.wacker.com/cms/de/products-markets/products/product.jsp?product=10466.*

87. Yamamoto, M., *Stimulation of elemental mercury oxidation in the presence of chloride ion in aquatic environments.* Chemosphere, 1996. **32**(6): p. 1217-1224.

88. Canela, M.C. and W.F. Jardim, *The fate of Hg° in natural waters.* Journal of Brazilian Chemical Society, 1997. **8**: p. 421-426.

89. Brandon, N.P., et al., *Thermodynamics and electrochemical behaviour of Hg---S---Cl---H2O systems.* Journal of Electroanalytical Chemistry, 2001. **497**(1-2): p. 18-32.

90. Amyot, M., F.M.M. Morel, and P.A. Ariya, *Dark Oxidation of Dissolved and Liquid Elemental Mercury in Aquatic Environments.* Environmental Science & Technology, 2004. **39**(1): p. 110-114.

91. Cheng, K.Y., et al., *Cement Stabilization/Solidification Techniques: pH Profile Within Acid-Attacked Waste form*, in *Studies in Environmental Science*. 1991, Elsevier. (Amsterdam) p. 371-372.

92. Stepanova, I.V., et al., *High-strength concrete, contains complex mixture of iron hydroxide sol and aluminium sulfate with, iron hydroxide sol aluminium sulfate*, UNIV ST PETERSBURG SUPPLY NETWORK (UYST-Soviet Institute). 2008.

93. Baker, P.G. and P.L. Bishop, *Prediction of metal leaching rates from solidified/stabilized wastes using the shrinking unreacted core leaching procedure.* Journal of Hazardous Materials, 1997. **52**(2-3): p. 311-333.

94. Schuster, E., *The Behavior of Mercury in the Soil with Special Emphasis on Complexation and Adsorption Processes - a Review of the Literature.* Water Air and Soil Pollution, 1991. **56**: p. 667-680.

95. Wang, J.S., et al., *Kinetics of the desorption of mercury from selected freshwater sediments as influenced by chloride.* Water, Air, & Soil Pollution, 1991. **56**(1): p. 533-542.

96. Bishop, P.L., R. Gong, and T.C. Keener, *Effects of leaching on pore size distribution of solidified/ stabilized wastes.* Journal of Hazardous Materials, 1992. **31**(1): p. 59-74.

97. Perlot, C., J. Verdier, and M. Carcasses, *Influence of cement type on transport properties and chemical degradation: Application to nuclear waste storage.* Materials and Structures, 2006. **39**(5): p. 511-523.

98. Svensson, M. and B. Allard, *Diffusion tests of mercury through concrete, bentonite-enhanced sand and sand.* Journal of Hazardous Materials, 2007. **142**(1-2): p. 463-467.

99. Svensson, M. and B. Allard, *Leaching of mercury-containing cement monoliths aged for one year.* Waste Management, 2008. **28**(3): p. 597-603.

100. Svensson, M., A. Dueker, and B. Allard, *Formation of cinnabar - estimation of favorable conditions in a proposed Swedish repository.* J. Hazard. Mater., 2006. **136**(3): p. 830-836.

101. Davis, A.R. and D.E. Irish, *Infrared and Raman spectral study of aqueous mercury(II) nitrate solutions.* Inorganic Chemistry, 2002. **7**(9): p. 1699-1704.

102. Tan, K. and M.J. Taylor, *Vibrational spectra of mercury(I) nitrate in aqueous solution and of the crystalline hydrolysis products.* Australian Journal of Chemistry, 1978. **31**(12): p. 2601-2608.

103. Kiss, J. and A.A. Rehim, *The formation of cinnabar-metacinnabar at hydrothermal conditions (between 25°- 300℃ temperature) and it s genetical interpretation*. Report, 1976, Department of Mineralogy, Eötvös University: Budapest. p. 32-68.

9. Appendix

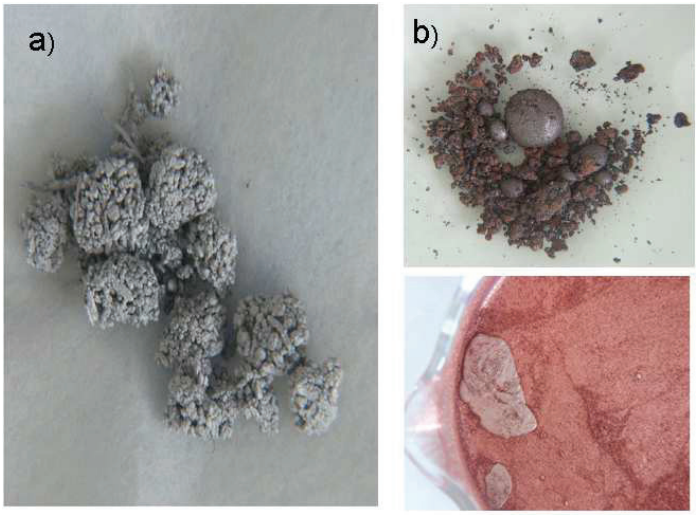

App. Fig 1: a) Silver amalgam b) copper amalgam prepared for irradiation experiments at room temerature

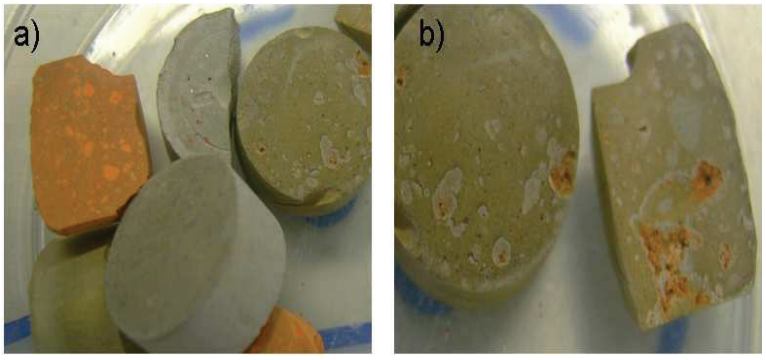

App. Fig 2: a) Hg compounds encapsulated in cement (HgS (red), HgSe (gray). b) Hg(I) nitrate encapsulated in cement

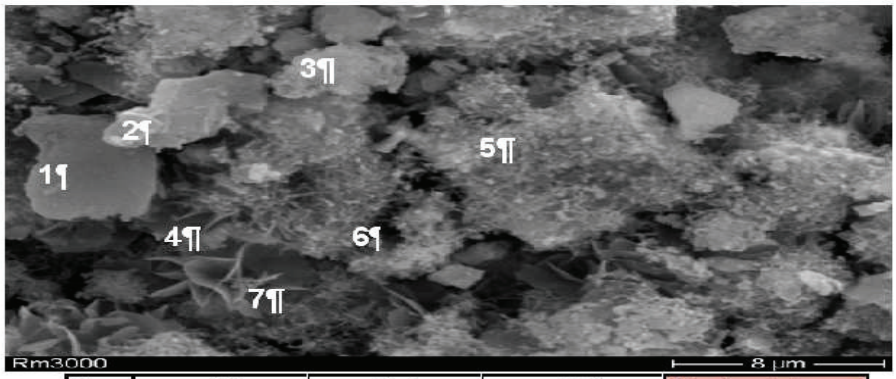

Nr.	Si*		Ca*		Hg*		Dominant phase
	Wt%	At%	Wt%	At%	Wt%	At%	
1	2,3	3,7	83,2	93,1	14,5	14,5	Ca_3SiO_5
2	34,5	50,4	44,2	42,2	21,3	4,4	Ca_3SiO_5 +SiO_2
3	7,5	13,6	62,2	78,6	30,5	7,7	Ca_3SiO_5
4	6,6	11,8	64,2	80,8	29,2	7,4	Ca_3SiO_5 + Hg
5	< 1	< 1	8,3	31,2	91,7	68,8	Hg-Phase
6	5,7	9,8	69,1	84,1	25,2	6,1	Ca_3SiO_5 + Hg
7	5,6	9,5,	71,2	84,9	23,1	5,5	Ca_3SiO_5

App. Fig 3: Enlarged picture of HgS in cement with Hg/Ca/Si compositions measured at specific points

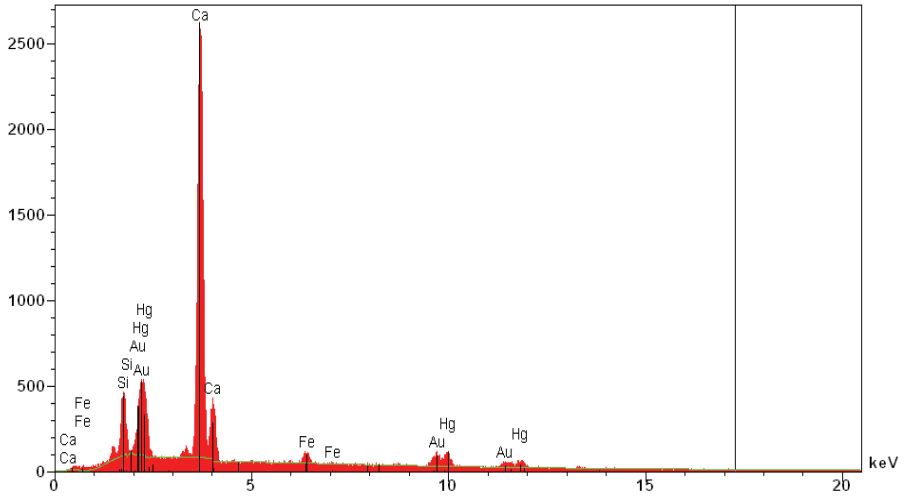

App. Fig 4: EDX spectrum of coverage of Hg-cement matrix after 3 months leaching distilled water under γ-irradiation (Au sputtering was used)

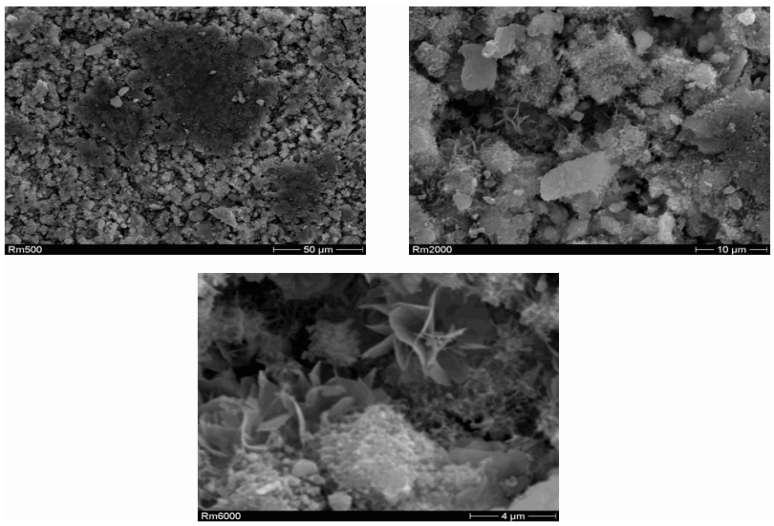

App. Fig 5 : SEM photosgraphs of degraded HgS-cement matrix

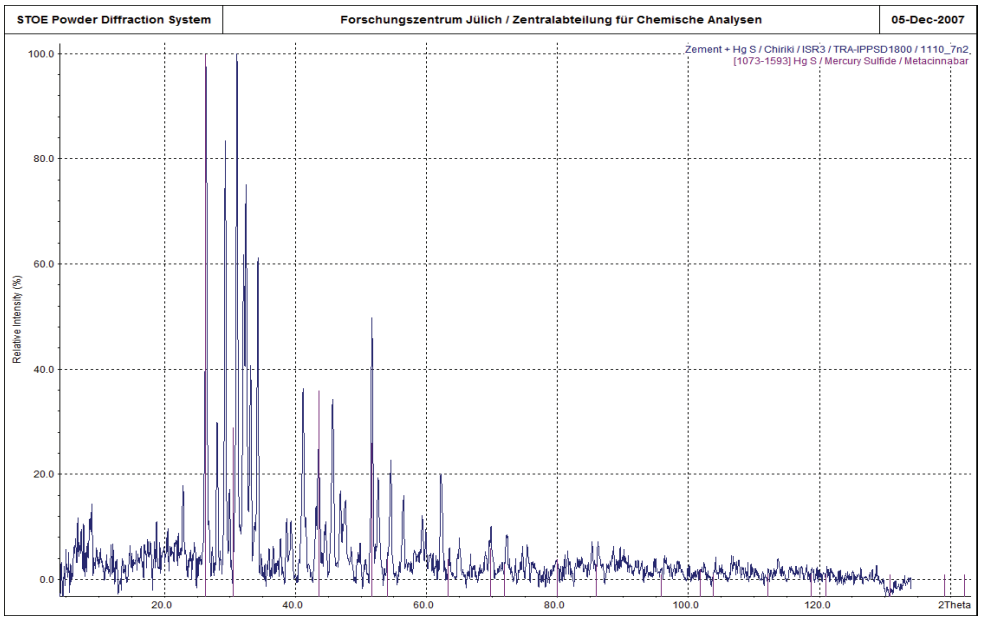

App. Fig 6 : XRD information of Cement-HgS phase

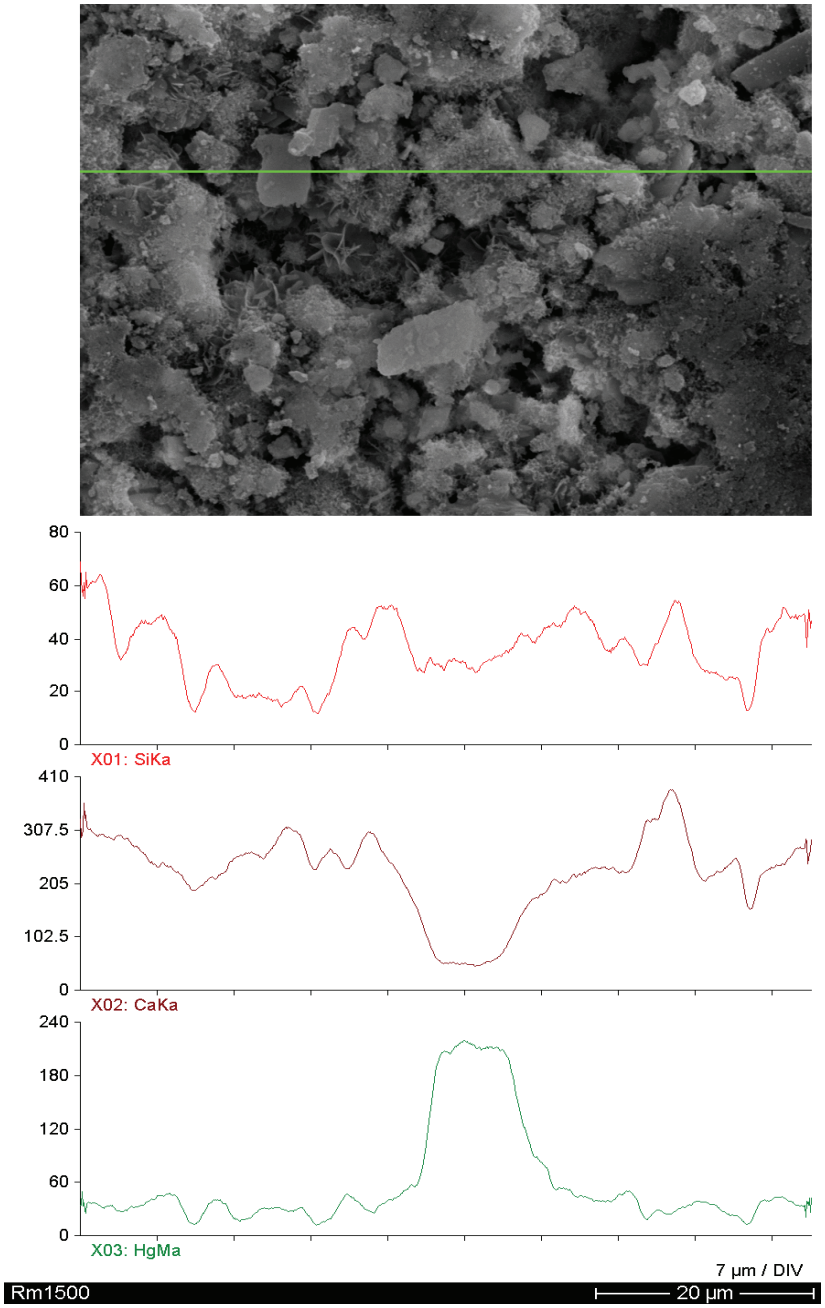

App. Fig 7: SEM photograph of degraded HgS-cement matrix with EDX line scan through inner surface

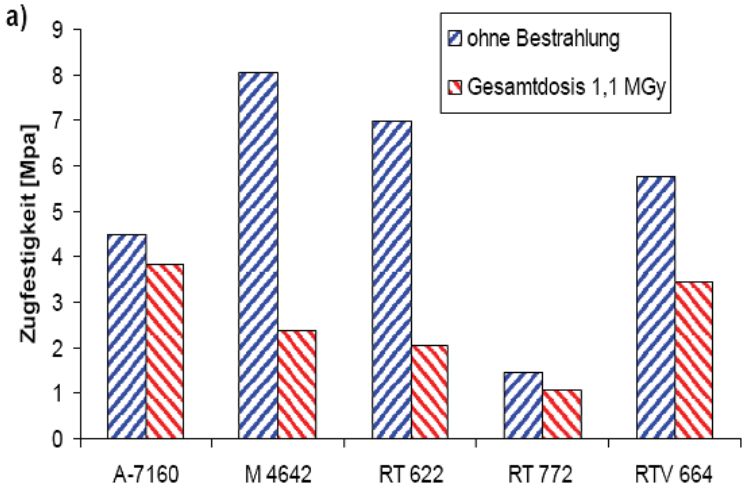

App. Fig 8: The influence of gamma-irradiation on the tensile strength after a total dose rate of 1.1 mGy [84]

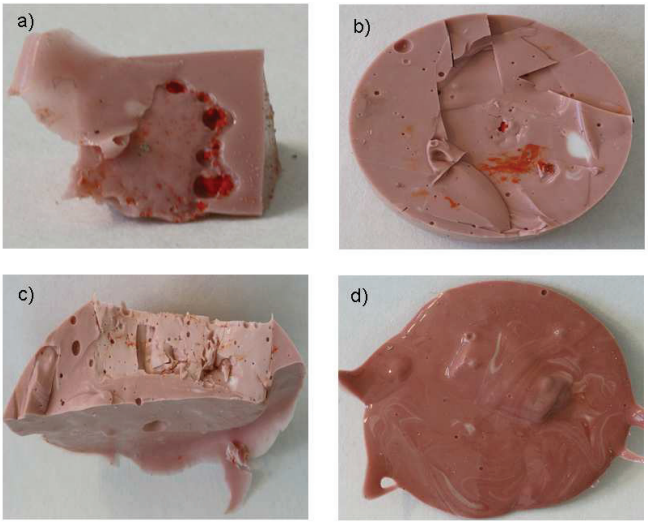

App. Fig 9: HgS/polysiloxane specimen – a) &b) unlayered (top), layered (c) and (d) HgS+cement+polysiloxane layered

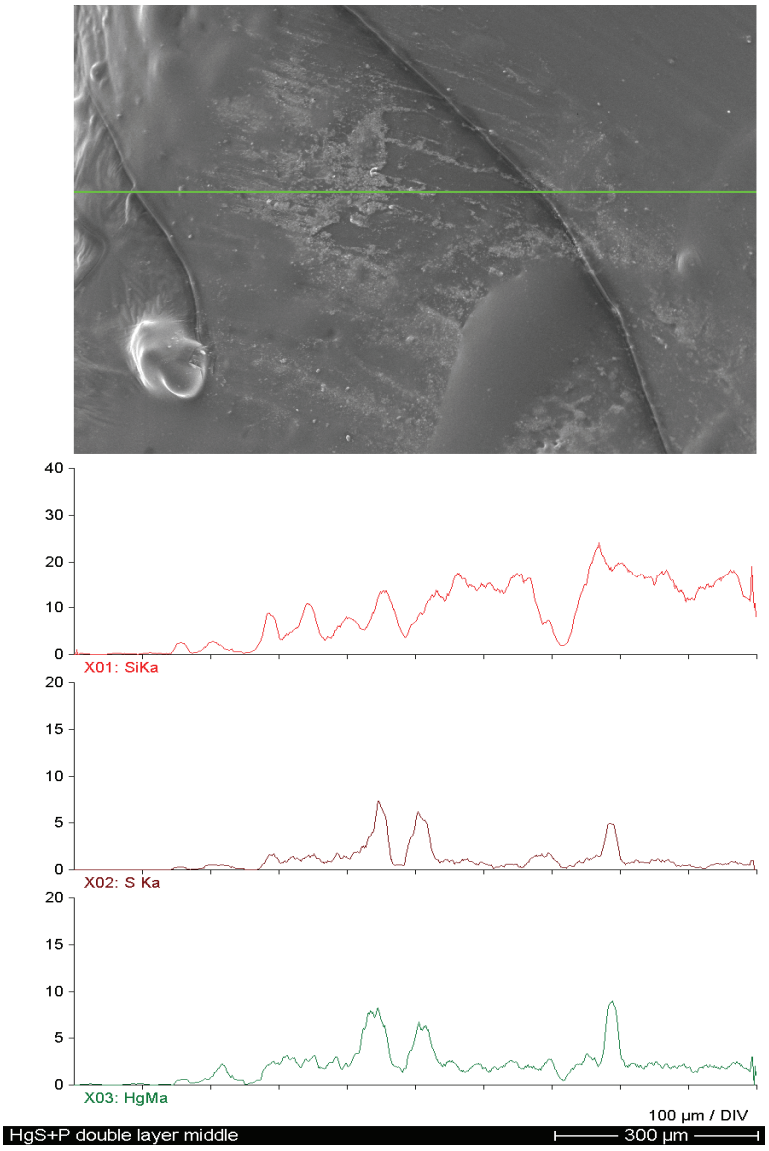

App. Fig 10: SEM photograph of degraded HgS-polysiloxane matrix with EDX line scan through outersurface

Species	ΔG_f°/kJ mol^{-1}
Hg_2^{2+}	153.607
Hg^{2+}	164.703
HgO (c, red, orthorh.)	−58.555
HgO (c, yellow, orthorh.)	−58.450
HgO (c, red, hexag.)	−58.325
$Hg(OH)^+$	−52.01
$HHgO_2^-$	−190
$Hg(OH)_2$ (undissociated)	−274.5
HgH (g)	216
$HgCl^+$	−5.0
$HgCl_2$ (c)	−180.3
$HgCl_2$ (undissociated)	−172.8
$HgCl_3^-$	−308.8
$HgCl_4^{2-}$	−446.4
Hg_2Cl_2 (c)	−210.374
HgS (c, red)	−46.4
HgS (c, black)	−44.4
$HgSO_4$ (c)	−594
$HgSO_4$ (dissociated)	−587.9
Hg_2SO_4 (c)	−626.34
HgS_2^{2-}	ca. 20.7–22.7
$Hg(S_2O_3)_2^{2-}$	−1039.741 [11,12]
$Hg(S_2O_3)_3^{4-}$	−1566.361 [11,12]
$Hg(SO_3)_2^{2-}$	−945.888 [19]
$Hg(SO_3)_3^{4-}$	−1443.276 [19]
H_2O	−237.178
OH^-	−157.293

App. Table 1: Standard Gibbs energy formation of species in Hg-S-Cl-H_2O system at 298℃ [89]

The following chemical reactions were used to analyze the Hg-S-H_2O system in different aqueous solution containing solution HgS. [89]

$$HgS(c,\ red) + H_2O$$

$$\leftrightarrow HgO(c,\ red,\ hexag) + HS^- + H^+$$

$$\log(HS^-) = -41.53 + pH$$

$$Hg_2SO_4(c) \leftrightarrow Hg_2^{2+} + SO_4^{2-}$$

$$\log(Hg_2^{2+}) = -6.19 - \log(SO_4^{2-})$$

$$Hg^{2+} + HSO_4^- \leftrightarrow HgSO_4(aq) + H^+$$

$$\log\{(HgSO_4(aq)/(Hg^{2+})\} = pH - 0.60 + \log(HSO_4^-)$$

$$HgSO_4(c) \leftrightarrow HgSO_4(aq)$$

$$\log(HgSO_4(aq)) = -1.07$$

$$HgSO_4(c) \leftrightarrow Hg^{2+} + SO_4^{2-}$$

$$\log(Hg^{2+}) = 2.465 - \log(SO_4^-)$$

$$Hg^{2+} + HSO_4^- \leftrightarrow HgSO_4(c) + H^+$$

$$\log(Hg^{2+}) = -0.47 - pH - \log(HSO_4^-)$$

$$Hg(OH)_2(aq) + SO_4^{2-} + 2H^+ \leftrightarrow HgSO_4(aq) + 2H_2O$$

$$\log\{(HgSO_4)/(Hg(OH)_2\} = 7.56 - 2\ pH + \log(SO_4^{2-})$$

$$HgO(c,\ red,\ hexag) + 2H^+ + SO_4^{2-} \leftrightarrow HgSO_4(c) + H_2O$$

$$\log(SO_4^{2-}) = 2\ pH - 4.90$$

$$Hg^{2+} + 2S_2O_3^{2-} \leftrightarrow Hg(S_2O_3)_2^{2-}$$

$$\log(Hg(S_2O_3)_2^{2-}) - \log(Hg^{2+}) - 2\log(S_2O_3^{2-}) = 29.23$$

$$Hg^{2+} + 3S_2O_3^{2-} \leftrightarrow Hg(S_2O_3)_3^{4-}$$

$$\log(Hg(S_2O_3)_3^{4-}) - \log(Hg^{2+}) - 3\log(S_2O_3^{2-}) = 30.6$$

$$Hg^{2+} + 2SO_3^{2-} \leftrightarrow Hg(SO_3)_2^{2-}$$

$$\log(Hg(SO_3)_2^{2-}) = 24.07 + 2\log(SO_3^{2-}) + \log(Hg^{2+})$$

$$Hg^{2+} + 3SO_3^{2-} \leftrightarrow Hg(SO_3)_3^{4-}$$

$$\log(Hg(SO_3)_3^{4-}) = 25.96 + 3\log(SO_3^{2-}) + \log(Hg^{2+})$$

Raman frequencies					Vibrational assignment
HNO_3 (4 M)	$HgNO_3$ (3M)	$HgNO_3$ (3M*)	$HgNO_3$ (10 M)	$HgNO_3$ (pur)	
		3626 sh	3626 sh		$\upsilon(OH)^{2}$; OH str from M-OH^{8};
3466 s v-br	3466 s v-br	3472 s v-br	3494 s v-br	3497 s v-br	$\upsilon(OH)^{2}$; OH str from M-OH^{8};
2100 w		2095 w	2090 vw	2095 vw	coordinated M-NO $(NO^{+})^{8}$;
2055 w		2056 w	2059 vw	2061 vw	coordinated M-NO $(NO^{+})^{8}$;
1973 sh		1986 sh			coordinated M-NO $(NO^{+})^{8}$;
1933 vw					$(NO^{+})^{8}$;
			1662 sh	1665 sh	def. of bulk water and overtone of the op fundamental of bound nitrate ion[1];
1642 w-br	1641 w-br	1638 w-br	1629 w-br	1624 w-br	def. of bulk water and overtone of the op fundamental of bound nitrate ion[1];
			1463 ms-br		$\upsilon_{as}(NO_3^{-}Hg^{+})$****^{1,8};
1416 m-br	1414 m-br	1413 m-br		1417 wm-br	$\upsilon_{as}(NO_3^{-})^{1}$;
1346 sh	1343 sh	1342 sh			$\upsilon_{as}(NO_3^{-}Hg)^{1,8}$;
			1306 ms-br	1302 sh	$\upsilon_{as}(NO_3^{-}Hg^{+})$***^{1,7};
				1130 wm-br	$\upsilon_{as}(NO_3^{-}Hg^{+})$***^{1};
1051 s	1049 s	1050 s	1045 s	1043 ms	$\upsilon_{s}(NO_3^{-}Hg^{+})$*^{1,2,7};

			965 sh		$\upsilon_s(NO_3^-Hg^+)$*[1,2,7];
				878 s	$\upsilon_1(Hg)$[6];
813 vvw		818 vvw	816 vvw	815 vvw	$\delta^{op}(NO_3^-Hg^+)$[1,2,7]; $\upsilon_3(Hg)$[6];
	745 sh	745 sh	728 sh	746 vw-br	$NO_3^-Hg^+$ def..[1,2,7];
717 w-br	721 w-br	722 w-br	719 vw	715 vw-br	$NO_3^-Hg^+$ def..**[1,7];
			691 vw-br		$\rho(H_2O)$[2]; δ(O-N=O)[4,5,7];
			642 vw-br		$\rho(H_2O)$[2]; δ(O-N=O)[4,5];
		475 vw			υ(Hg-OH_2)[2]; δ(HgON, ONO)[4,5];
				362 sh	υ(Hg-OH_2)[2]; δ(HgON)[4]; $\upsilon_2(Hg)$[6];
				298 vs-br	δ(Hg-O)[2,4];
	170 sh	171 vs	171 sh	171 sh	υ(O-Hg-Hg-O)*****[2-4];
	167 sh				translatory lattice mode and skel. def.[2]; δ(HgHgO)[4];
152 sh	156 sh				translatory lattice mode and skel. def.[2]; δ(HgHgO)[4];
143 sh					translatory lattice modes and skel. def.[2]; δ(HgHgO)[4];
61 vvs	59 vvs	60 vvs	61 vvs	61 vvs	translatory lattice modes and skel. def.[2];

App. Table 2: Raman frequencies vs Vibrational assignment of different Hg-nitrate bonds

*The Raman peak at 1050 cm^{-1} was assigned to the $\upsilon_s(NO_3^-)$. If the peak shifts to lower wavenumbers, this vibration can be assigned to the $\upsilon_s(NO_3^-Hg^+)$.

**The Raman signal at about 718 cm^{-1} was assigned to the NO_3^- deformation mode. In the case that this vibrational mode shifts to higher wavenumbers, then it will be assigned to the $NO_3^-Hg^+$ deformation mode.

***unidentate cation-nitrate binding

****bidentate orientation

*****A very strong band at wavenumbers higher than 170 cm^{-1} can be assigned to the large non-bonded Hg···Hg stretching mode in the crystal.

1. **Einsatz von multispektralen Satellitenbilddaten in der Wasserhaushalts- und Stoffstrommodellierung – dargestellt am Beispiel des Rureinzugsgebietes**
   von C. Montzka (2008), XX, 238 Seiten
   ISBN: 978-3-89336-508-1

2. **Ozone Production in the Atmosphere Simulation Chamber SAPHIR**
   by C. A. Richter (2008), XIV, 147 pages
   ISBN: 978-3-89336-513-5

3. **Entwicklung neuer Schutz- und Kontaktierungsschichten für Hochtemperatur-Brennstoffzellen**
   von T. Kiefer (2008), 138 Seiten
   ISBN: 978-3-89336-514-2

4. **Optimierung der Reflektivität keramischer Wärmedämmschichten aus Yttrium-teilstabilisiertem Zirkoniumdioxid für den Einsatz auf metallischen Komponenten in Gasturbinen**
   von A. Stuke (2008), X, 201 Seiten
   ISBN: 978-3-89336-515-9

5. **Lichtstreuende Oberflächen, Schichten und Schichtsysteme zur Verbesserung der Lichteinkopplung in Silizium-Dünnschichtsolarzellen**
   von M. Berginski (2008), XV, 171 Seiten
   ISBN: 978-3-89336-516-6

6. **Politikszenarien für den Klimaschutz IV – Szenarien bis 2030**
   hrsg.von P. Markewitz, F. Chr. Matthes (2008), 376 Seiten
   ISBN 978-3-89336-518-0

7. **Untersuchungen zum Verschmutzungsverhalten rheinischer Braunkohlen in Kohledampferzeugern**
   von A. Schlüter (2008), 164 Seiten
   ISBN 978-3-89336-524-1

8. **Inorganic Microporous Membranes for Gas Separation in Fossil Fuel Power Plants**
   by G. van der Donk (2008), VI, 120 pages
   ISBN: 978-3-89336-525-8

9. **Sinterung von Zirkoniumdioxid-Elektrolyten im Mehrlagenverbund der oxidkeramischen Brennstoffzelle (SOFC)**
   von R. Mücke (2008), VI, 165 Seiten
   ISBN: 978-3-89336-529-6

10. **Safety Considerations on Liquid Hydrogen**
    by K. Verfondern (2008), VIII, 167 pages
    ISBN: 978-3-89336-530-2

11. **Kerosinreformierung für Luftfahrtanwendungen**
von R. C. Samsun (2008), VII, 218 Seiten
ISBN: 978-3-89336-531-9

12. **Der 4. Deutsche Wasserstoff Congress 2008 – Tagungsband**
hrsg. von D. Stolten, B. Emonts, Th. Grube (2008), 269 Seiten
ISBN: 978-3-89336-533-3

13. **Organic matter in Late Devonian sediments as an indicator for environmental changes**
by M. Kloppisch (2008), XII, 188 pages
ISBN: 978-3-89336-534-0

14. **Entschwefelung von Mitteldestillaten für die Anwendung in mobilen Brennstoffzellen-Systemen**
von J. Latz (2008), XII, 215 Seiten
ISBN: 978-3-89336-535-7

15. **RED-IMPACT**
Impact of Partitioning, Transmutation and Waste Reduction Technologies on the Final Nuclear Waste Disposal
SYNTHESIS REPORT
ed. by W. von Lensa, R. Nabbi, M. Rossbach (2008), 178 pages
ISBN 978-3-89336-538-8

16. **Ferritic Steel Interconnectors and their Interactions with Ni Base Anodes in Solid Oxide Fuel Cells (SOFC)**
by J. H. Froitzheim (2008), 169 pages
ISBN: 978-3-89336-540-1

17. **Integrated Modelling of Nutrients in Selected River Basins of Turkey**
Results of a bilateral German-Turkish Research Project
project coord. M. Karpuzcu, F. Wendland (2008), XVI, 183 pages
ISBN: 978-3-89336-541-8

18. **Isotopengeochemische Studien zur klimatischen Ausprägung der Jüngeren Dryas in terrestrischen Archiven Eurasiens**
von J. Parplies (2008), XI, 155 Seiten, Anh.
ISBN: 978-3-89336-542-5

19. **Untersuchungen zur Klimavariabilität auf dem Tibetischen Plateau - Ein Beitrag auf der Basis stabiler Kohlenstoff- und Sauerstoffisotope in Jahrringen von Bäumen waldgrenznaher Standorte**
von J. Griessinger (2008), XIII, 172 Seiten
ISBN: 978-3-89336-544-9

20. **Neutron-Irradiation + Helium Hardening & Embrittlement Modeling of 9%Cr-Steels in an Engineering Perspective (HELENA)**
by R. Chaouadi (2008), VIII, 139 pages
ISBN: 978-3-89336-545-6

21. **in Bearbeitung**

22. **Verbundvorhaben APAWAGS (AOEV und Wassergenerierung) – Teilprojekt: Brennstoffreformierung – Schlussbericht**
von R. Peters, R. C. Samsun, J. Pasel, Z. Porš, D. Stolten (2008), VI, 106 Seiten
ISBN: 978-3-89336-547-0

23. **FREEVAL**
Evaluation of a Fire Radiative Power Product derived from Meteosat 8/9 and Identification of Operational User Needs
Final Report
project coord. M. Schultz, M. Wooster (2008), 139 pages
ISBN: 978-3-89336-549-4

24. **Untersuchungen zum Alkaliverhalten unter Oxycoal-Bedingungen**
von C. Weber (2008), VII, 143, XII Seiten
ISBN: 978-3-89336-551-7

25. **Grundlegende Untersuchungen zur Freisetzung von Spurstoffen, Heißgaschemie, Korrosionsbeständigkeit keramischer Werkstoffe und Alkalirückhaltung in der Druckkohlenstaubfeuerung**
von M. Müller (2008), 207 Seiten
ISBN: 978-3-89336-552-4

26. **Analytik von ozoninduzierten phenolischen Sekundärmetaboliten in *Nicotiana tabacum* L. cv Bel W3 mittels LC-MS**
von I. Koch (2008), III, V, 153 Seiten
ISBN 978-3-89336-553-1

27. **IEF-3 Report 2009. Grundlagenforschung für die Anwendung**
(2009), ca. 230 Seiten
ISBN: 978-3-89336-554-8

28. **Influence of Composition and Processing in the Oxidation Behavior of MCrAlY-Coatings for TBC Applications**
by J. Toscano (2009), 168 pages
ISBN: 978-3-89336-556-2

29. **Modellgestützte Analyse signifikanter Phosphorbelastungen in hessischen Oberflächengewässern aus diffusen und punktuellen Quellen**
von B. Tetzlaff (2009), 149 Seiten
ISBN: 978-3-89336-557-9

30. **Nickelreaktivlot / Oxidkeramik – Fügungen als elektrisch isolierende Dichtungskonzepte für Hochtemperatur-Brennstoffzellen-Stacks**
von S. Zügner (2009), 136 Seiten
ISBN: 978-3-89336-558-6

31. **Langzeitbeobachtung der Dosisbelastung der Bevölkerung in radioaktiv kontaminierten Gebieten Weißrusslands – Korma-Studie**
von H. Dederichs, J. Pillath, B. Heuel-Fabianek, P. Hill, R. Lennartz (2009), Getr. Pag.
ISBN: 978-3-89336-532-3

32. **Herstellung von Hochtemperatur-Brennstoffzellen über physikalische Gasphasenabscheidung**
von N. Jordán Escalona (2009), 148 Seiten
ISBN: 978-3-89336-532-3

33. **Real-time Digital Control of Plasma Position and Shape on the TEXTOR Tokamak**
by M. Mitri (2009), IV, 128 pages
ISBN: 978-3-89336-567-8

34. **Freisetzung und Einbindung von Alkalimetallverbindungen in kohlebefeuerten Kombikraftwerken**
von M. Müller (2009), 155 Seiten
ISBN: 978-3-89336-568-5

35. **Kosten von Brennstoffzellensystemen auf Massenbasis in Abhängigkeit von der Absatzmenge**
von J. Werhahn (2009), 242 Seiten
ISBN: 978-3-89336-569-2

36. **Einfluss von Reoxidationszyklen auf die Betriebsfestigkeit von anodengestützten Festoxid-Brennstoffzellen**
von M. Ettler (2009), 138 Seiten
ISBN: 978-3-89336-570-8

37. **Großflächige Plasmaabscheidung von mikrokristallinem Silizium für mikromorphe Dünnschichtsolarmodule**
von T. Kilper (2009), XVII, 154 Seiten
ISBN: 978-3-89336-572-2

38. **Generalized detailed balance theory of solar cells**
by T. Kirchartz (2009), IV, 198 pages
ISBN: 978-3-89336-573-9

39. **The Influence of the Dynamic Ergodic Divertor on the Radial Electric Field at the Tokamak TEXTOR**
von J. W. Coenen (2009), xii, 122, XXVI pages
ISBN: 978-3-89336-574-6

40. **Sicherheitstechnik im Wandel Nuklearer Systeme**
von K. Nünighoff (2009), viii, 215 Seiten
ISBN: 978-3-89336-578-4

41. **Pulvermetallurgie hochporöser NiTi-Legierungen für Implanat- und Dämpfungsanwendungen**
von M. Köhl (2009), XVII, 199 Seiten
ISBN: 978-3-89336-580-7

42. **Einfluss der Bondcoatzusammensetzung und Herstellungsparameter auf die Lebensdauer von Wärmedämmschichten bei zyklischer Temperaturbelastung**
von M. Subanovic (2009), 188, VI Seiten
ISBN: 978-3-89336-582-1

43. **Oxygen Permeation and Thermo-Chemical Stability of Oxygen Permeation Membrane Materials for the Oxyfuel Process**
by A. J. Ellett (2009), 176 pages
ISBN: 978-3-89336-581-4

44. **Korrosion von polykristallinem Aluminiumoxid (PCA) durch Metalljodidschmelzen sowie deren Benetzungseigenschaften**
von S. C. Fischer (2009), 148 Seiten
ISBN: 978-3-89336-584-5

45. **IEF-3 Report 2009. Basic Research for Applications**
(2009), 217 Seiten
ISBN: 978-3-89336-585-2

46. **Verbundvorhaben ELBASYS (Elektrische Basissysteme in einem CFK-Rumpf) - Teilprojekt: Brennstoffzellenabgase zur Tankinertisierung - Schlussbericht**
von R. Peters, J. Latz, J. Pasel, R. C. Samsun, D. Stolten
(2009), xi, 202 Seiten
ISBN: 978-3-89336-587-6

47. **Aging of ^{14}C-labeled Atrazine Residues in Soil: Location, Characterization and Biological Accessibility**
by N. D. Jablonowski (2009), IX, 104 pages
ISBN: 978-3-89336-588-3

48. **Entwicklung eines energetischen Sanierungsmodells für den europäischen Wohngebäudesektor unter dem Aspekt der Erstellung von Szenarien für Energie- und CO_2 - Einsparpotenziale bis 2030**
von P. Hansen (2009), XXII, 281 Seiten
ISBN: 978-3-89336-590-6

49. **Reduktion der Chromfreisetzung aus metallischen Interkonnektoren für Hochtemperaturbrennstofzellen durch Schutzschichtsysteme**
von R. Trebbels (2009), iii, 135 Seiten
ISBN: 978-3-89336-591-3

50. **Bruchmechanische Untersuchung von Metall / Keramik-Verbundsystemen für die Anwendung in der Hochtemperaturbrennstoffzelle**
von B. Kuhn (2009), 118 Seiten
ISBN: 978-3-89336-592-0

51. **Wasserstoff-Emissionen und ihre Auswirkungen auf den arktischen Ozonverlust**
Risikoanalyse einer globalen Wasserstoffwirtschaft
von T. Feck (2009), 180 Seiten
ISBN: 978-3-89336-593-7

52. **Development of a new Online Method for Compound Specific Measurements of Organic Aerosols**
by T. Hohaus (2009), 156 pages
ISBN: 978-3-89336-596-8

53. **Entwicklung einer FPGA basierten Ansteuerungselektronik für Justageeinheiten im Michelson Interferometer**
von H. Nöldgen (2009), 121 Seiten
ISBN: 978-3-89336-599-9

54. **Observation – and model – based study of the extratropical UT/LS**
by A. Kunz (2010), xii, 120, xii pages
ISBN: 978-3-89336-603-3

55. **Herstellung polykristalliner Szintillatoren für die Positronen-Emissions-Tomographie (PET)**
von S. K. Karim (2010), VIII, 154 Seiten
ISBN: 978-3-89336-610-1

56. **Kombination eines Gebäudekondensators mit H2-Rekombinatorelementen in Leichwasserreaktoren**
von S. Kelm (2010), vii, 119 Seiten
ISBN: 978-3-89336-611-8

57. **Plant Leaf Motion Estimation Using A 5D Affine Optical Flow Model**
by T. Schuchert (2010), X, 143 pages
ISBN: 978-3-89336-613-2

58. **Tracer-tracer relations as a tool for research on polar ozone loss**
by R. Müller (2010), 116 pages
ISBN: 978-3-89336-614-9

59. **Sorption of polycyclic aromatic hydrocarbon (PAH) to Yangtze River sediments and their components**
by J. Zhang (2010), X, 109 pages
ISBN: 978-3-89336-616-3

60. **Weltweite Innovationen bei der Entwicklung von CCS-Technologien und Möglichkeiten der Nutzung und des Recyclings von CO_2**
Studie im Auftrag des BMWi
von W. Kuckshinrichs et al. (2010), X, 139 Seiten
ISBN: 978-3-89336-617-0

61. **Herstellung und Charakterisierung von sauerstoffionenleitenden Dünnschichtmembranstrukturen**
von M. Betz (2010), XII, 112 Seiten
ISBN: 978-3-89336-618-7

62. **Politikszenarien für den Klimaschutz V – auf dem Weg zum Strukturwandel, Treibhausgas-Emissionsszenarien bis zum Jahr 2030**
hrsg. von P. Hansen, F. Chr. Matthes (2010), 276 Seiten
ISBN: 978-3-89336-619-4

63. **Charakterisierung Biogener Sekundärer Organischer Aerosole mit Statistischen Methoden**
von C. Spindler (2010), iv, 163 Seiten
ISBN: 978-3-89336-622-4

64. **Stabile Algorithmen für die Magnetotomographie an Brennstoffzellen**
von M. Wannert (2010), ix, 119 Seiten
ISBN: 978-3-89336-623-1

65. **Sauerstofftransport und Degradationsverhalten von Hochtemperatur-membranen für CO2-freie Kraftwerke**
von D. Schlehuber (2010), VII, 139 Seiten
ISBN: 978-3-89336-630-9

66. **Entwicklung und Herstellung von foliengegossenen, anodengestützten Festoxidbrennstoffzellen**
von W. Schafbauer (2010), VI, 164 Seiten
ISBN: 978-3-89336-631-6

67. **Disposal strategy of proton irradiated mercury from high power spallation sources**
by S. Chiriki (2010), xiv, 124 pages
ISBN: 978-3-89336-632-3

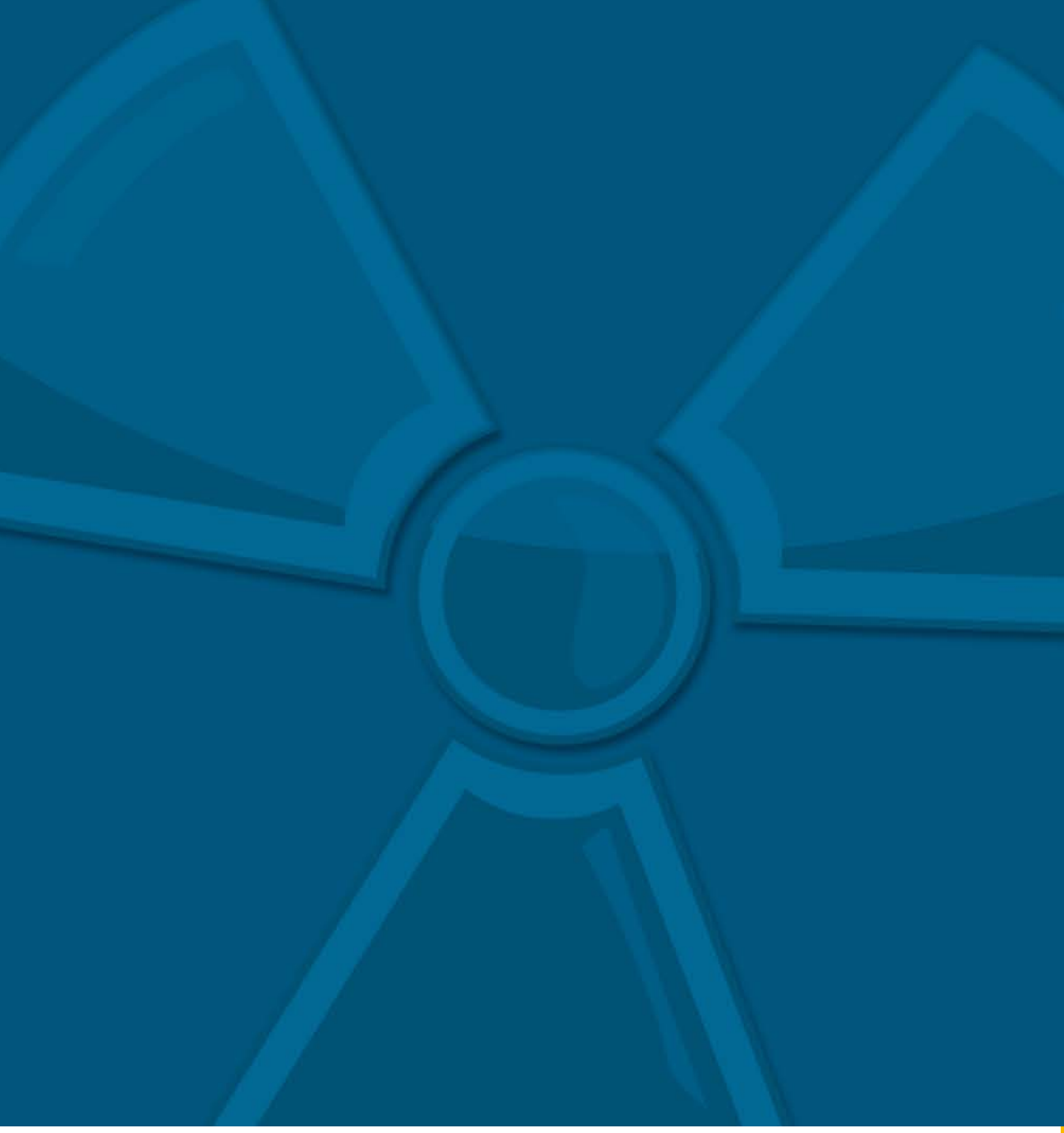

Energie & Umwelt / Energy & Environment
Band / Volume 67
ISBN 978-3-89336-632-3

JÜLICH
FORSCHUNGSZENTRUM